A STUDY OF CREEP IN LIGHTWEIGHT AND CONVENTIONAL CONCRETES

By

MICHAEL A. CASSARO

A DISSERTATION PRESENTED TO THE GRADUATE COUNCIL OF
THE UNIVERSITY OF FLORIDA
IN PARTIAL FULFILLMENT OF THE REQUIREMENTS FOR THE
DEGREE OF DOCTOR OF PHILOSOPHY

UNIVERSITY OF FLORIDA

April, 1967

TO

Kay

Mike
Kevin
Molly
Katie
Maggie
Matt

ACKNOWLEDGMENTS

This report was prepared as a part of a study under Research Project DR-5025 at the University of Florida under contract with the Florida State Road Department and in cooperation with the United States Bureau of Public Roads.

For the University of Florida, the work covered in this report was carried out under the general administrative supervision of T. L. Martin, Jr., Dean of the College of Engineering; M. E. Forsman, Director of the Engineering and Industrial Experiment Station; R. W. Kluge, Chairman of the Department of Civil Engineering.

The author wishes to thank James Gammage, Engineer of Materials, Research and Training of the Florida State Road Department, R. W. Kluge, Chairman, Department of Civil Engineering, University of Florida, K. Majidzadeh, Associate Professor of Civil Engineering at Ohio State Univeraity, and D. Sawyer, Professor of Civil Engineering, Auburn University, Alabama, for their valuable contributions to this study. This study was started under the direction of D. Sawyer while he was with the University of Florida and most of the planning is credited to him. Appreciation is also rendered to J. L. Holsonback for his efforts in development of computer programs used in the study.

The opinions, findings, and conclusions expreased in this publication are those of the author and not necessarily those of the Florida State Road Department or the Bureau of Public Roads.

TABLE OF CONTENTS

LIST OF FIGURES

LIST OF TABLES

LIST OF SYMBOLS

ϵ = concrete strain

$\dot{\epsilon}$ = strain rate, time derivative of strain

ϵ_{vis} = all non recoverable components of total strain

f = concrete stress in psi

f_o = initial concrete stress

f_D = decaying concrete stress

t = time in days

E = elastic modulus of concrete in psi

λ = viscosity in psi-days

λ_∞ = final viscosity

λ_o = initial viscosity

ϕ = fluidity, the reciprocal of viscosity

E_e, ϕ_e = spring and dashpot constants respectively of the elastic element in the rheological equation for creep

E_n, ϕ_n = similar constants for any Kelvin element

e = base of the natural logarithms

k = Boltzmann's constant 1.380×10^{-16} erg deg^{-1}

h = Planck's constant 6.624×10^{-27} erg sec

T = absolute temperature

E_o = free energy of activation

c_t = time dependent component of the coefficient of structural stability

c_f = coefficient of the stress dependent component of the coefficient of structural stability

A, B = coefficients in the equation governing strain rate based on the rate process theory

w = weighted flow distance over which a particle of moisture must flow before reaching the surface of a specimen

Abstract of Dissertation Presented to the Graduate
Council in Partial Fulfillment of the
Requirements for the Degree of
Doctor of Philosophy

A STUDY OF CREEP IN LIGHTWEIGHT AND CONVENTIONAL CONCRETE

By

Michael A. Cassaro

April, 1967

Chairman: Professor R. W. Kluge
Major Department: Civil Engineering

Statistical Mechanics and Rheological approaches have been utilized to establish a mathematical model to represent the long term creep of concrete.

The generalized model presented predicts behavior of lightweight and conventional concretes irrespective of size and shape variations. A coefficient of structural stability has been introduced to incorporate the effect of aging and of stress variations in the analysis of data. The use of the age and stress dependent components of the stability coefficient permits the calculation of creep at any time and for any stress level.

CHAPTER I

INTRODUCTION

The mechanical properties of concrete, and perhaps all matter, may be treated from three distinct viewpoints; each viewpoint attempts to satisfy an engineering need for predictability concerning the mechanical behavior of the material in specific structural applications; each viewpoint used to satisfy this need takes a basically separate route; each viewpoint has distinct advantages which when applied, are complementary. These viewpoints are the Statistical Mechanics, the Structural, and the Phenomenological approaches to material behavior.[20]

The Statistical Mechanics approach considers the material as an association of discrete particles held together by bonds of high energy content. At this level behavior of the discrete particles is described by their relative positions in space, their velocities, and the interaction forces between them. The Structural approach considers the material to be continuous but non-homogeneous, being formed of elements of different properties, distributed randomly throughout the material, and having finite dimensions. The Phenomenological approach considers the observed or macroscopic material behavior. It deals with the observation of the relation between forces and resulting states of motion of finite bodies assumed to be homogeneous. Mechanical behavior of the material is described in terms of the relations between stresses and strains, and their derivatives. This approach usually involves extensive testing and bases the material behavior on observed responses obtained from the test and its environment.

A. Objective

In this investigation, an attempt has been made to combine the best findings of each approach. The primary concern is with an understanding of the behavior of a specific structural lightweight aggregate concrete and normal limestone aggregate concrete as the behavior is influenced by creep alone. In an attempt to clarify the existing theories for the mechanism of creep as they pertain to concretes of the type tested, this study has endeavored to link molecular hypothesis and rheological models with macroscopic observations of the concrete structures under investigation. In this endeavor it is hoped that a clear understanding of creep behavior of concrete as a function of time and stress will result.

The parameters in the model developed are material constants related to the rheological structure of the concrete in question. If it is possible to determine the nature of the changes of these material constants for the concrete structure with respect to stress independently of aging it is reasonable to expect that it will be possible to predict creep for the concrete under any condition of stress and time.

In all previous methods developed to explain creep it has not been possible to make a general prediction of creep behavior for a specific concrete relative to time and stress based on the results from a single test. The advantages for being able to do so are obvious. By linking molecular hypothesis to rheological description of the concrete it appears possible to separate aging effects from stress variation effects. When the two effects are separated variation in each may be handled separately thereby producing the desired model.

B. Scope

This investigation has three objectives.

1. To determine the difference in the nature of creep between lightweight Solite concrete and normal limestone concrete.
2. To determine the influence of shape without size interaction on concrete creep.
3. To investigate the possibility of establishing a model to represent the creep of concrete under any stress history from a single test of the concrete which is to be represented by the model.

In establishing the general creep model with respect to stress and time based on the observed creep response from a test series under sustained stress, conventional viscoelastic[2, 3] and statistical mechanics[6, 19] approaches are employed to develop the coefficients of the creep equation for the model. Following the conventional viscoelastic approach the material behavior is separated into type of response as follows:

1. instantaneous elastic response
2. steady state irrecoverable creep
3. transient delayed elastic response
4. transient viscous response for early stage creep
5. transient irrecoverable creep representing long term responses.

The model is established by converting the last four responses listed into three parameters in the model:

1. The rate of transition of the gel from fluid to solid.
2. The total expected change in the structure of the gel as measured by its fluidity.
3. The purely elastic transient action of the gel and aggregate system.

The first parameter constitutes the rate of change of the concrete structure under the action of stress and due to normal aging. The second parameter represents the difference in the nature of the structure from before load is applied to some final state. These two parameters are involved in the stability of the concrete structure with respect to aging and stress.

The third parameter is purely elastic in nature and represents the delayed elasticity term of the model. It is shown that this term may be employed to determine the delayed elastic recovery for the unloaded specimen.

If the model is to be acceptable it must be capable of predicting creep behavior of lightweight and normal concretes alike; the model developed does so. The model developed also attempts to predict creep behavior irrespective of size and shape variations. The variations in the material constants of the model due to shape appear to adequately explain the creep mechanism as it pertains to shape. Size was not a parameter of the experiment. However the anticipated nature of the interaction between size and shape is developed and is presented in the interpretation of the results. Since mix variations and environment were not parameters in this experiment and in view of a lack of sufficient correlation between size and creep, the scope of this experiment precludes the formulation of a more generalized model.

CHAPTER II

REVIEW OF THE CREEP BEHAVIOR OF CONCRETE

Many variables influence the magnitude of creep. This test program was limited to only a few among which are:

Coarse aggregate ingredients

Mix proportions

Shape of the specimen

A. Coarse Aggregate Ingredients

In general it is believed that hard dense aggregates, with low absorption and a high elastic modulus produce a concrete with low creep tendencies. Troxell and Davis[1] indicate that particle shape, surface texture, pore structure and unit weight may also influence concrete creep. These influences are all involved in the differences between the two aggregates used in this study. An individual evaluation of each influencing factor is difficult if not impossible. However, it may be possible to speculate on the more prominent characteristics which are considered to be the modulus of elasticity and the permeability of the aggregate. Particle shape and surface texture are not considered to be major factors in creep behavior according to Best.[15]

B. Mix Proportions

Cement paste content and water-cement ratio appear to be intimately involved in creep activity of concrete. Many authors have testified to

the direct relationship between paste content and creep.[18] This study was not intended to resolve the questions concerning the nature of the involvement of cement, water or paste. Therefore, in an attempt to minimize complications in the behavior of concrete due to variations in these ingredients the paste contents were made equal for the concrete mixes.

The water-cement ratios for the two mixes could not be so easily equated. No problem resulted from the selection of a given water-cement ratio for the limestone concrete. However, a water-cement ratio for the lightweight aggregate concrete may not be established since a portion of the free water contained in the aggregate used must be considered to add to the mix water for the concrete. By preliminary experimentation the strength of the lightweight concrete was controlled by selection of an effective mix water content to establish near equal strengths for the two structural concretes.

C. Shape of Specimen

Very little work has been done to determine the effect of shape on creep. Several in vestigations have been reported involving the influence of size of specimen on creep. These reports indicate a decrease in creep with increase in size of specimen.[1, 2, 16] The effect is usually explained as a result of the increased seepage path to the free surface. This apparent interaction of stress dependent seepage and shrinkage which is related to creep bears directly on the shape effect of the concrete specimen. Thus by varying the free surface area and maintaining a constant cross-sectional area it is possible to evaluate the stress

dependent seepage effect on creep as distinguished from pure shrinkage for these two concrete types.

D. Nature of Creep in Concrete

The deformation characteristics of concrete are related to its internal structure.[11,13] The mortar paste constitutes the active part of the concrete in binding coarse aggregate to form a stone-like material. It is composed of cement, water, interspersed graded fine aggregate, and air. The relative proportions of these ingredients vary from one concrete mix to another. This variation is the essential factor which results in all behavioral variations of concrete.

The aggregate particles are bound together by the cement paste matrix. The aggregate plays a less active role in the creep response of the concrete than the cement paste.

At any stage of hydration, the structure of the cement paste consists of unhydrated cement grains, hydrated cement, water, and air. The cement paste structure is called cement gel which has a more rigid structure with aging and a less rigid structure under increasing load. It is the action of the gel which gives concrete its viscoelastic nature. Initially as the cellular structure of the hydrated cement is developing, the colloidal-liquid phase predominates. If a load is applied at this early stage the cement gel behaves as a liquid in that it flows under any nonisotropic stress, however small. The degree to which the liquid-colloidal phase exists is manifested in the amount of creep which results. As the gel matures, due to continued hydration, the solid cellular structure becomes dominant over the liquid phase.

An applied stress at this time results in less creep since the gel would behave more like a solid, exhibiting elastic tendencies.

The nature of the action of the aggregate dispersed throughout the cement gel has been termed passive.[2] If, as stated above, it is the cement gel which creeps, then by including solid aggregate particles into the gel its resistance to creep should be increased according to Reiner.[3] This condition further complicates the problem of determining the action of the coarse aggregate. As it was explained in connection with the coarse aggregate effects discussed in section A of this chapter, this additional volume concentration effect cannot be evaluated for the lightweight aggregate because it is not known how the moisture contained in the lightweight aggregate influences its volume concentration in the concrete.

Therefore, like most creep findings reported in the literature, the findings of this report may only be applied to the specific concretes being investigated. The model constants are applicable only to the range of specimen sizes used and under similar ambient conditions of humidity and temperature.

CHAPTER III

THE VISCOELASTIC APPROACH

A. Basic Mathematical Models

The most successful simple phenomenological form of the data from a creep study follows Ross's[7] parametric equation relating strain and time. Most strain data may first be prepared in this form from which creep, ϵ , may be determined at any time t from

$$\epsilon = \frac{at}{b + t} \quad , \tag{1}$$

where a is a dimensionless constant and b is a constant with the units of time.

The most general phenomenological form for creep data is obtained from rheological theory. Rheology is the science of flow of materials; it offers a transition between classical theory of elasticity and classical hydrodynamics and has been proposed as a theory of the general behavior of materials on the assumption that every real material must be supposed to possess all basic deformational properties in varying proportions. Strain relations may be developed as viscoelastic strains employing the conventional theory of rheology.[2, 17] Using the data from test series A a creep model with four linear elements was developed which was similar to Freudenthal's[4] model in the simplified form. The detailed model used is shown in Figure 1. The model consists of the following elements in series.

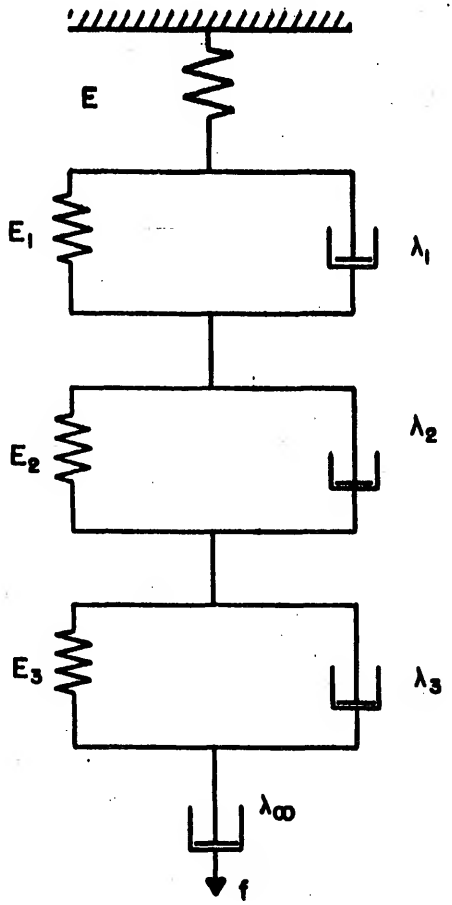

LINEARIZED RHEOLOGICAL MODEL FOR CONCRETE

FIGURE 1

1. A Maxwell element with linear spring and dashpot in series representing the elastic strain and the long time irrecoverable creep resulting from inelastic strain.
2. A Kelvin element with linear spring and dashpot in parallel representing the short time viscoelastic effects. This influence was attributed to consolidation due to seepage of pore water.
3. A Kelvin element with linear spring and dashpot in parallel representing intermediate time viscoelastic effects. This influence was attributed, after Freudenthal, to retarded elasticity or recoverable creep.
4. A Kelvin element with linear spring and dashpot in parallel representing long time viscoelastic effects. This influence was attributed to destruction of the gel structure under stress.

The equation[17] representing the simple rheological model for constant f is

$$\epsilon = \frac{f}{E} + \frac{ft}{\lambda_\infty} + \sum_{n=1}^{3} \frac{f}{E_n} \left(1 - e^{-\phi_n E_n t}\right) \quad . \tag{2}$$

The first two terms represent the Maxwell element. The three terms in the summation represent the Kelvin elements. All terms in equation (2) are defined in the list of symbols.

Most creep curves may be satisfied by simply extending the number of terms in the summation to provide a transition curve which fits the data between the elastic response (first term) and the final or steady state response (second term).

B. The Nature of the Rheological Model

Rheological equations define ideal bodies which serve as models of comparison in the analysis of material behavior. The rheological

variables are stress, deformation and time; the rheological parameters are viscosity and elasticity. The parameters in the rheological equations characterize the material behavior; they may be constants from which we obtain linear viscoelastic equations or they may be functions of time or stress from which we obtain non-linear viscoelastic equations.

Many models have been proposed for the creep behavior of concrete. However, the many factors influencing the gel structure seem to preclude the development of a single model for all conditions. The nature of hydration in the gel is believed to contribute the major source of variability in the creep behavior. It is the gel which supplies the viscoelastic nature of concrete because it is a varying form of matter lying between the solid and fluid physical states. The gel in concrete, which is formed initially from a fluid, is distinguished by a change in its mechanical properties, by a transition into a solid state having high viscosity, elasticity, and limiting values of stress related to strain. Some authors[5] have experienced completely solid state responses (no viscous creep) from concretes which have been fully dried and cured.

Concrete undergoes the transition from fluid to solid over a period of several years. After a few hours, however, the solid phase cellular structure may have developed sufficient elastic strength to withstand a test load. At that time the concrete is put into service and loads are imparted to it. It is clear that the degree of fluidity of the gel at the time of loading will greatly influence the elastic and creep properties of the concrete. Rheological models are unable to cope with the many variables which influence these phase changes of the gel not to mention the added variation of aggregate interaction with the gel. It would

appear that a single model, no matter how general it may be, is not the basic answer to prediction of creep in concrete; rather, a general procedure for predicting creep behavior is more in order. Such a procedure will provide for the development of an equation which incorporates the significant parameters for the concrete being investigated into a specific rheological model.

All the influences on creep may be categorized by their influence on three factors:

1. The rate of transition of the gel from fluid to solid.
2. The purely elastic action of the gel and aggregate system.
3. The total change in the structure of the gel.

If these three factors are used as parameters for the rheological model then it would seem that the creep behavior of every concrete may be interpreted.

For a more detailed study of the rheological approach refer to items 2, 4, and 17 in the bibliography. A supplementary study to this report, of rheology, and the basis for development and behavior of the model presented in figure 1 is found in reference 22.

CHAPTER IV

THE STATISTICAL MECHANICS APPROACH

A. The Rate Process Theory

Glasstone, Laidler and Eyring[6] extended classical quantum mechanics theory to include statistical treatment of reaction rates. Since all matter is composed of molecules or assemblies of molecules which vibrate about some equilibrium position, when the quantum state (or energy level) is changed new equilibrium positions are obtained. Eyring, et al. employed a concept of potential energy surfaces to describe the conversion from vibrational energy to translational kinetic energy and vice-versa. The essential requirements in the development are that:

1. Energy is conserved, following the first law of thermodynamics.
2. The number of assemblies is constant.
3. There exists definite energy levels (second law of thermodynamics).
4. All possible energy levels (or quantum states) for the entire system have equal probability.

Since there is a given probability that any molecule or assembly shall have a free energy in any quantum state which is a function of the entropy of the assembly, the total probability of the occurrence of an assembly with given entropy is proportional to the sum of all the energy terms for the assembly. The sum is called the partition function of the assembly for a given volume of matter. The partition function may include energy terms for nuclear, electrical, vibrational, rotational, and translational energy.

In evaluating the reaction rate of an assembly we are concerned about the velocity at which an activated assembly travels over the potential energy barrier (Figure 2)[9] thus passing from one equilibrium state to another. The magnitude of the energy barrier is equal to the work or thermal energy which must be applied to the assembly in order to activate it. The assembly is considered to be activated when it is at the level of energy equal to the energy barrier level. The net rate at which the reaction occurs is determined by the average velocity of the activated assemblies passing over the top of the barrier.

Eyring et al. have evaluated the partition functions involved in the thermodynamics of reaction rates to develop an equation for the specific reaction rate. The specific reaction rate defines the frequency, v, with which an activated assembly crosses the barrier and is displaced a distance Δ (Figure 2) from one equilibrium position to another.

$$v = \frac{kT}{h} e^{-E_o/kT} \tag{3}$$

in which:

T = absolute temperature

k = Boltzmann's constant

h = Planck's constant

E_o = the free energy of activation; for a rheological assembly it is defined by $E_o = V - T \cdot S$ where V is the total energy of the assembly and S is the entropy (a measure of the disorder of the assembly) accompanying the activation process.

In the presence of an applied stress the energy barrier is modified (Figure 2). The effect of the stress is to reduce the height of the

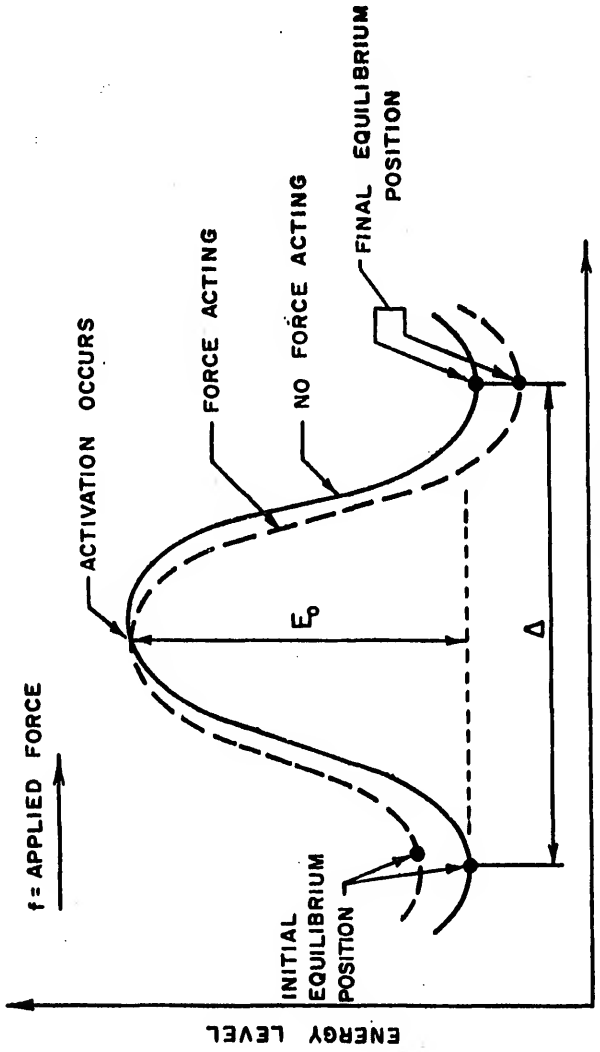

POTENTIAL ENERGY BARRIER OPPOSING MOVEMENT OF FLOW ASSEMBLIES TO NEW EQUILIBRIUM POSITIONS

FIGURE 2

energy barrier in the direction of the stress thereby permitting a flow assembly with given free energy level to pass freely over the barrier. Since there exists an equal probability for the existence of all free energy levels, a greater stress will result in activation of a greater portion of the population of flow assemblies.

If the potential energy surface is considered symmetrical, then the energy level required for flow opposite to the applied stress is increased an amount equal to the decrease in the energy level in the direction of the applied stress. That is, activation occurs midway between equilibrium positions.

The passage of an activated assembly over the potential energy barrier represents the jump of the assembly from one equilibrium position to the next. Let Δ be the distance between two equilibrium positions. The applied force acting on an assembly is f/D^2 where D is a structure factor which is equal to the number of flow assemblies per unit length and f is the applied stress. Hence, the energy that the assembly acquires in advancing to the activated state is

$$\Delta f/D^2 \times 1/2 \quad , \text{ that is, } 1/2\ f\Delta\ /D^2.$$

A creep condition may be analyzed by evaluating the coefficients for the specific reaction rate of the concrete specimen loaded under sustained stress. The frequency of activation for movement of the flow assemblies in the direction of the stress, that is, for flow in the forward direction, is

$$v_f = \frac{kT}{h} \exp\left[\frac{-\left(E_o - \frac{f\Delta}{2D^2}\right)}{kT}\right] \qquad (3a)$$

and the frequency for movement opposed to the stress, that is, for flow in the backwards direction, is

$$v_b = \frac{kT}{h} \exp \left[\frac{-(E_o + \frac{f\,\Delta}{2D^2})}{kT} \right] . \qquad (3b)$$

The net frequency of movement of the flow assemblies combining motions in the forward and backward directions becomes

$$v_f - v_b = 2\,\frac{kT}{h} \exp \left[\frac{-E_o}{kT} \right] \sinh \left(\frac{f\,\Delta}{2kTD^2} \right) . \qquad (3c)$$

The creep rate may now be related to the frequency of movement of flow assemblies. Let

L = the axial component of displacement due to the movement of an assembly to a new equilibrium position, and recall that

D = a structure factor which is equal to the number of flow assemblies per unit length.

The creep rate is

$$\dot{\epsilon} = DL\,(v_f - v_b)$$

or

$$\dot{\epsilon} = 2\,DL\,\frac{kT}{h} \exp \left[\frac{-E_o}{kT} \right] \sinh \left(\frac{f\,\Delta}{2kTD^2} \right) \qquad (4)$$

which may be written[10]

$$\dot{\epsilon} = A \sinh B f . \qquad (4a)$$

The coefficients, A and B are evaluated based on the findings of the rheological investigation of the parametric equations obtained from

the observed responses. Using the simple viscoelastic model of Figure 1 described in Chapter III with the rate process solution, the data may be further evaluated for a better understanding of the creep behavior.

The rate process equation (4a) relates creep rate to stress. The viscoelastic equation (2) for the simple rheological model of Figure 1 related creep to time for a given sustained stress. The two applications are therefore complementary and may facilitate separation of influences on creep due to aging and stress variations.

CHAPTER V

EXPERIMENTAL PROCEDURE

A. Description of the Test

It is generally considered that creep and shrinkage are intimately related. Their true interaction, however, is not completely understood. Shrinkage has been defined as the change in length of concrete members without the influence of applied stresses. Creep is defined as the change in length of concrete members under the influence of applied stresses. These definitions provide only a superficial distinction between creep and shrinkage. In fact, differential shrinkage in concrete is known to result in stress gradients causing compressive stresses in the interior of the concrete.[21] Therefore any contribution to the shortening of the member by these stresses should be classified as creep according to the definition. On the other hand, moisture forced to the vicinity of the surface of a creep specimen by applied stresses may be removed from the specimen by the same phenomena that cause shrinkage. In spite of this awareness, it is traditional to separate the two effects, shrinkage and creep, according to the definitions presented above. This separation is desirable in this investigation since the basic theories being employed are contingent upon a knowledge of the applied forces. Consequently creep strains in this investigation were obtained by subtraction of shrinkage strains obtained from unstressed specimens, from the total strains obtained from creep specimens.

The purpose of this investigation, concerning the comparative creep behavior of a typical Florida limestone aggregate concrete and a Florida lightweight aggregate concrete (Florida Solite - an expanded clay product) was to determine some structurally important aspects of the mechanism of creep in concrete. Three test series investigated creep. Series A investigated creep under sustained stress. Test series B and C investigated creep under different decreasing stress situations. A fourth test series investigated shrinkage.

Shrinkage of the test specimens is illustrated in Figures 12, 13, and 14. Total strains for creep series A are illustrated in Figures 15, 16, and 17. Both sets of strain data display seasonal influences beyond the initial stage of their responses. Shrinkage and creep specimens were maintained in the laboratory environment where periodic ambient readings were recorded of humidity (Figure 6) and temperature (Figure 7).

B. Materials

In an attempt to minimize effects from mix variations, strength, variations and environment variations between pours, a single pour was made for each concrete type. Table I contains proportions for the two mixes used. Equal paste contents as nearly as could be determined were selected to minimize the effects of a difference between the concrete gels influencing creep. As a result of the desire to obtain near equal strength for the two concrete types, the water contents were selected to compensate for the aggregate influence on strength. Figure 3 illustrates the concrete strength gain for both concretes. Each point represents the average of four 6 x 12 inch test cylinders.

TABLE I

MIX PROPORTIONS PER CUBIC YARD OF CONCRETE

All Specimens

Conventional Limestone Concrete		Lightweight (Solite) Concrete	
Cement - (Type III, Hi-Early):	6.73 sacks	Cement - (Type III, Hi-Early):	8.7 sacks
Sand - (Interlachen, FM = 2.42):	1220 #	Sand - (Interlachen, FM = 2.42):	1213 #
Stone - (3/4" Brooksville Limestone):	1755 #	Stone - (3/4" Florida Solite):	1080 # (23.9% moisture)
Water - 36.6 gallons:	303 #	Water - 27.9 gallons:	232 #
Weight per cubic foot:	145 #/c.f.	Weight per cubic foot:	123 #/c.f.
Slump:	5 "	Slump:	2 1/2"
W/C Ratio by Weight:	.477	W/C Ratio by Weight:	.284
Paste Content:	80 #/c.f.	Paste Content:	83 #/c.f.

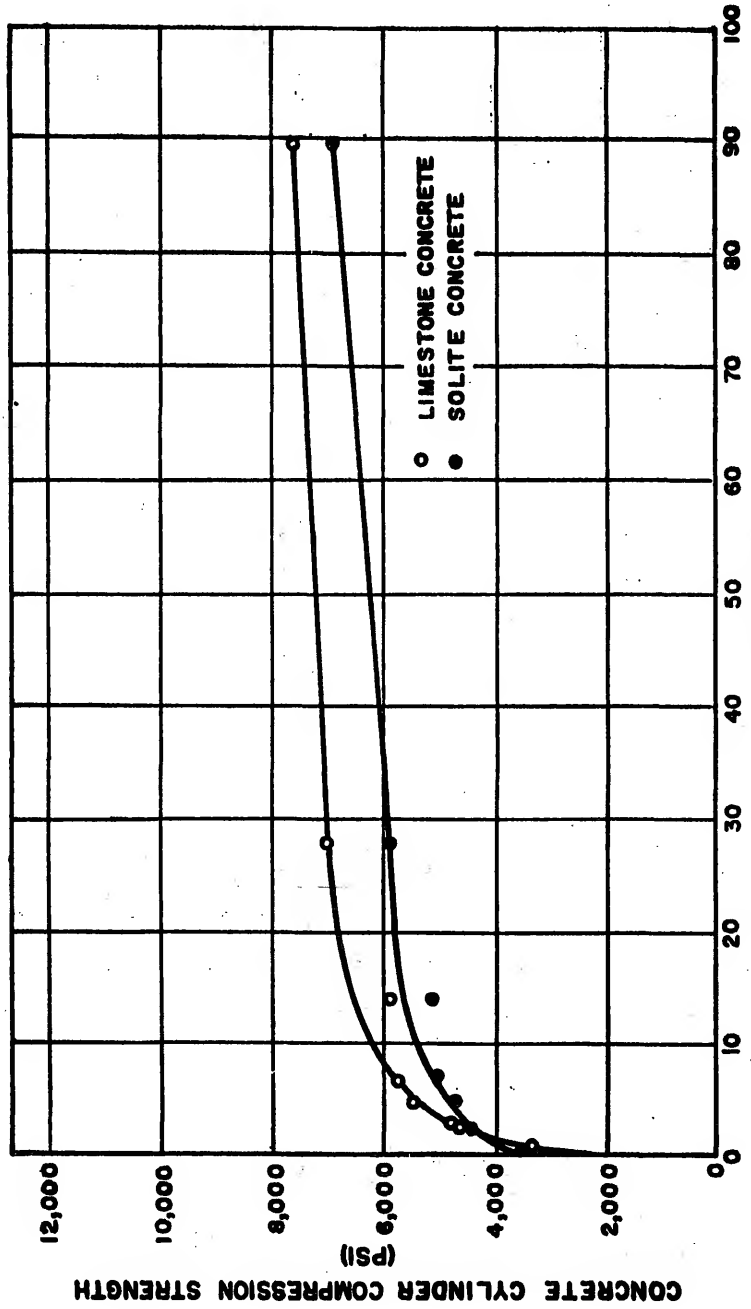

STRENGTH GAIN FOR STANDARD MOIST CURED CONCRETE

FIGURE 3

— The concrete used in the specimen contained type III, high early strength cement as would be used in most prestressed concrete bridge construction. The coarse aggregates had maximum sizes of 3/4". The fine aggregate used in all specimens was Interlachen sand normally used for construction in the north Florida area.

C. Description of Specimens

Special shapes were selected to test an hypothesis about the shape factor effect on the rate of creep. Three shapes with identical cross-sectional areas equal to 28.27 square inches but with unlike perimeters were cast. The specimens obtained contained equal volumes but varying volume-to-surface area ratios (Table II). The shapes selected, which had cross, rectangular, and circular cross-sections, are shown in Figure 4. The selection of equal volumes was made in order to evaluate shape effect by blocking out size effect.

The flow path from any point at the interior of the specimen to the surface is measured by the average weighted distance over which a particle of moisture must travel before reaching the surface of the specimen. The average weighted distances for the specimen may be calculated by summing the products of the incremental areas of the specimen cross-section and the least distance from these incremental areas to the surface of the specimen, and dividing the sum by the area of the specimen. The average weighted distances are given in Table II for each shape of specimen. Although perimeter-to-cross-section area ratio is frequently used as a measure of shape effect[16] it is convenient and perhaps more accurate to use the weighted distance as the significant measure of shape effect.

TABLE II

TEST CONDITIONS

Test Series	Shape	Coarse Aggregate Type	Cross-sectional Area to Perimeter Ratio	Average Length of Flow Path	Initial Stress (psi)	Concrete Strength at Stressing (psi)	Age at Stressing (days)	Stress Character
A (control)	Cylinder	Limestone	1.49	1.00	914	4700	3	Sustained
		Solite	1.49	1.00	914	4600	3	
	Rectangle	Limestone	1.23	0.77	914	4700	3	
		Solite	1.23	0.77	914	4600	3	
	Cross	Limestone	0.99	0.55	914	4700	3	
		Solite	0.99	0.55	914	4600	3	
B	Cylinder	Limestone	1.49	1.00	914	4700	3	Decreasing
		Solite	1.49	1.00	914	4600	3	
	Rectangle	Limestone	1.23	0.77	914	4700	3	
		Solite	1.23	0.77	914	4600	3	
	Cross	Limestone	0.99	0.55	914	4700	3	
		Solite	0.99	0.55	914	4600	3	
C	Cylinder	Limestone	1.49	1.00	904	5700	7	Decreasing
		Solite	1.49	1.00	904	5200	7	
	Rectangle	Limestone	1.23	0.77	904	5700	7	
		Solite	1.23	0.77	904	5200	7	
	Cross	Limestone	0.99	0.55	904	5700	7	
		Solite	0.99	0.55	904	5200	7	

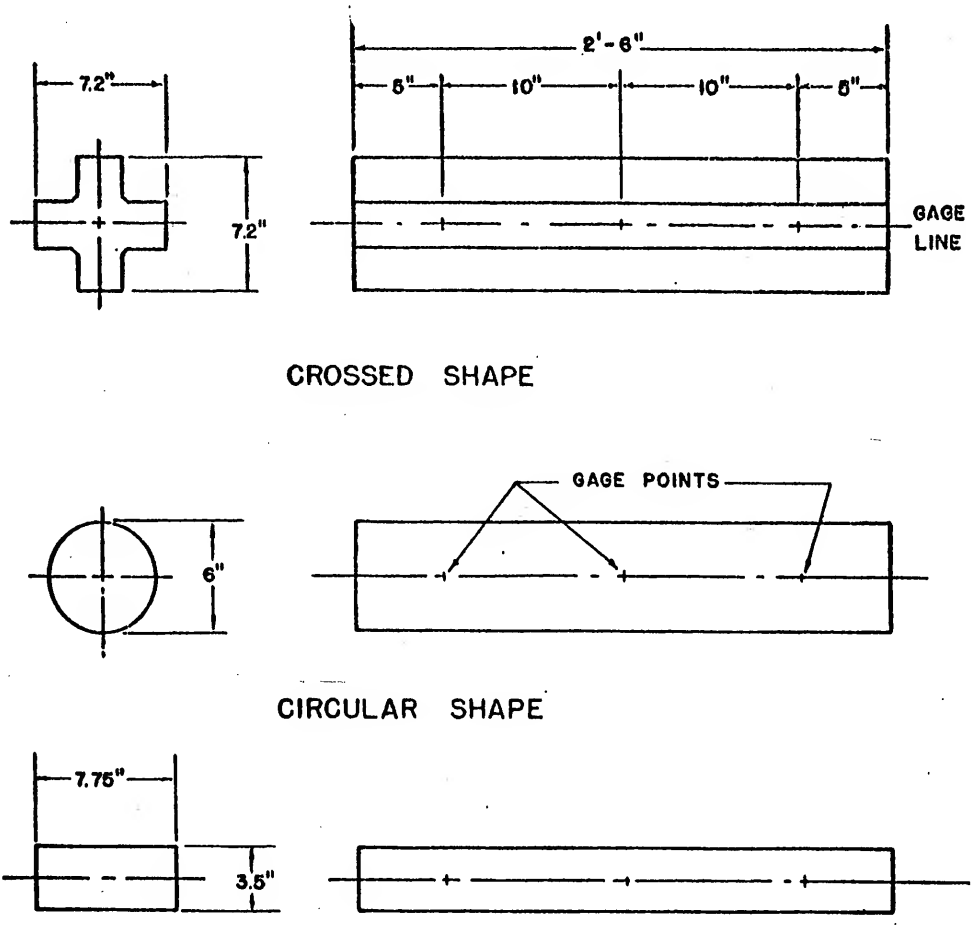

SHRINKAGE AND CREEP SPECIMEN

FIGURE 4

When this substitution is made, it becomes immediately evident that shape and size effects interact since length of flow path is the primary variable governing their influences on creep. In this regard the specimen behavior in this investigation may be considered to give some indication of size effect even though the investigation seemingly blocks out size effects.

All specimens were thirty inches long. This provided space for two gage lengths of ten inches over which measurements were made plus six inches on each end. The six specimens comprising a creep test series were strung together end to end with a transition plate between each specimen. The ends of all specimens were capped with standard capping compound consisting of flyash and sulfur. Each specimen was cast with a metal conduit along its axis through which the stress rod was placed for loading of the specimen. A ten inch concrete bearing clock and steel plate were used at the ends of the strung specimens to accept and distribute the applied test load.

Shrinkage specimens were made identical to creep specimens. Their end faces were sealed with a layer of wax and metal foil which resulted in having their exposed surface identical to the exposed surface of the creep specimens.

Shrinkage strains were taken on individual unstressed specimens. Creep stains were taken on specimens under identical stress conditions in each test series. One specimen of each shape for each of the two concrete types was used in each creep test series as shown in Figure 5. Table II summarizes the test conditions for each specimen. Specimens in test series A were maintained under constant sustained stress of 914 ± 10 psi.

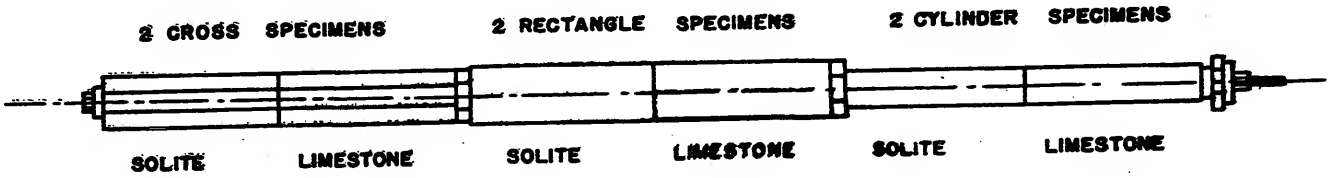

PLAN

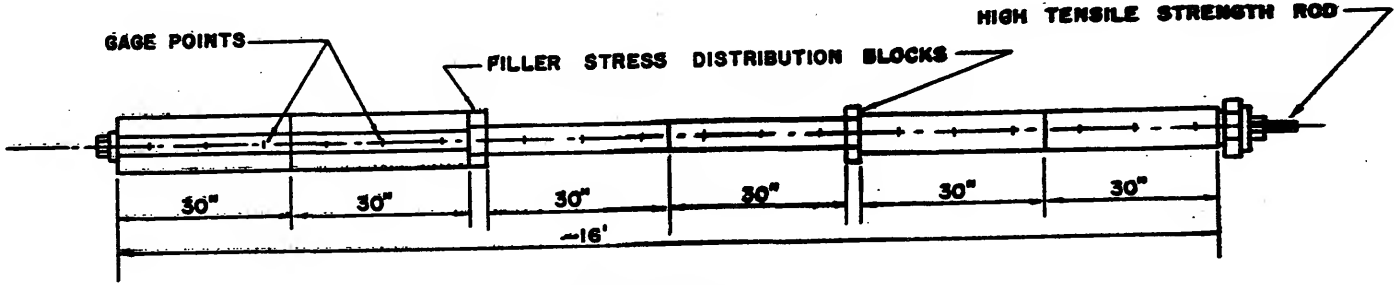

ELEVATION

DIAGRAM OF CREEP SPECIMEN UNDER STRESS

FIGURE 5

Stresses in specimen for test series B and C were permitted to decrease as shown in Figure 8. The decrease in stress associated with series C resulted from normal prestress loss due to creep and shrinkage. Test series B contained filler blocks of concrete and high strength plaster between the specimens which permitted a greater initial stress decay.

D. Instrumentation

All specimen were instrumented with standard Whittemore gage points spaced at ten inches as indicated in Figures 4 and 5. Shrinkage and creep specimens were maintained in laboratory environment where periodic concrete strain readings were recorded along with ambient readings of humidity (Figure 6) and temperature (Figure 7). Strain adjustments were made for temperature variation by assuming a thermal coefficient of 0.0000055 inches per inch per degree Fahrenheit. However, no adjustments were made for humidity variations because there is no way of determining the integration effects of humidity on concrete behavior.

Load readings on the creep specimen were obtained from SR-4 strain gages on the stress rods. Loads were applied with hydraulic jacks.

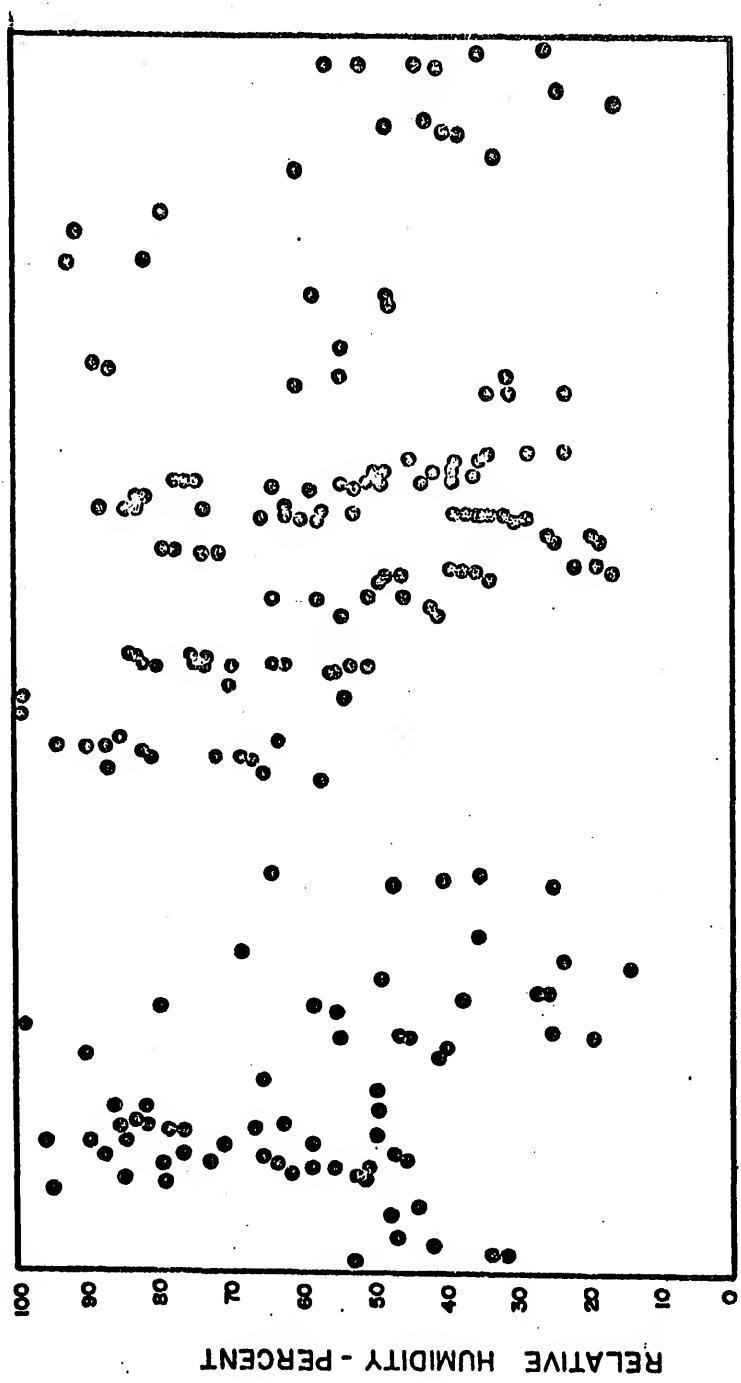

HISTORY OF RELATIVE HUMIDITY IN LABORATORY

FIGURE 6

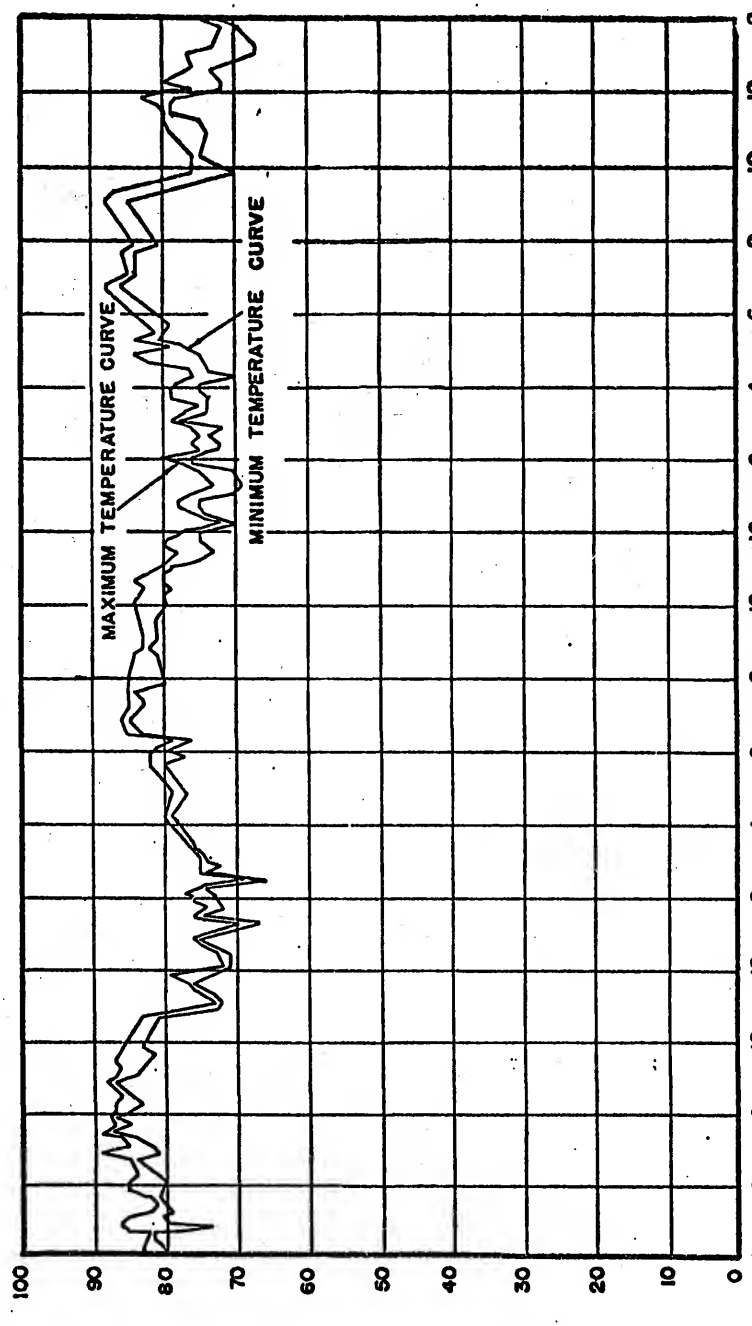

HISTORY OF AMBIENT TEMPERATURE IN LABORATORY

FIGURE 7

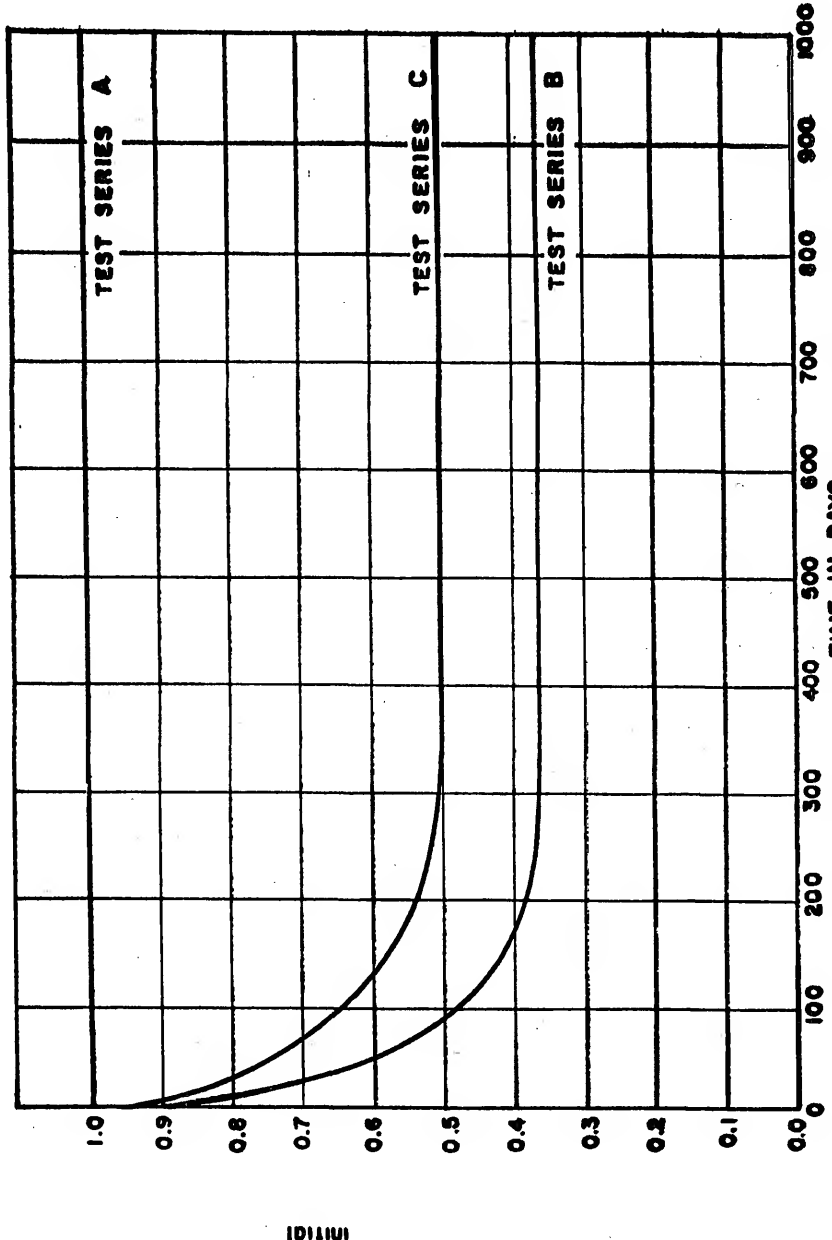

STRESS HISTORY OF CONCRETE SPECIMEN

FIGURE 8

CHAPTER VI

DEVELOPMENT OF A MODEL FOR THE CREEP MECHANISM

A. Separation of Creep Components

There are two fundamental types of viscoelastic creep:

1. Delayed elasticity -- a completely recoverable strain phenomenon.
2. Viscous creep -- an irrecoverable strain which may contain transient and steady state components.

Creep has been associated with rearrangement of molecules due to thermal movement. According to quantum theory, the movement must result in a different and stable equilibrium configuration of molecules. Since fluids contain many vacant sites in their molecular structure, large voids (holes) exist into which the migrating molecules may relocate. Any motion of one molecular assembly may, of course, result in relocation of neighboring assemblies. The rearrangement of these assemblies is always in the general direction of the applied stress but, the motion may have components in any direction thereby resulting in shear distortion. These shear distortions are viewed as macroscopic creep. When the applied stress is removed some of these migrated assemblies return to their initial equilibrium states. The resulting strain recovery is viewed as delayed elasticity. It is necessary to separate the two fundamental types of creep, the irrecoverable from the recoverable creep, in the development of the model for a creep mechanism because under decreasing stresses the elastically recoverable component will be active.

(a) Elastic Creep

Elastic creep has been described by Orowan[8] as resulting from an applied stress which alters the statistical equilibrium position for each assembly. A time dependent strain results which continues as the assemblies seek new equilibrium positions within their stressed configuration. If the force is suddenly removed, the instantaneous elastic response returns the molecular structure to its former equilibrium configuration. The assemblies now seek their original equilibrium positions and recoverable strains are observed. It is tacitly assumed that no deterioration or damage occurs to the molecular structure during the load cycle and no additional thermal energy sources are introduced into the system. The strain recovery will therefore be complete by definition of elasticity.

(b) Viscous Creep

During the transition period, while fluidity characterizes the nature of the gel matrix, the flow assemblies are more mobile. The crystalline structure is not sufficiently rigid to behave completely elastically and therefore, once it has moved to a new equilibrium position the flow unit is completely stable in this position. Upon removal of the load there is no tendency for the flow unit to return to its original position.

B. The Generalized Model for the Creep Mechanism

The development of a model which is to represent the creep behavior of concrete must contain the two elements, delayed elasticity and viscous creep.[14] The basic strain equation must then be of the form

$$\epsilon = \frac{f}{E} + q\,(f, t)_{vis.} + q\,(f, t)_{el.} \quad , \tag{5}$$

where the terms represent the elastic strain, the viscous component of creep, and the elastic component of creep respectively.

Since the last term has an elastic nature, a Kelvin element should be sufficient to represent this component. In its simplest form the term may have constant coefficients to represent average effects of delayed elasticity in the concrete. It represents the basic elastic structure of the gel.

The second term contains all phenomena which result in permanent changes in the rheological structure. Such phenomena are for example:

1. Hydration effects.
2. Irrecoverable strain effects resulting from structural deterioration due to stress.
3. Viscous flow.

Each of the two creep terms in the model must contain coefficients which relate the structural changes of the concrete due to the various influences to the two major variables, aging and stress. The objective is to establish coefficients which include as many influencing factors as possible so as to make the model applicable in a greater number of situations. For example, if it would be possible to incorporate such factors as size and shape, environment conditions, mix proportions, and physical characteristics of the mix ingredients into the model, then the enigma of creep behavior would truly be considered resolved. It should be emphasized at this point that this study will not attempt to develop such a general form of the model for the creep mechanism. It is hoped, however, that the ground work will be adequately accomplished toward such a development. Obviously to achieve such a result will involve a study of much greater depth and scope than this investigation encompasses.

Equation (5) may be revised to include the delayed elastic component referred to and is therefore written in the form:

$$\epsilon = \frac{f}{E} + \phi\,(f,\, t)\, ft + \frac{f}{E_e}\,(1 + e^{-\phi_e E_e t}) \quad . \tag{5a}$$

(a) Coefficients of Structural Stability

Reiner[3] has introduced a coefficient (X) called "The Coefficient of Structural Stability" which relates viscosity, or more accurately its reciprocal, fluidity, to stress. The scope of this coefficient may be broadened to include structural variations in fluidity due to aging also. As described in Appendix B let

$$X = (\phi - \phi_\infty) \Big/ - \frac{\partial^2 \phi}{\partial (f^2/4)\, \partial (t)} \qquad (6)$$

where ϕ represents the fluidity at any time,

ϕ_∞ represents the ultimate fluidity,

f is the normal stress.

The partial derivatives are taken with respect to stress squared (f^2) and time (t). Reiner has shown that fluidity is influenced by the square of the shear stress ($f^2/4$). The negative sign is required because an increase in time results in a decrease in fluidity.

In order to understand the Structural Stability Coefficient consider the extreme cases of $X = 0$ and $X = \infty$. When $X = 0$, $\phi = \phi_\infty$ which means that the viscosity of the material is at its steady state value. The material is fully aged and, under applied stress, it strains at constant rate. When $X = \infty$, the partial derivatives of fluidity with respect to time and stress are equal to zero. This implies that the viscosity of the material is not changed due to applied stress or due to aging. This latter case is obviously not possible with concrete since aging, through hydration, will always produce some finite value for the change in viscosity with time. Therefore the smaller values for the structural stability coefficient, X, indicate greater structural stability of the material. The material is less subject to creep, since ϕ is smaller because of aging or stress influences.

Either factor, stress or aging, may have a greater influence or a lesser influence on structural changes. It is therefore necessary to separate the aging and stress components of the coefficient of structural stability. Accordingly components for aging, c_t, and stress change, c_f, have been developed in Appendix B.

It can be shown (Appendix B) that the coefficient of structural stability will influence the fluidity in the following way:

$$\phi = \phi_\infty + (\phi_o - \phi_\infty) \exp \left[- (c_t + c_f (f_o^2 - f^2)) \right] , \qquad (7)$$

where

ϕ_∞ = steady state or ultimate fluidity

ϕ_o = initial fluidity

f_o = initial stress

f = stress at any time (t)

The coefficient of structural stability contains two components:

1. c_f represents the extent of influence of stress change on the structural stability.

2. c_t is independent of stress change and represents the natural influences, such as hydration, on the structural stability.

Substituting equation (7) into equation (5a), the strain may now be written

$$\epsilon = \frac{f}{E} + \left[\phi_\infty + (\phi_o - \phi_\infty) \exp (- (c_t + c_f (f_o^2 - f^2))) \right] ft + \frac{f}{E_e} \left[1 - e^{-\phi_e E_e t} \right] . \qquad (8)$$

This equation represents a general function for creep following the mechanical model of Figure 9. It becomes necessary to evaluate the coefficients an parameters of the second and third elements in Figure 9. The parameters appear

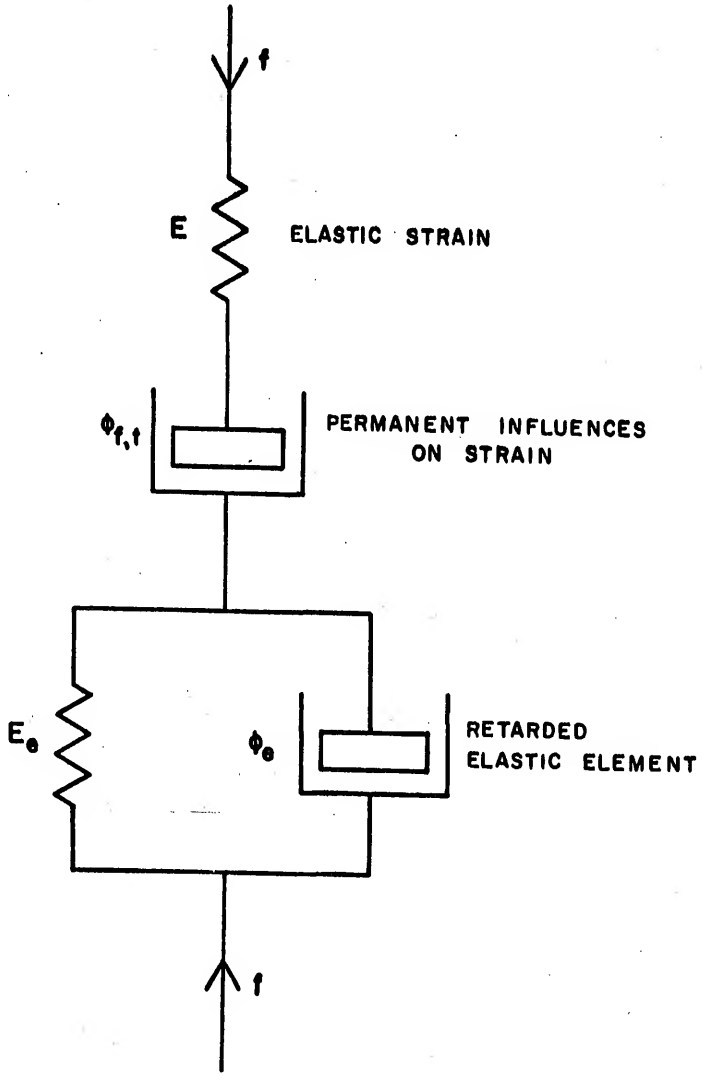

PROPOSED RHEOLOGICAL MODEL TO REPRESENT CREEP IN CONCRETE

FIGURE 9

in the form of fluidity ϕ and elasticity E in equation (8). The coefficients are c_t and c_f.

(b) The Rheological Parameters in the Creep Equation

The proposed model contains structural coefficients and rheological parameters. Define creep compliance as creep per unit stress. Employing the linear viscoelastic model for creep (Figure 1), the creep compliance for each specimen under sustained stress is obtained and the rheological parameters evaluated. Table III presents the parameters for equation (2) and the linear viscoelastic model. The resulting creep compliance ($c\epsilon$) is

$$c\epsilon = \frac{t}{\lambda_\infty} + \sum_{n=1}^{3} \frac{1}{E_n}\left(1 - e^{-\phi_n E_n t}\right) \qquad (9)$$

The first term in the creep compliance, containing the steady state (ultimate) viscosity of the concrete may be used directly to obtain the ultimate fluidity (ϕ_∞) required for equation (7).

$$\phi_\infty = \frac{1}{\lambda_\infty} \qquad (10)$$

The remaining Kelvin elements form the basis for determination of the remaining parameters in equation (8). Since there will be several (usually three are sufficient) Kelvin elements in the creep compliance, it is reasonable to assume that one of these elements may be used as the single linear element comprising the elastic term of equation (8). It may not be obvious, however, which element represents the delayed elastic component. Therefore all Kelvin terms should be investigated by the rate process theory.

Initial fluidity (ϕ_o) may be determined when it is known which rheological elements contribute to the inelastic portion of the creep.

TABLE III

COEFFICIENTS FOR THE LINEAR VISCOELASTIC MODEL OF FIGURE 1

Data From the Control Specimen, Series A

	Lightweight (Solite) Concrete			Limestone Concrete		
	Circle	Rectangle	Cross	Circle	Rectangle	Cross
Stress f psi	914	914	914	914	914	914
Initial Strain ϵ_i (10^{-6}) in/in	361	341	329	196	179	191
Final Strain Rate $\dot{\epsilon}$ (10^{-6}) in/in/day	.02830	.04362	.06336	.01483	.02905	.03499
E (10^6) psi	2.533	2.682	2.779	4.665	5.108	4.787
E_1 (10^6) psi	5.071	3.581	2.683	9.022	4.905	4.105
E_2 (10^6) psi	3.809	3.438	3.284	5.321	3.609	3.091
E_3 (10^6) psi	7.160	11.612	20.275	5.394	6.491	5.843
$\lambda_\infty(10^6)$ psi day	32,311.	20,961.	14,431.	61,679.	31,474.	26,134.
$\lambda_1(10^6)$ psi day	1005.4	726.86	557.36	1763.2	970.68	814.09
$\lambda_2(10^6)$ psi day	218.85	203.16	198.98	303.04	206.80	177.64
$\lambda_3(10^6)$ psi day	148.54	249.49	447.07	111.27	134.50	121.29

That is, after it has been determined which rheological element will be used to represent the delayed elastic component, the remaining Kelvin terms of the creep compliance will be used to determine ϕ_o. The strain rate function for two or more Kelvin elements may be obtained from the creep compliance by differentiating with respect to time, thus for Kelvin elements 1 and 3

$$c\epsilon = \frac{1}{E_1}(1 - e^{-\phi_1 E_1 t}) + \frac{1}{E_3}(1 - e^{-\phi_3 E_3 t}) \tag{9a}$$

$$c\dot{\epsilon} = \phi_1 e^{-\phi_1 E_1 t} + \phi_3 e^{-\phi_3 E_3 t}. \tag{9b}$$

At $t = 0$, $c\dot{\epsilon}_o = \phi_o$, by definition, therefore

$$\phi_o = (\phi_1 + \phi_3). \tag{11}$$

C. The Analysis of Rheological Assemblies from a Statistical Mechanics Viewpoint

In the previous section it was proposed that a rate process study of each Kelvin element in the creep compliance be made. Such a study will provide an insight into the stress dependent nature of each element considered as a rheological assembly. Each assembly contains the characteristics of a molecular structure having energy levels representing the bonds between similar assemblies and spacings between equilibrium positions of the assemblies which regulate the rate at which activation occurs. The rate process equations presented in Chapter IV are therefore applicable for this rheological structure.

For the elastic condition there is expected a uniform statistical spacing between equilibrium positions (Figure 2). This assumption is based on the premise that for any concrete the molecular structure is randomly oriented and elasticity implies a certain rigidity of the crystalline structure, therefore the material would be expected to exhibit uniform elastic

behavior throughout the specimen. By the same argument the free energy of activation should also be uniform throughout the specimen. In cases where no specimen variation is introduced to form comparisons, such as was done in this experiment with regard to shape, it may be difficult to separate the elastically retarded element from the other elements. In some cases it may be assumed that the intermediate activation energy is related to the elastic element. This may not always be true, however, where severe elastic deterioration is present. In general, however, elastic deterioration will require the largest energies and viscous flow will require the smallest energies of activation leaving intermediate levels of activation energy for assignment to elastic characteristics.

The analysis of the Kelvin elements employing the statistical mechanics approach is derived generally from Herrin's work[9] and Majidzadeh's work[10] with asphalts. The application of statistical mechanics to portland cement concretes is straight forward. The rheological equation for the Kelvin elements is known. For each element the strain is

$$\epsilon = \frac{f}{E_n} (1 - e^{-\phi_n E_n t}) \quad . \tag{12}$$

It is required to obtain an expression of the element behavior in terms of the rate theory. According to the rate theory the strain rate, $\dot{\epsilon}$, is a function of stress.

$$\dot{\epsilon} = A \sinh B f_D \, , \tag{13}$$

where f_D is the decaying stress resulting from activation of rheological assemblies into new equilibrium positions. For each Kelvin element we have

$$f = f_S + f_D \tag{14}$$

and

$$\epsilon = \epsilon_S = \epsilon_D \quad . \tag{15}$$

The total stress and strain for an element is f and ϵ respectively. The subscripts S and D refer to the spring and dashpot components of each Kelvin element. From equations (14) and (15) we may obtain

$$f_D = f - \epsilon E_n \quad . \tag{16}$$

Differentiating the strain with respect to time for the Kelvin elements represented by equation (12) yields

$$\dot{\epsilon} = \phi_n f e^{-\phi_n E_n t} \quad . \tag{17}$$

Using calculated values from equations (16) and (17), equation (13) may now be solved by simultaneous application of least squares and successive approximations for the coefficients A and B. Herrin[9] has prepared a computer program for this solution which was employed in this investigation.

In evaluating these data it was considered that the Kelvin elements represented four distinct effects of the creep behavior:

1. an elastic response
2. a viscous response
3. a deterioration or separation of elastic bonds
4. a structural growth of strength and viscosity due to hydration and aging.

Since these responses represent behavior of the entire concrete mass rather than responses of the separate phases comprising the concrete, it may be assumed that the free energy of activation and the equilibrium spacing are uniform for each rheological assembly (representing each Kelvin element) which is taken as the basic assembly or flow unit in the rate process.

Table IV contains the computed values for the coefficients in the rate function for each type of rheological assembly in the specimen under sustained stress. The method used to determine these coefficients is described and illustrated in Appendix C. Some immediate relationships are evident, and are described in the following.

(a) Spacing of Equilibrium States

Within each concrete type the spacings between states of equilibrium are relatively independent of shape for each rheological assembly.

Furthermore in this investigation, it appears that these spacings are also independent of type of concrete. Since only the coarse aggregate type and water-cement (w/c) ratio differed between these two concretes it seems that aggregate and w/c ratio would have a compensating influence on the spacing of equilibrium states. A small influence is evident for rheological assembly number one, which represents the long term deterioration effects, wherein the less dense structure of the lightweight aggregate yields a slightly greater spacing than in the denser limestone concrete. In like manner, rheological assembly number three, representing short term viscous action, indicates slightly greater spacing for the limestone concrete which may be attributed to the greater w/c ratio in the limestone concrete.

The effects of these two factors, w/c ratio and aggregate strength, also compensated each other from a structural standpoint to yield nearly equal concrete strengths which has been considered by some authors to be an important factor in creep.[12] The major factor in determining the equilibrium spacing of rheological assemblies appears to be related to the concrete structure as measured physically by strength but it appears that

TABLE IV

COMPUTED STRUCTURE COEFFICIENTS IN THE RATE FUNCTION

For Control Specimen (Series A)

Concrete Type	Shape	Rheological Assembly (Corresponds to Kelvin elements)	Computed Structure Coefficients for = A sinh Bf at 1000 days A $x10^{-6}$/day	B $x10^{-3}$/psi	Computed Structure Coefficients at 20 days A $x10^{-6}$/day	B $x10^{-3}$/psi
Limestone Concrete	Circle	1	2.4×10^{-6}	$.23 \times 10^{-3}$	4.7×10^{-6}	$.12 \times 10^{-3}$
		2	23.0	.18	34.0	.14
		3	95.0	.090	100.6	.087
	Rectangle	1	4.4	.23	8.5	.12
		2	25.6	.18	36.9	.13
		3	82.5	.090	85.0	.087
	Cross	1	5.2	.23	10.1	.12
		2	28.0	.18	40.9	.14
		3	97.6	.084	94.4	.087
Lightweight (Solite) Concrete	Circle	1	4.2	.23	8.2	.12
		2	25.1	.18	34.0	.14
		3	79.1	.084	61.6	.109
	Rectangle	1	5.7	.24	11.4	.12
		2	27.3	.18	36.8	.14
		3	48.3	.083	37.3	.106
	Cross	1	7.5	.24	14.8	.12
		2	28.0	.18	36.9	.14
		3	25.6	.087	21.0	.106

the most important factor governing strength is related to the thermodynamic bonds between rheological assemblies in the mix.

(b) Free Energy of Activation

The most significant influence on the physical behavior of the concrete is the level of free energy of activation (height of the potential energy barrier) for each rheological assembly. This level determines the extent of the thermodynamic bonds and the frequency of activation for the contribution to creep from each rheological assembly. It can be expected that deterioration effects resulting from permanent separation of elastic bonds will require most energy and that viscous flow would require least energy for activation.

1. The second rheological assembly.

The second rheological assembly representing elastic behavior is only slightly influenced by shape as it affects hydration during the first twenty days approximately. After about the first month shape has no effect on the change in the free energy of activation in the limestone aggregate concrete. However shape appears to have a slight influence on the change in free energy of activation in the lightweight concrete (refer to Table V). The slightly larger average value of the coefficient A from Table IV for the lightweight concrete is indicative of a slightly greater elastic contribution than for the normal concrete. Therefore, a greater delayed elastic recovery may be expected from the lightweight concrete than from the limestone concrete. In Section D elastic recovery is calculated for the specimens in test series A. The lightweight specimen display a greater recovery than the limestone concrete specimen.

TABLE V

CHANGE IN RATE FUNCTION STRUCTURE COEFFICIENTS

For Control Specimen (Series A)
Between 20 days and 1000 days

Concrete Type	Rheological Assembly Number	Specimen Shape	Change From 20 day to 1000 day values		% Change	
			A	B	A	B
Limestone Concrete	1	Circle	-2.3	+.11	-49.	+92.
		Rectangle	-4.1	+.11	-48.	+92.
		Cross	-4.9	+.11	-49.	+92.
	2	Circle	-11	+.04	-33.	+29.
		Rectangle	-11.3	+.05	-31.	+38.
		Cross	-12.9	+.04	-32.	+29.
	3	Circle	-5.6	+.003	-1.	+3.
		Rectangle	-2.5	+.003	-3.	+3.
		Cross	+3.2	-.003	+3.	-3.
Lightweight (Solite) Concrete	1	Circle	-4.0	+.11	-49.	+92.
		Rectangle	-5.7	+.12	-50.	+100.
		Cross	-7.3	+.12	-49.	+100.
	2	Circle	-9	+.04	-27.	+29.
		Rectangle	-9.5	+.04	-26.	+29.
		Cross	-8.9	+.04	-24.	+29.
	3	Circle	+17.5	-.025	+28.	-23.
		Rectangle	+11.0	-.023	+30.	-22.
		Cross	+4.6	-.02	+22.	-18.

For the second rheological assembly, representing elastic behavior of the concrete, the results of the statistical mechanics approach shown in Tables IV and V indicate the nature of the stability of the elastic structure. In the limestone concrete the first twenty days produce an energy level which is influenced by shape. However, following the first twenty days shape has no apparent influence on the increase in energy as seen from Table V. These effects appear to be related to the shrinkage characteristics of the concrete specimen.

In the lightweight concrete the influence of shape extended beyond the first twenty days. This effect was probably caused by the moisture contribution from the coarse aggregate to continued hydration. In spite of this continuing supply of water in the lightweight aggregate concrete and a greater quantity of cement, the lightweight concrete was apparently deficient in moisture to achieve its potential activation energy level. The limestone concrete gained energy at a greater rate than the lightweight concrete. The limestone concrete also contained a greater amount of water in the mix, though not an excessive amount, from which a greater amount of water was colloidally contained by chemical bond in the gel. It appears, therefore, that the rate of strength gain may be related to the quantity of free mix water in the concrete. That is, even though water may be included in the mix as mechanically contained moisture in the coarse aggregate, only a portion of this water will become chemically activated in the hydration process after the water is released from the aggregate. The remainder, and perhaps the largest portion, will be treated as capillary moisture, ultimately becoming associated with shrinkage characteristics of the concrete in moderate to small size specimens. In large specimens a

greater portion of this moisture originating in the coarse aggregate may become chemically hydrated resulting in strength gain.

If the level of energy for the elastic state of the structure is considered to be directly related to the strength, a study of the difference in energy levels in the two concretes for the circular shaped specimens would be informative. The circular shaped specimens were identical in cross section to the strength test cylinders. The limestone aggregate specimen showed a larger energy by about 10 per cent from Table IV. The limestone aggregate specimen indicated a greater strength by about 12 per cent from strength tests. These results appear to represent reasonably acceptable trends but not enough data are presented to justify any hypothesis relating strength with activation energy level of the selected elastic rheological assembly.

2. The third rheological assembly.

The third rheological assembly represents short time deformation and exhibits a decidedly different behavior for the normal limestone concrete than for the lightweight concrete. In the former, the rate coefficients A are large indicating a small activation energy resulting from the high water-cement ratio leading consequently to greater fluidity. Uniformity of the activation energy levels for each shape means that the fluidity of the system is not influenced by the escape of free capillary water resulting from shrinkage nor is the quantity of water molecules held in chemical bond influenced by the movement of free water as it evacuates the concrete.

On the other hand, the lightweight concrete exhibits a significant influence of shape on activation energy. For greater flow paths the energy required for activation decreases implying greater fluidity. Since it was

seen that free water loss from the cement gel does not influence fluidity or the free energy level, it is evident that moisture discharged from the lightweight aggregate contributes to this variation. Evidently, as moisture is discharged from the coarse lightweight aggregate as free water and moves toward the surface of the concrete, portions of this free water are chemically absorbed along the way. With longer flow paths, greater quantities of water are chemically absorbed, causing greater fluidity to result thereby producing a lower activation energy. This absorption of free water would also be expected to occur in the normal concrete, however, the rate of evacuation of the capillaries is considerably reduced in the lightweight concrete due to the slow emission of water from the aggregate. This retarded moisture activity is evident in the shrinkage curves (Figures 12, 13, and 14). The absorption of water released by the aggregate may also be considered to increase the water-cement ratio for the concrete. The significance of this absorption is evident in Table V from the observed reduction in activation energy by about 30 per cent in the lightweight specimen.

The third rheological assembly is changing during the early life of the structure. As seen from Table V practically no change occurs in the limestone concrete after twenty days. This activity means that a steady state condition is achieved early in so far as creep associated with flow is concerned. Viscous activity is extended in the lightweight concrete due to the reserve moisture supply held in the coarse aggregate.

It appears reasonable to assume that specimens of larger sizes or which are maintained in high humidity environments will exhibit this viscous state through a longer period of time and possibly throughout their life.

Under these conditions the simple Kelvin element from which the rheological assembly is developed may be bifurcated according to a period of true fluidity and a longer period of quasi fluidity. The former state represents the condition between initial pouring of the concrete and setting of the rigid gel structure. The latter state represents fluid action of the elements still in a colloidal state imposed upon the restrictive nature of the gel structure.

3. The first rheological assembly.

The first rheological assembly exhibiting long time strain activity is associated with large values of activation energy which appear to be equally influenced by shape for both concretes. The more rapid evacuation of free moisture from capillaries of the gel in the concrete specimen with greater surface area-to-volume ratios results in a reduction of the required energy of activation due to a reduction in the rate of increase of chemical bonding forces. This effect is directly related to the amount of hydration associated with each shape.

The larger values of the coefficient A for the lightweight concrete represent a lower activation energy which results from weaker bonds and less hydration. Weaker bonds can be attributed to the gel in the lightwaight concrete and to the less dense Solite aggregate. The gel may be contributing to this weakness because of insufficient mix water to hydrate a sufficient quantity of cement to form a strong and rigid gel structure. However, the rate coefficient A also contains a factor L (equation (3c)) related to the displacement resulting from activation of an assembly, which may be considered to be a modifying factor for non uniformity of behavior. Stress concentrations and so-called plastic zones contributing to permanent deformations result from

piling-up of rheological assemblies at internal obstructions that are present within the gel matrix. Such obstructions may be, for example, dense coarse aggregate particles and reinforcement. The conditions under which deformations of this type occur require suitably oriented obstructions in the path of the migrating assemblies with sufficiently greater density and crystalline rigidity to prevent penetration of, or displacement by the migrating assemblies. This piling-up of assemblies results in bridging between hard coarse aggregate particles which transfers the stresses throughout the specimen. In soft aggregate concrete the gel matrix is more uniformly stressed and bridging will not be well developed if it is developed at all. Consequently, the strains resulting from activation in the lightweight concrete are greater than in normal concrete where assemblies which have created fully developed bridging prevent large deformation when activation occurs in regions between the bridges.

For each of the assemblies discussed it must be remembered that hydration will influence the level of energy of activation and perhaps the equilibrium spacing also. Hydration will change the properties of flow units and adjust free energy levels causing formation of bonds thereby affecting the potential energy barrier with time. Table IV contains coefficients A and B in the rate function for the first twenty days only. These values may be compared with corresponding final values at 1000 days from Table IV for an illustration of the influence of energy changes beyond the first twenty days on creep rates. When little change occurs in the level of activation energy for a rheological element the steady state condition is said to exist for that element. Achievement of a steady state condition does not preclude further variations, however, if conditions in the concrete

structure are changed so as to cause a variation in the quantum energy level. For example, the lightweight concrete experienced changes in energy due to a moisture transfer from the coarse aggregate to the gel. In this case the increase in fluidity can be ascribed to the discharge of free internal moisture from the Solite aggregate. If the moisture had not been discharged into the gel, a steady state condition would have been expected to occur sooner.

Rheological assemblies one and two experienced increases in activation energy beyond twenty days as a consequence of hydration. Equilibrium spacings in general change proportionately with changes in the free energy of activation except in the first rheological assembly. The large increase in this case probably represents the effect of greater separation of molecules resulting from activation as the material loses viscous damping capacity and elastic strain energy is converted directly to kinetic energy upon rupture of the bonds.

D. Application of the Structure Parameters for the Rheological Assemblies to the Rheological Model

(a) Retarded Elastic Recovery

Development of equation (8) representing the model for the creep mechanism may now be completed based on the interpretations of the rate process theory discussed in the preceding sections. Since the first and third rheological elements contained stress and time dependent variations of non-recoverable creep they are to be included in the second, non-linear term of equation (8). The second rheological element satisfies elastic conditions, and it will therefore comprise the third term of equation (8).

A check of the elastic influence of this element may be accomplished by comparing its response with the complete relaxation data for the actual specimen.

The strain accumulated in the elastic rheological assemblies may be computed at any time

$$\epsilon = A \frac{\lambda_n}{E_n} \left[\frac{B (f - f_o)}{1 \cdot 1 !} + \frac{B^3 (f^3 - f_o^3)}{3 \cdot 3 !} + \frac{B^5 (f^5 - f_o^5)}{5 \cdot 5 !} + \ldots \right]. \quad (18)$$

This equation, derived from the rate process theory for a rheological element, is developed in Appendix A.

Table VI, comparing results obtained from equation (18) by pooling all specimens into lightweight and normal concrete categories against actual test data supports the use of the second Kelvin element to represent retarded elastic behavior. The calculated elastic recovery should be related to the activation energy level at the time of removal of stress. For a greater period under sustained loading the activation energy increases thus the factor A decreases, thereby reducing the recoverable elastic strain. The approximated final value of the coefficient A is determined by assuming that the 1000 day value from Table IV is the average of the initial value of A, assumed equal to the 20 day value from Table IV, and the desired final value.

(b) Total Change in Fluidity of the Concrete

Earlier, initial and final values of the fluidity terms ϕ_o and ϕ_∞ were determined from a consideration of the basic rheological equations. From a rate theory standpoint the fluidity at any time is

$$\phi = \frac{d\epsilon}{df} = AB \cosh Bf \quad . \quad (19)$$

TABLE VI

ELASTIC RETARDED RECOVERY -- COMPARISON OF DATA AND THEORY

Average of All Shapes for Control Specimens (Series A)

of Each Concrete Type

$$\epsilon = A \frac{\lambda}{E} \sum_{j=1}^{\infty} \left[\frac{B^i (f_o^i - f^i)}{i \cdot i!} \right] \quad , i = 2j - 1$$

Concrete Type		Limestone	Lightweight (Solite)
Rheological Constants	E	4.0×10^6 psi	3.5×10^6 psi
	λ	229×10^6 psi-day	207×10^6 psi-day
Rate Theory Constants	A^*	13.7×10^{-6}/day	17.7×10^{-6}/day
	B	$.18 \times 10^{-3}$/psi	$.18 \times 10^{-3}$/psi
Initial Stress	f_o	914 psi	914 psi
Calculated Delayed Elastic Recovery		129×10^{-6} in/in	172×10^{-6} in/in
Actual Delayed Elastic Recovery		103×10^{-6} in/in	154×10^{-6} in/in

*Assume: Final A = $2 A_{1000} - A_{20}$ (approximately)

It was shown in the previous section that the free energy of activation increases with time due to the change in the gel structure. Therefore the values of A and B in the rate process equation are average values predicting the behavior to any arbitrarily selected time just as the rheological parameters are average values for any applied stress. If we set f = 0 in equation (19) then

$$\phi_o = AB, \tag{20}$$

which gives values equal to the results from equation (11) when the average A and B values at any age are used. However, any value of f greater than zero will result in greater fluidity than ϕ_o when employing equation (19). Therefore it becomes obvious that the fluidity change must include the true variation in internal energy and equilibrium spacing for an accurate account of the non recoverable strains at any stage of the creep process.

An understanding of the nature of the change in the quantum states of the concrete is not within the scope of this study. The true value of ϕ_o should be approximately equal to the value determined from equation (20). For the statistical mechanics approach which is represented by equation (20), the values of $\phi_o = AB$ do not change when using the data at twenty days or at 1000 days from Table IV.

Equation (11) provides a decrease in fluidity with respect to time whereas equation (20) provides an increase in fluidity with respect to stress. The true fluidity is probably a non linear function of time and stress requiring a knowledge of the physico-chemical thermodynamic variations affecting the quantum states of the mix.

Assuming the ultimate fluidity ϕ_∞ to be established by equation (10) the total change in fluidity may be approximated by assuming a variation between the values established by equations (11 or 20) for ϕ_o and equation (10) for ϕ_∞ .

The total change in fluidity is influenced primarily by the mix proportions of the concrete and by the ambient conditions of the environment in which the concrete will be used. For most structural concretes in any environment the gel structure becomes sufficiently rigid after a long time that little or no viscous creep occurs even in the presence of high humidity. Therefore it may be justified to use zero as a value for ϕ_∞. If this expedient step is taken it only becomes necessary to evaluate ϕ_o from test data obtained from the concrete under initial loading.

(c) Inelastic Behavior and the Coefficients of Structural Stability

The coefficients of structural stability for equation (7) may be determined by evaluating the responses from the control specimens.

$$\phi = \phi_\infty + (\phi_o - \phi_\infty)\, e^{-(c_t + c_f (f_o^2 - f^2))} \quad . \tag{7}$$

From a consideration of the behavior of the control specimens (Series A) for which $f = f_o$, a determination of the time dependent component in the structural stability coefficient may be made by solving for the aging component, c_t. Substituting $f = f_o$ into equation (7) yields the solution for the time dependent component of creep only,

$$\frac{\phi - \phi_\infty}{\phi_o - \phi_\infty} = e^{-c_t} \quad . \tag{21}$$

Taking the log of both sides results in a solution for c_t

$$c_t = -\ln \frac{\phi - \phi_\infty}{\phi_o - \phi_\infty} \tag{22}$$

in which

$$\phi = \frac{\epsilon_{vis}}{f \cdot t} \quad . \tag{23}$$

ϵ_{vis} is simply obtained by subtracting shrinkage, initial elastic strains and delayed elastic strains from the total creep strain for each specimen. Time dependent coefficients (c_t) for the non-recoverable creep component are presented in Figures 10 and 11. The coefficient c_t is assumed to be a function of time only, therefore it is entirely independent of stress variations. Equation (22) is used to obtain the value of c_t for the concrete from experimental data. However equation (22) may not be used as a general relation for the prediction of creep behavior. The coefficient c_t must include, in addition to the variable time, all of the influencing factors which contribute to the aging characteristics of creep of concrete. Hansen and Mattock[16] have evaluated shape effect on creep and presented a relationship between creep and shape in an exponential form. It is not incongruous to assign a similar relationship to other factors which influence creep. Accordingly the coefficient c_t is assigned an exponential form

$$c_t = t^n \epsilon^{-(F_n(t))}, \qquad (24)$$

where $F_n(t)$ is a polynomial function of time. The equations c_t are given in Table VII for each control specimen. The constants in the c_t function are related to the time dependent factors influencing concrete aging, hydration for example, which cause variation of the energy states in the concrete independently of stress. The polynomial exponent has been limited to a cubic function. The limitation is based partly on an acceptable fit of the function to the experimental data as represented by the error sum of squares in Table VII. The closeness of fit is indicated in Figures 10 and 11. The plots were made from a computerized curve fitting program. The exponent was limited to a cubic function also becauae it was quite

TABLE VII

EQUATIONS FOR THE AGING COEFFICIENTS, c_t ,

OF STRUCTURAL STABILITY FROM COMPUTERIZED LEAST SQUARE FIT

Concrete Type	Shape of Specimen	Equation: $c_t = t^a \exp(-(b_1 + b_2 t + b_3 t^2 + b_4 t^3))$					Error Sum of Squares
		a	b_1	b_2	b_3	b_4	
Limestone Concrete	Circle	.971	3.699	4.524×10^{-3}	-4.851×10^{-6}	2.085×10^{-9}	2.038×10^{-3}
	Rectangle	.965	3.762	4.774×10^{-3}	-5.437×10^{-6}	2.429×10^{-9}	2.569×10^{-3}
	Cross	.969	3.787	4.824×10^{-3}	-5.493×10^{-6}	2.439×10^{-9}	3.530×10^{-3}
Lightweight (Solite) Concrete	Circle	.959	3.753	4.676×10^{-3}	-5.270×10^{-6}	2.334×10^{-9}	3.414×10^{-3}
	Rectangle	.965	3.988	4.831×10^{-3}	-5.740×10^{-6}	2.604×10^{-9}	5.224×10^{-3}
	Cross	.993	4.422	5.006×10^{-3}	-6.377×10^{-6}	3.014×10^{-9}	11.880×10^{-3}

obvious that higher power terms would only tend to influence the creep at advanced ages and in not a highly significant manner. A reasonably successful fit may be obtained in the early ages by substitution of a constant for the polynomial function as was done by Hansen and Mattock.[16]

The complete form of the aging component c_t of the structural stability coefficient is

$$c_t = t^a e^{-(b_1 + b_2 t + b_3 t^2 + b_4 t^3)} \quad . \tag{24a}$$

From Table VII the constant a is relatively independent of shape or concrete mix. Further, it is reasonably close to unity so that setting a = 1 does not result in a serious error for the concrete specimens tested. The polynomial exponent is, however, related to shape. By employing the circular shape as a standard, since it has a weighted flow path length equal to unity for a six inch diameter specimen, all other shapes or sizes may be related to the six inch diameter cylinder as a standard. Redesignating the coefficients b_n in the polynomial function to c_n for the six inch diameter cylinder, the coefficients b_n may be approximately determined from

$$b_n = c_n \left[\frac{K\,(1 - w)}{\sum_{n=1}^{4} c_n} + 1 \right] , \tag{25}$$

where w is the weighted flow distance for the concrete specimen from Table II and K is a constant associated with the concrete mix. K is equal to six for the lightweight Solite concrete used in this experiment and K is equal to three for the limestone concrete.

The stress dependent component, c_f, in the structural stability coefficient is obtained from the control specimens employing the rate coefficients from the rate process theory presented in Table IV. In Appendix A, the creep for a single rheological assembly was determined. The combined strain for two such assemblies representing the Kelvin elements one and three from the rheological model of Figure 1 may be written in the form of an infinite series,

$$\epsilon_1 + \epsilon_3 = \sum_{j=1,2}^{\infty} \left[(AB^i \lambda / E)_1 + (AB^i \lambda / E)_3 \right] \frac{(f_o^i - f^i)}{i \cdot i!} \qquad (26)$$

where $i = 2j - 1$.

The component c_f is related to stress changes in the concrete beyond the initial applied stress f_o. If the stress remains unchanged then only aging influences the creep rate and the c_f component is not effective. However under any change in stress, increase or decrease, the creep rate will be influenced according to the effect of the stress on the energy required for activation of a rheological assembly. If a creep test is performed on a standard cylindrical specimen and the macroscopic creep data evaluated by viscoelastic methods, the resulting rheological solution for the viscous non Newtonian elements, such as Kelvin elements one and three in this investigation, may be converted to the form represented by equation (26). This process results in an evaluation of non Newtonian concrete strain in terms of stress change and the linear viscoelastic parameters from the rheological study. The accuracy of the strains determined from equation (26) is limited to the accuracy of the rheological parameters ϕ_n and E_n in reflecting the true concrete behavior. This

limitation on accuracy is, however, directly related to the degree of work which the analyst is willing to expend in obtaining more accurate viscoelastic parameters. Surely if methods as described by Freudenthal and Roll[4] are employed, the greater effort will yield better results.

The important aspect of the relationship presented in equation (26) is in having a function which is sensitive to changes in stress rather than time. This relationship makes it possible for the structural analyst to evaluate the influence of stress changes on creep behavior with greater precision than was possible from just a rheological study.

In order to relate these non Newtonian strains to the component c_f of the structural stability coefficient, let

$$N_i = (AB^i \lambda / E)_1 + (AB^i \lambda / E)_3 \quad .$$

Equating the strains represented by equation (26) from the average states of the rheological assemblies one and three to the stress dependent creep term in equation (8) for the rheological model yields

$$(\phi_o - \phi_\infty) \exp\left[-c_f (f_o^2 - f^2)\right] ft = \sum_{j=1,2}^{\infty} \left[N_i \frac{(f_o^i - f^i)}{i \cdot i!}\right]_{i = 2j - 1.} \qquad (27)$$

Dividing by stress f and time t, substituting from Appendix A

$$t = -\frac{\lambda}{E} \ln \frac{f}{f_o} \qquad (A\text{-}4)$$

and taking the log of both sides of equation (27), the stress component of the structural stability coefficient is determined

$$c_f (f_o^2 - f^2) = \ln \left[\frac{\sum_{j=1,2}^{\infty} \left[(AB^i)_1 + (AB^i)_3\right] \frac{(f^{i-1} - f_o^i / f)}{i \cdot i!}}{(\phi_o - \phi_\infty) \ln f/f_o} \right], i=2j-1. \qquad (28)$$

The coefficients A, B, ϕ_o and ϕ_∞ have also been determined. Therefore knowing the stress variation, the right side of equation (28) may be substituted for the coefficient $c_f (f_o^2 - f^2)$ and the total creep may be calculated from equation (8),

$$\epsilon = \frac{f}{E} + \left[\phi_\infty + (\phi_o - \phi_\infty)\, e^{-(c_t + c_f (f_o^2 - f^2))}\right] ft + \frac{f}{Ee}\left[1 - e^{-\phi_e E_e t}\right]. \quad (8)$$

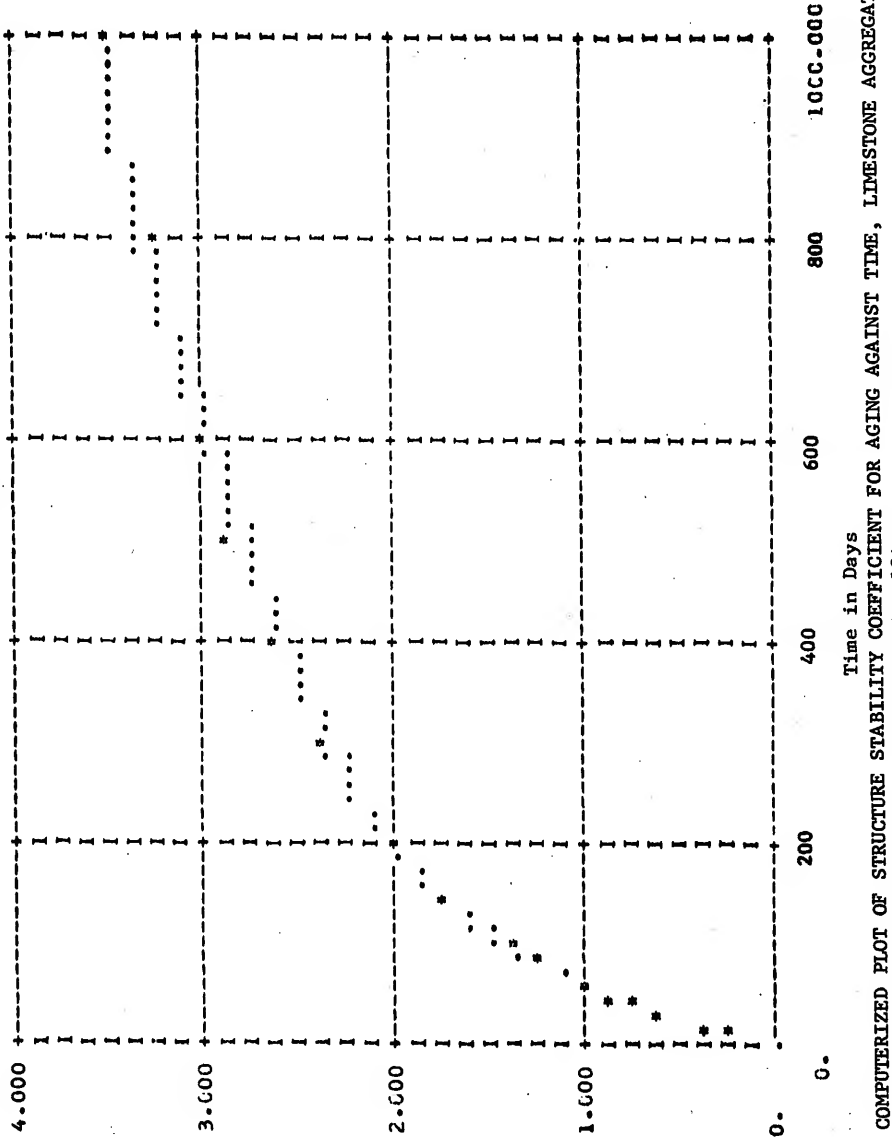

COMPUTERIZED PLOT OF STRUCTURE STABILITY COEFFICIENT FOR AGING AGAINST TIME, LIMESTONE AGGREGATE CONCRETE
FIGURE 10A

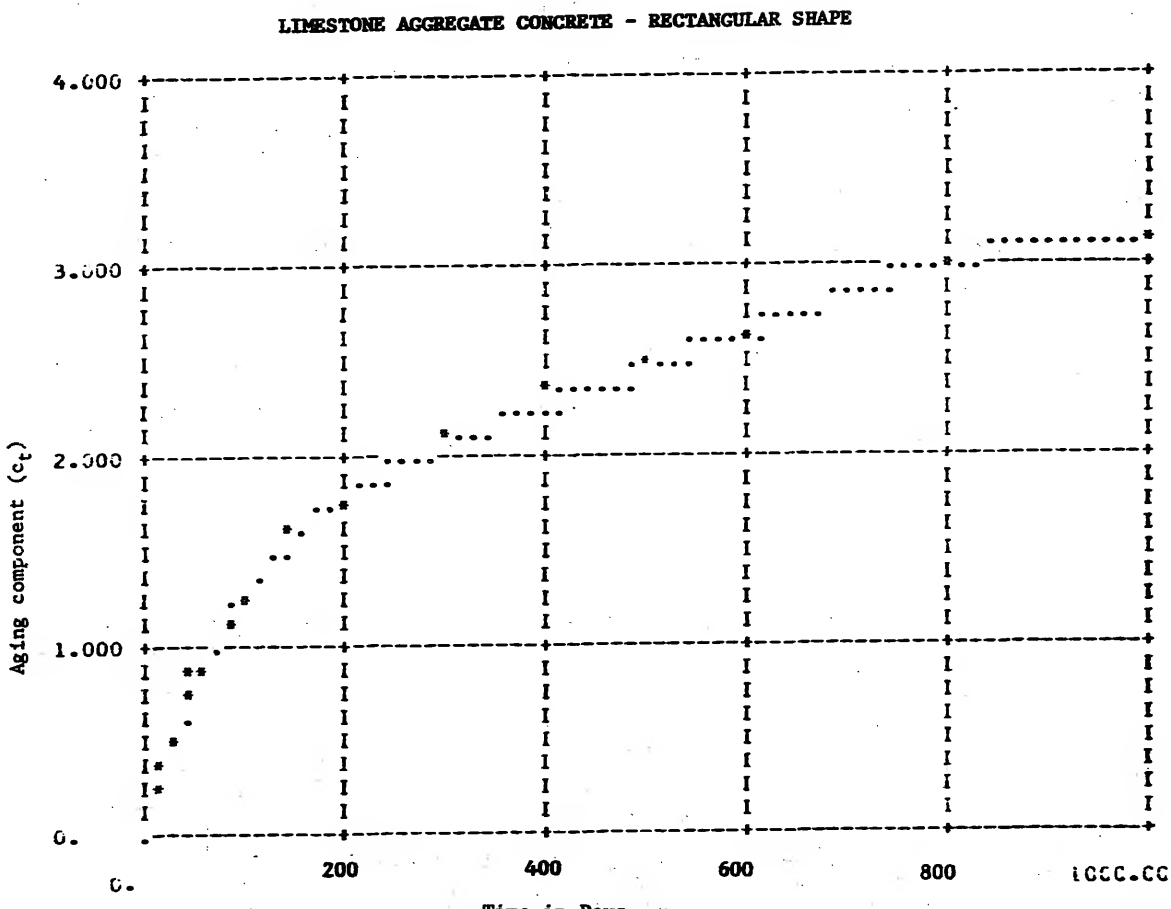

COMPUTERIZED PLOT OF STRUCTURE STABILITY COEFFICIENT FOR AGING AGAINST TIME, LIMESTONE AGGREGATE CONCRETE
FIGURE 10B

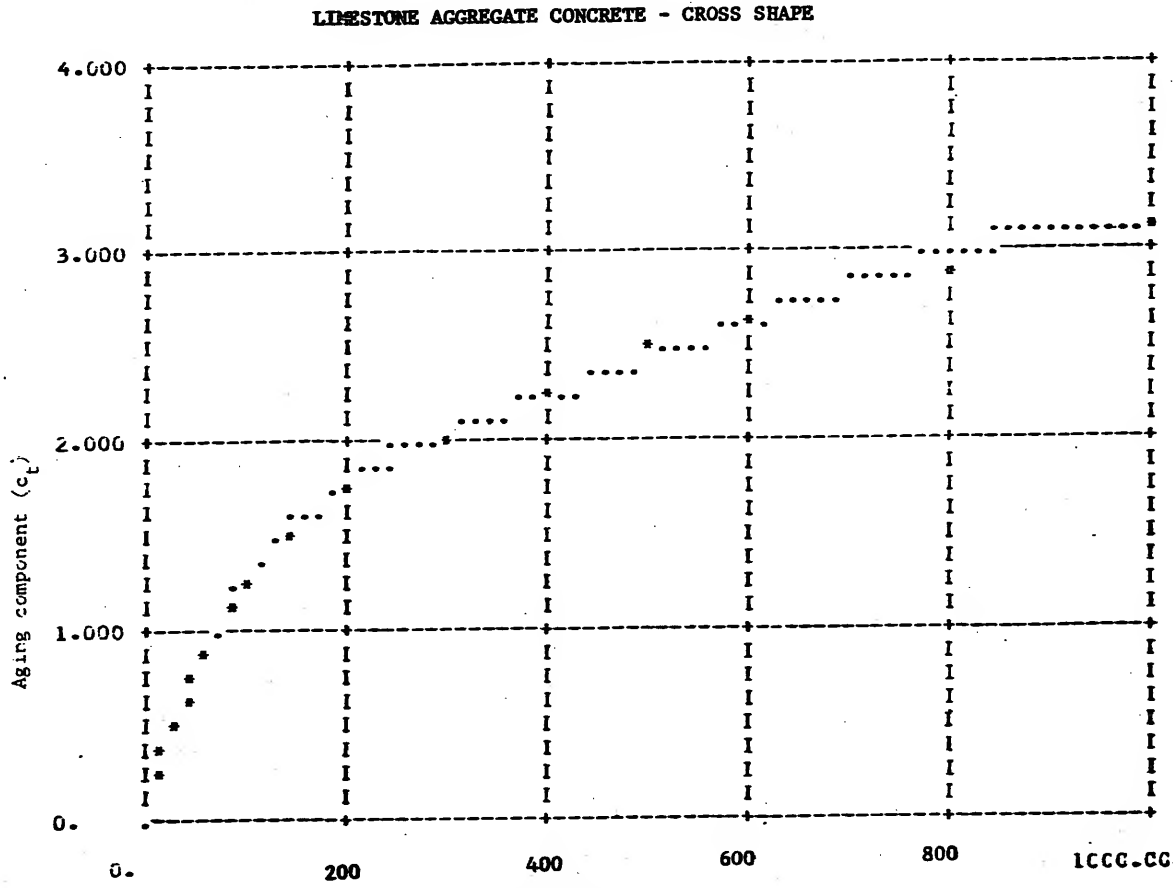

COMPUTERIZED PLOT OF STRUCTURE STABILITY COEFFICIENT FOR AGING AGAINST TIME, LIMESTONE AGGREGATE CONCRETE
FIGURE 10C

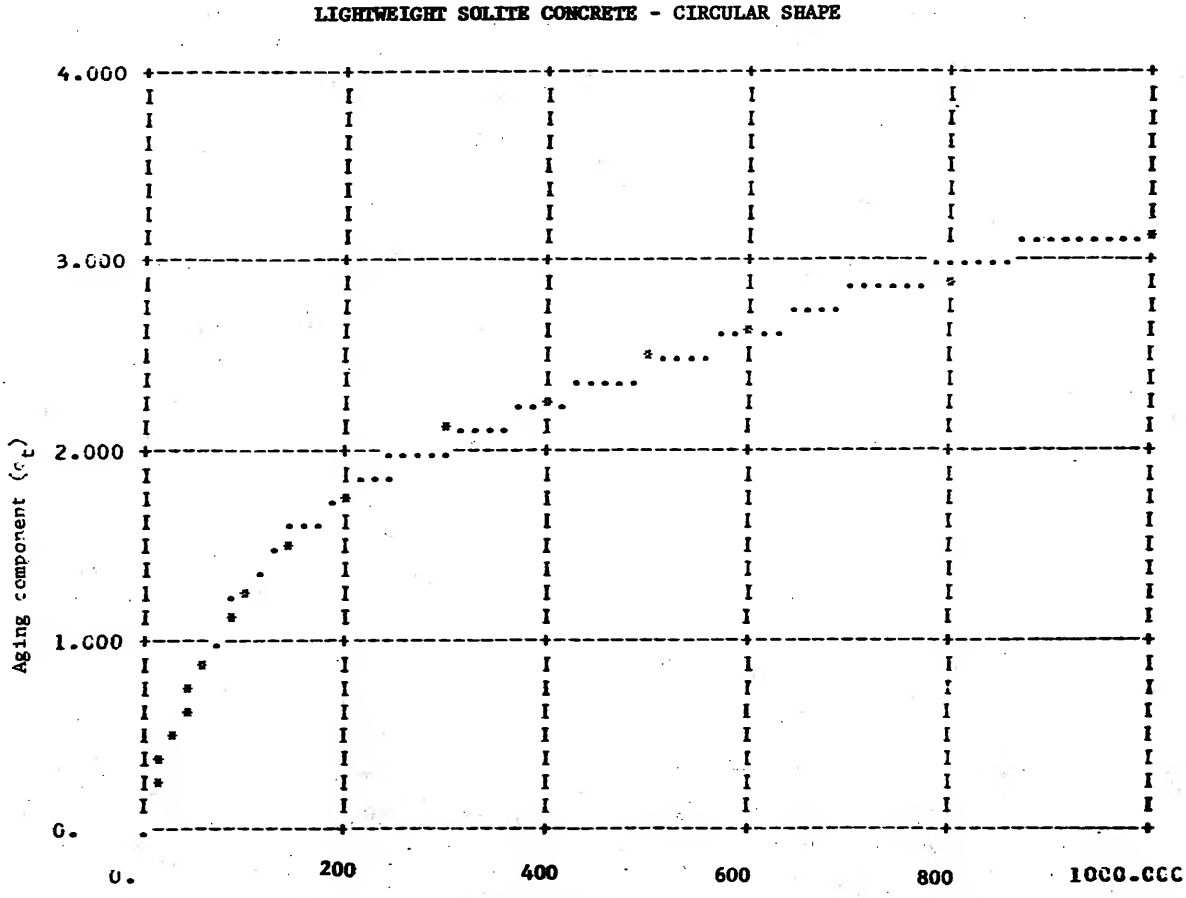

COMPUTERIZED PLOT OF STRUCTURE STABILITY COEFFICIENT FOR AGING AGAINST TIME, LIGHTWEIGHT AGGREGATE CONCRETE
FIGURE 11A

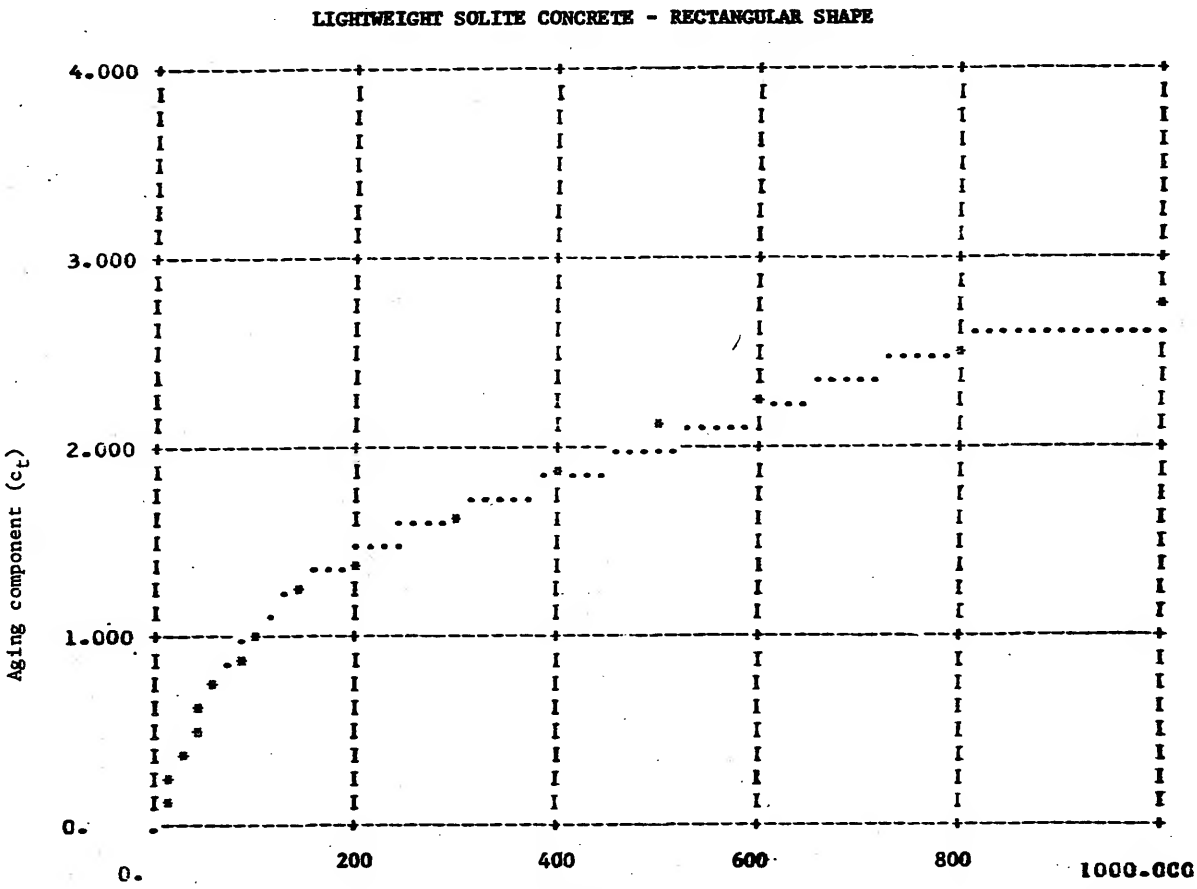

COMPUTERIZED PLOT OF STRUCTURE STABILITY COEFFICIENT FOR AGING AGAINST TIME, LIGHTWEIGHT AGGREGATE CONCRETE
FIGURE 11B

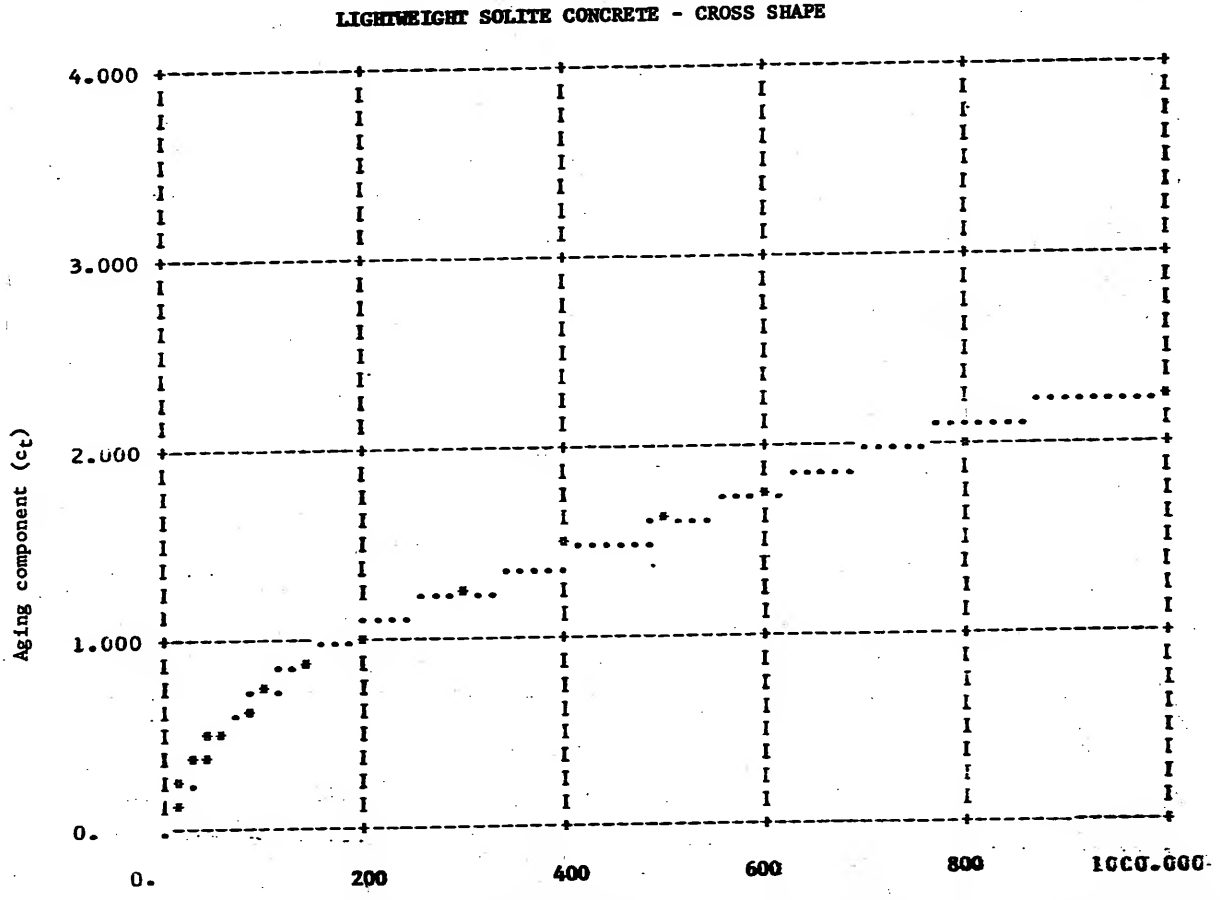

COMPUTERIZED PLOT OF STRUCTURE STABILITY COEFFICIENT FOR AGING AGAINST TIME, LIGHTWEIGHT AGGREGATE CONCRETE
FIGURE 11C

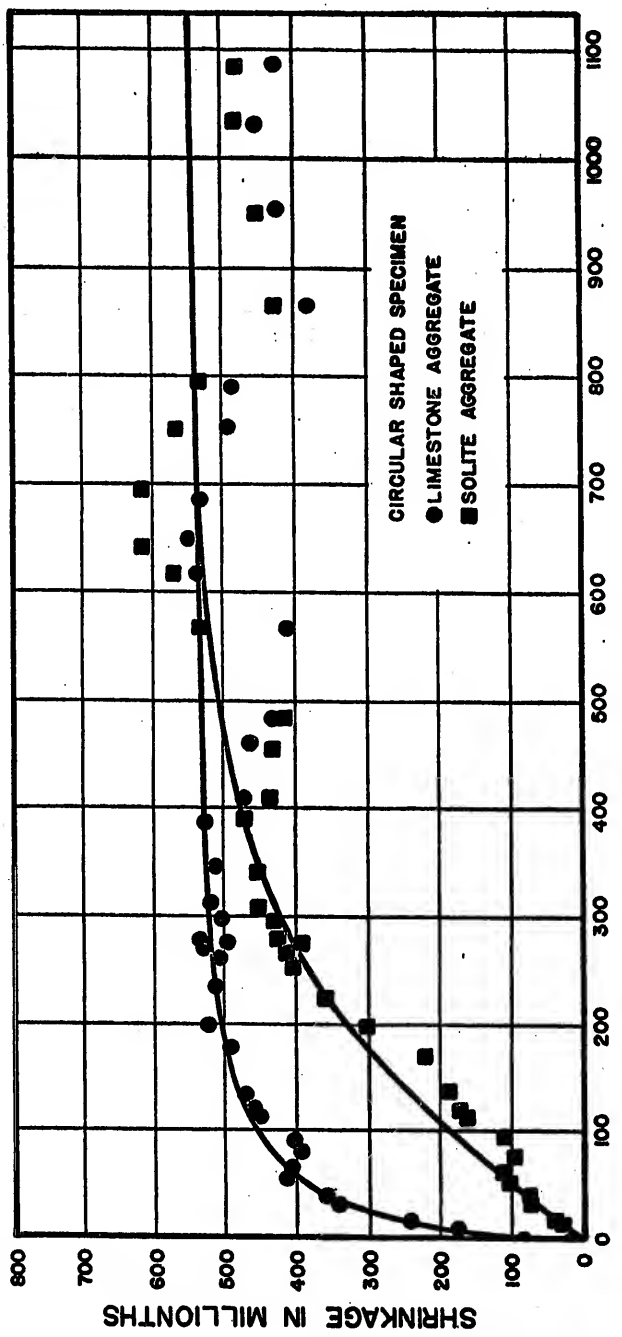

COMPARISON OF SHRINKAGE FOR LIMESTONE CONCRETE AND SOLITE CONCRETE

FIGURE 12

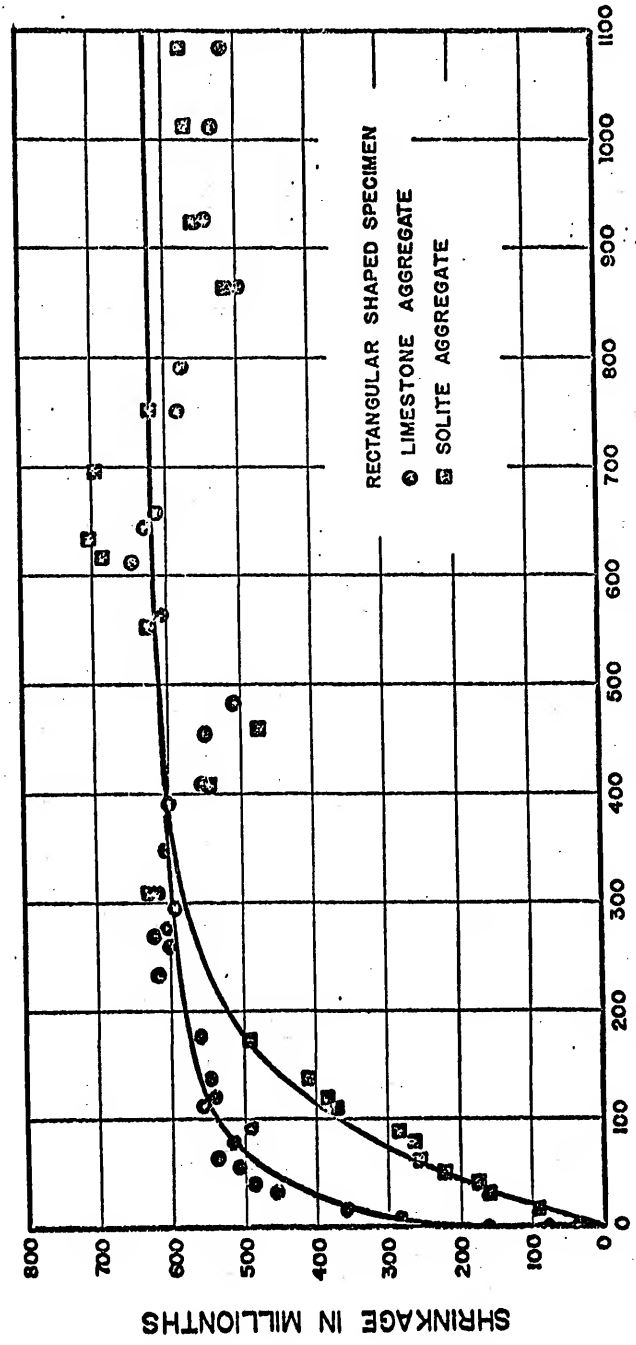

COMPARISON OF SHRINKAGE FOR LIMESTONE CONCRETE AND SOLITE CONCRETE

FIGURE 13

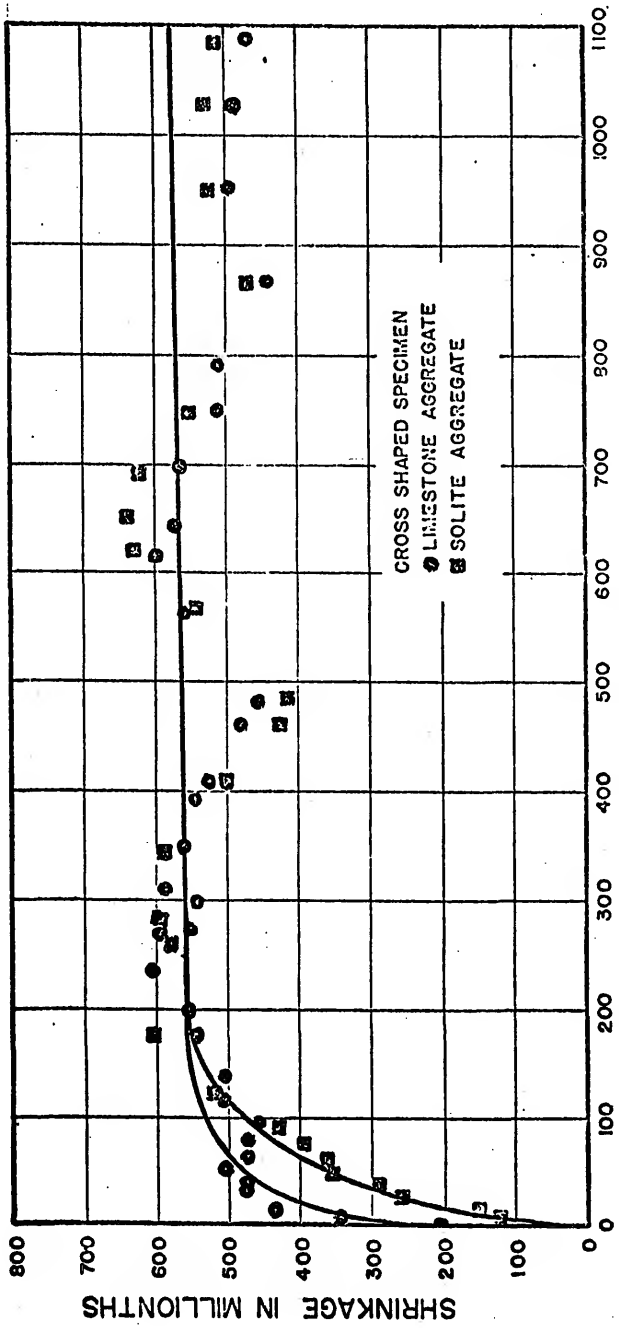

COMPARISON OF SHRINKAGE FOR LIMESTONE CONCRETE AND SOLITE CONCRETE

FIGURE 14

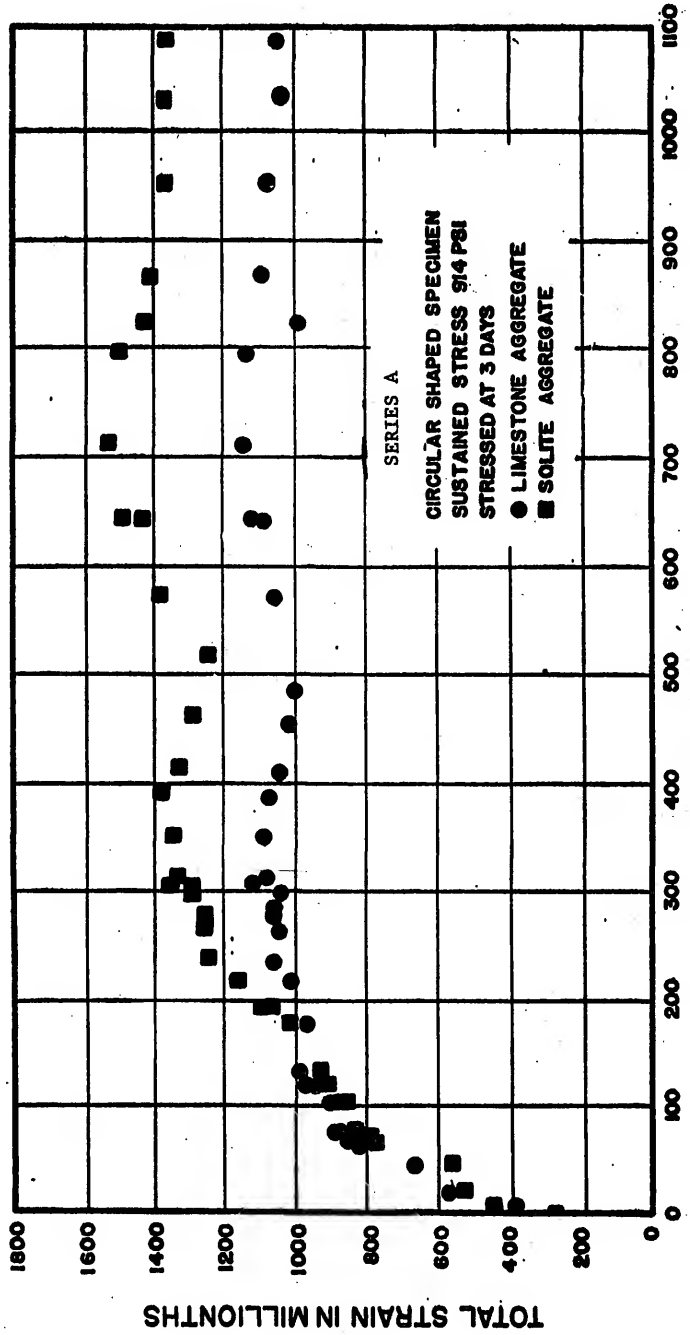

COMPARISON OF TOTAL STRAIN FOR LIMESTONE CONCRETE AND SOLITE CONCRETE

FIGURE 15

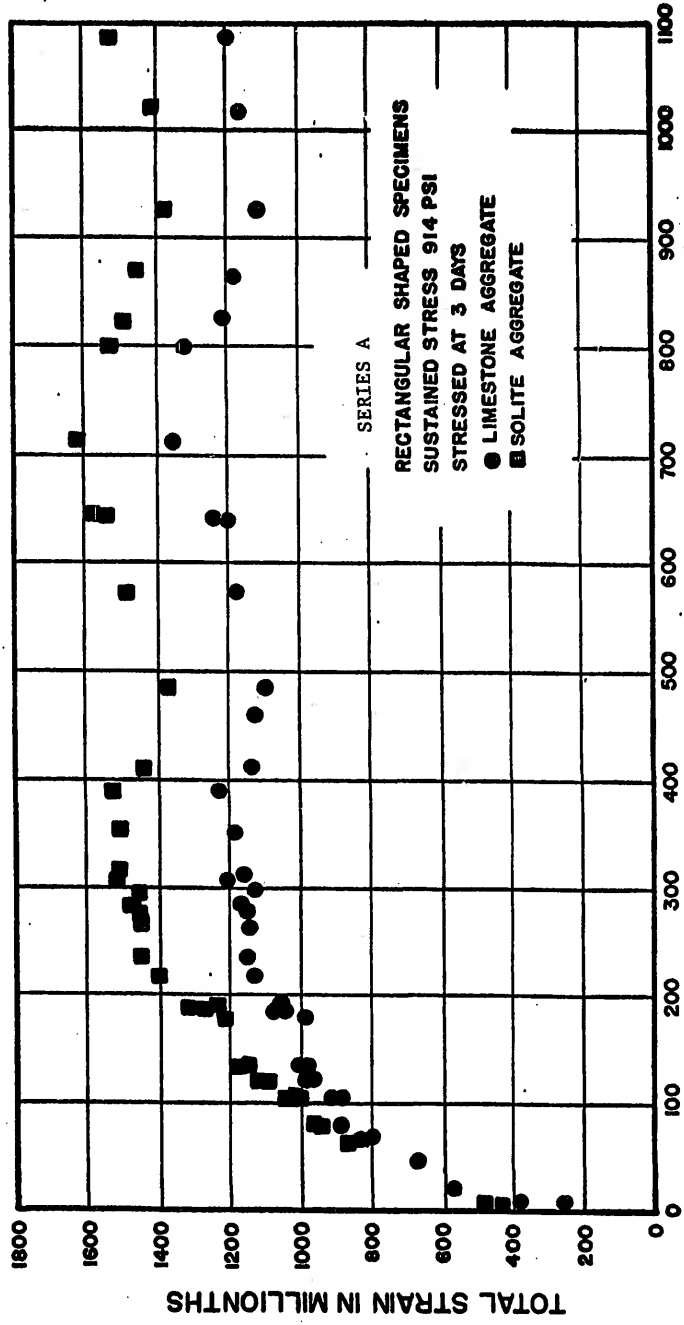

COMPARISON OF TOTAL STRAIN FOR LIMESTONE CONCRETE AND SOLITE CONCRETE

FIGURE 16

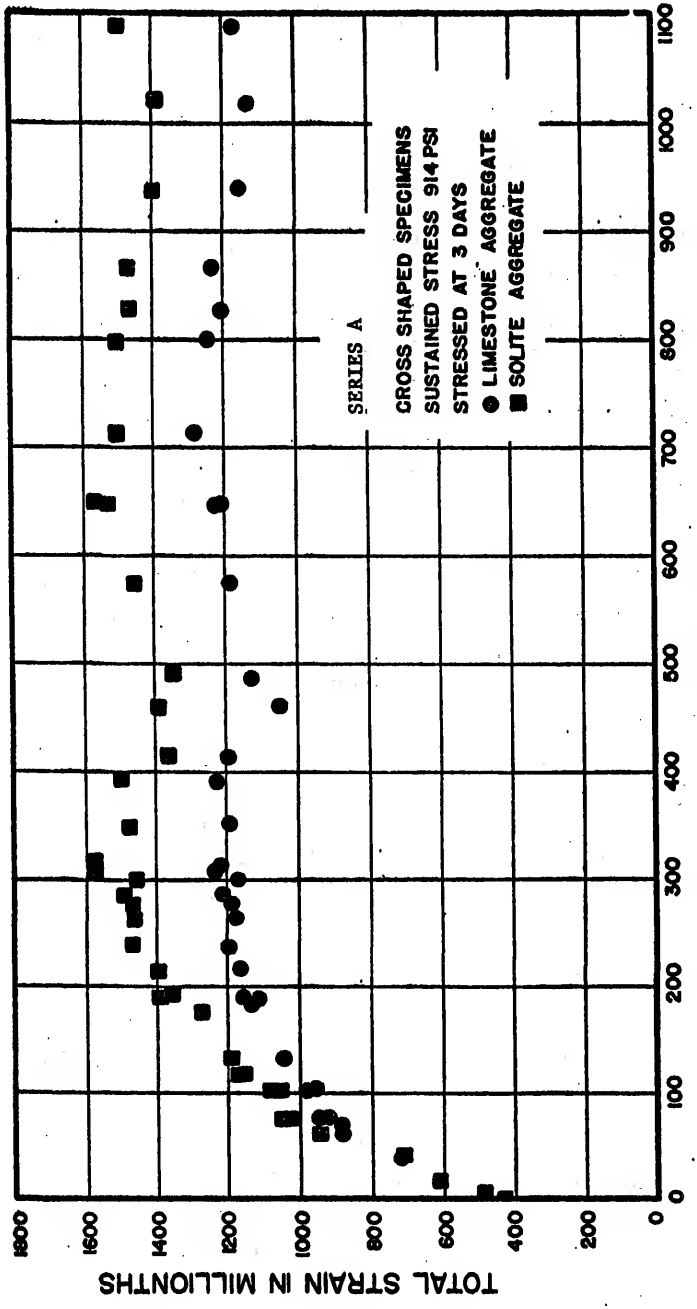

COMPARISON OF TOTAL STRAIN FOR LIMESTONE CONCRETE AND SOLITE CONCRETE

FIGURE 17

CHAPTER VII

ANALYSIS OF RESULTS

A. Application of the Model to Concrete Under Sustained Stress (Test Series A)

The model is designed from the response of test series A in which the concrete specimen were maintained under sustained stress for over 1000 days. Hence it is expected that the model will represent the behavior well. Figure 18 confirms the comparison between creep data and model for each condition of specimen shape and concrete mix.

The creep data for Figure 18 were obtained by subtracting the corresponding shrinkage from Figures 12, 13, or 14 from the total strain for the specimen shown in Figures 15, 16, or 17, with allowance made for shrinkage occurring up to the time of stressing. There is a prominent seasonal effect on shrinkage and total strain which becomes inconspicuous in the carry-over to the creep data. The extent of the seasonal effects in the creep data when compared with the effects in shrinkage is a measure of the interaction between creep and shrinkage of concrete.

The model which has been developed is in the general form represented by equation (8).

$$\epsilon = \frac{f}{E} + \left[\phi_\infty + (\phi_o - \phi_\infty)\, e^{-(c_t + c_f (f_o^2 - f^2))}\right] ft + \frac{f}{E_e}\left[1 - e^{-\phi_e E_e t}\right] \quad (8)$$

The elastic components are not considered to be influenced by shape. Therefore E, ϕ_e, E_e are the rheological parameters determined directly from the viscoelastic analysis of the data from the control specimen.

The inelastic component is a function of shape. The four parameters involved are ϕ_∞ , ϕ_o, c_t and c_f. Each parameter appears to be influenced by shape or flow path. The value for ϕ_∞ may be obtained from equation (10) employing the results in Table III.

$$\phi_\infty = \phi_\infty^c \; e^{-1.85\,(W_c - w)} \tag{29}$$

where ϕ_∞^c is the ultimate fluidity for the standard control specimen, the six inch diameter cylinder, and w is the weighted flow distance from Table II for the specimen under consideration. Equation (29) is applicable to either concrete. When the standard six inch diameter cylinder is used, $W_c = 1.0$ and equation (29) becomes

$$\phi_\infty = \phi_\infty^c \; e^{-1.85\,(1 - w)} \quad . \tag{29a}$$

The value for ϕ_o is obtained from equations (11) or (20). For the specimens tested, employing values from Table III in equation (11) results in no noticeable influence of shape on ϕ_o for the limestone concrete. However, the lightweight Solite concrete exhibited a variation in ϕ_o influenced by shape. The reason for this difference in behavior may be attributed to the proximity of the moisture laden Solite aggregate to the concrete surface. The apparent difference in viscosity is caused by differences in moisture loas from the aggregate. Employing equation (11) from page 41,

$$\phi_o = (\phi_1 + \phi_3)_c \; e^{-1.45\,M\,(1 - w)} \quad , \tag{30}$$

where the subscript c refers to the values for a standard control specimen, a six inch diameter cylinder in this case.

M = 0 for standard limestone concrete

M = 1 for Solite lightweight concrete as used in this experiment. A determination of the variation of M is not within the scope of this experiment.

The structural stability coefficients c_t and c_f have been fully described in the previous chapter. The aging component c_t was defined by equations (24a) and (25). For the concrete in this investigation the value of c_t was obtained by omitting the power of t in equation (24a).

$$c_t = t\, e^{-(b_1 + b_2 t + b_3 t^2 + b_4 t^3)} \quad , \tag{31}$$

where $$b_n = C_n \left[\frac{K\,(1 - w)}{\sum_{n=1}^{4} C_n} + 1 \right] \quad . \tag{25}$$

The values of C_n are determined by fitting equation (31), with C_n replacing b_n, to the creep data from a standard control specimen made from the concrete under investigation. The values for c_t are determined for any time t by use of equation (22). At least ten time intervals should be used in obtaining the values of C_n. Values for b_n for any other shape or size of specimen are obtained from equation (25) where K = 3 (1 + M)

K = 3 for limestone aggregate concrete

K = 6 for Solite aggregate concrete.

The value for the structural stability component c_f is determined by substitution defined by equation (28). Values for ϕ_o and ϕ_∞ are obtained as described earlier. Only the rate parameter A is dependent upon flow path or shape (see Table IV). Determination of the values for the parameter A to be used in equation (28) may be approximated from values obtained for a

standard control specimen of six inch diameter for each inelastic rheological assembly unit. For the first rheological assembly

$$A_1 = A_1^c \, e^{(1 - K/10)(1 - w)} \quad , \tag{32}$$

where A_1^c is the calculated value of A for the first rheological assembly of the cylindrical control specimen. K and w have been previously defined.

The value for the third rheological assembly is

$$A_3 = A_3^c \, e^{-2.5 M (1 - w)} \quad , \tag{33}$$

where M has been previously defined.

All parameters may be obtained from a single sustained creep test on a standard control specimen. However, in each of the relations above it is not possible to cross from one concrete mix to another. Therefore the test must be made on the type mix to be used in the prototype structure. The limited scope of this experiment precludes development of a model which will include mix variations and environmental variations in its prediction of creep behavior.

An analysis of the model (Figure 9) reveals certain characteristics of its behavior. Considering the first and third terms of equation (8) it is evident that these components of the model reflect no variations in the molecular structure. The variations due to irrecoverable viscous flow, destruction of bonds, and growth of new bonds are therefore all contained in the second term of equation (8). In the case of concrete under sustained stress these factors are all time dependent and the magnitudes of their influence on inelastic creep is directly proportional to the sustained stress level.

Proportionality of creep and stress is limited to low stress ranges. When the applied stress exceeds about 30 per cent of the twenty-eight day strength, f'_c, the creep rate increases and proportionality between creep and stress ceases. Freudenthal and Roll[4] have determined that only the inelastic components of creep are not proportional to stress. In the model represented by equation (8) therefore only the second term representing inelastic creep components would be non linear with respect to stress for high stress levels. This investigation did not include a study of stress level. Freudenthal and Roll[4] investigated stress level on different mixes producing concretes varying from very viscous to very fluid in nature. Employing their results equation (8) may be modified to include consideration of non proportional creep response under high stress conditions.

Since the second term of equation (8) is linear with respect to stress level any creep component obtained from it at any time would be the linear creep component only. In order to obtain the true creep the linear creep component must be multiplied by a factor which produces the non linear component of creep. The non linear component is related to the viscosity of the mix. A more viscous mix will yield a smaller non linear creep component. Since Freudenthal and Roll's results represented the extreme conditions of viscosity it is not known how the non linear creep component varies with viscosity. Therefore it is assumed that the non linear creep component is inversely proportional to the initial viscosity of the mix at the time the stress is applied.

In corporating non proportional relations between creep and stress into the model, equation (8) becomes

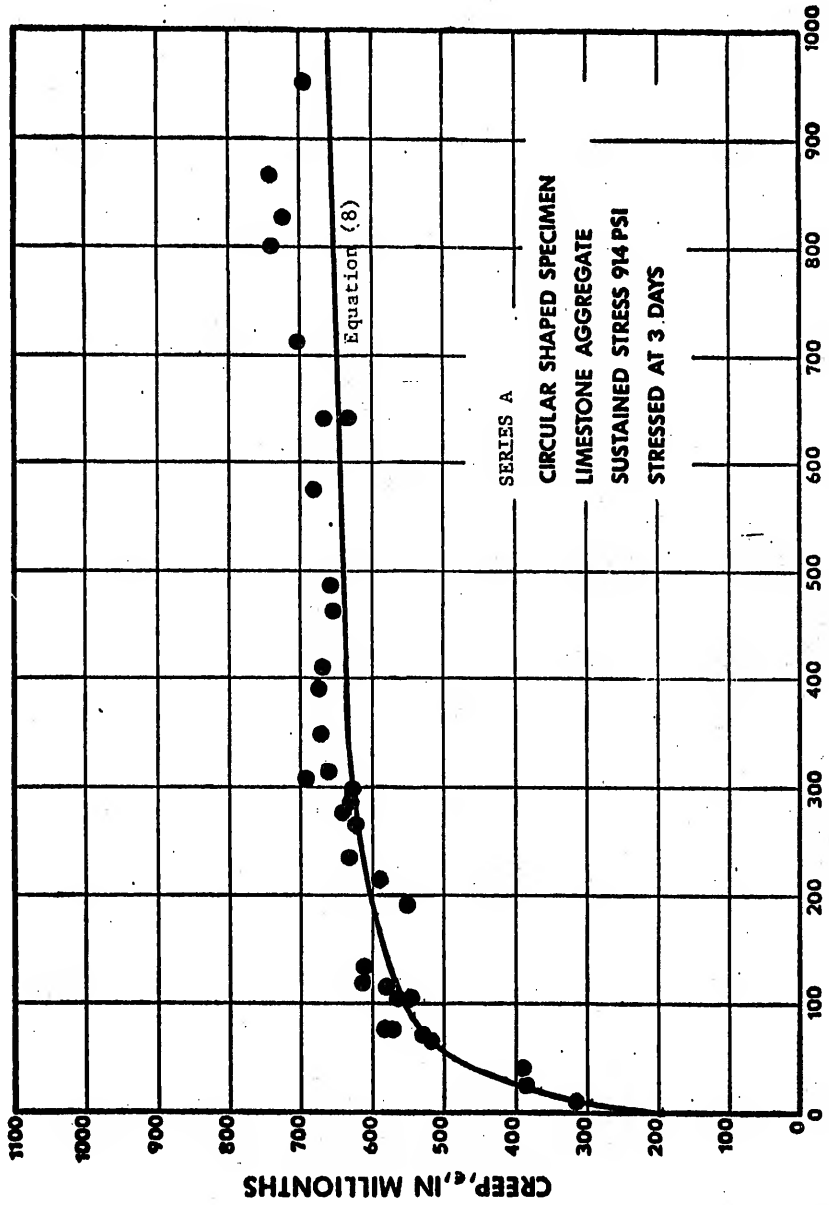

COMPARISON OF RHEOLOGICAL MODEL AND EXPERIMENTAL DATA

FIGURE 18 A

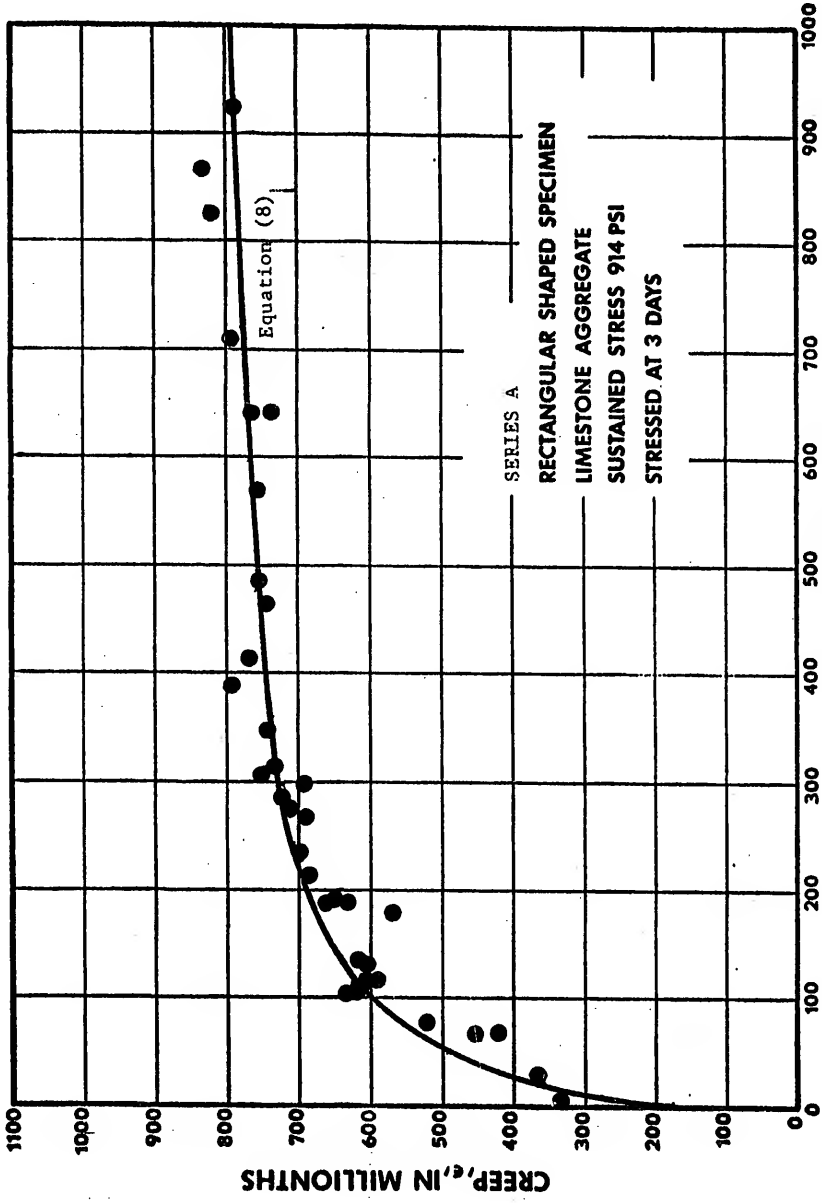

COMPARISON OF RHEOLOGICAL MODEL AND EXPERIMENTAL DATA

FIGURE 18 B

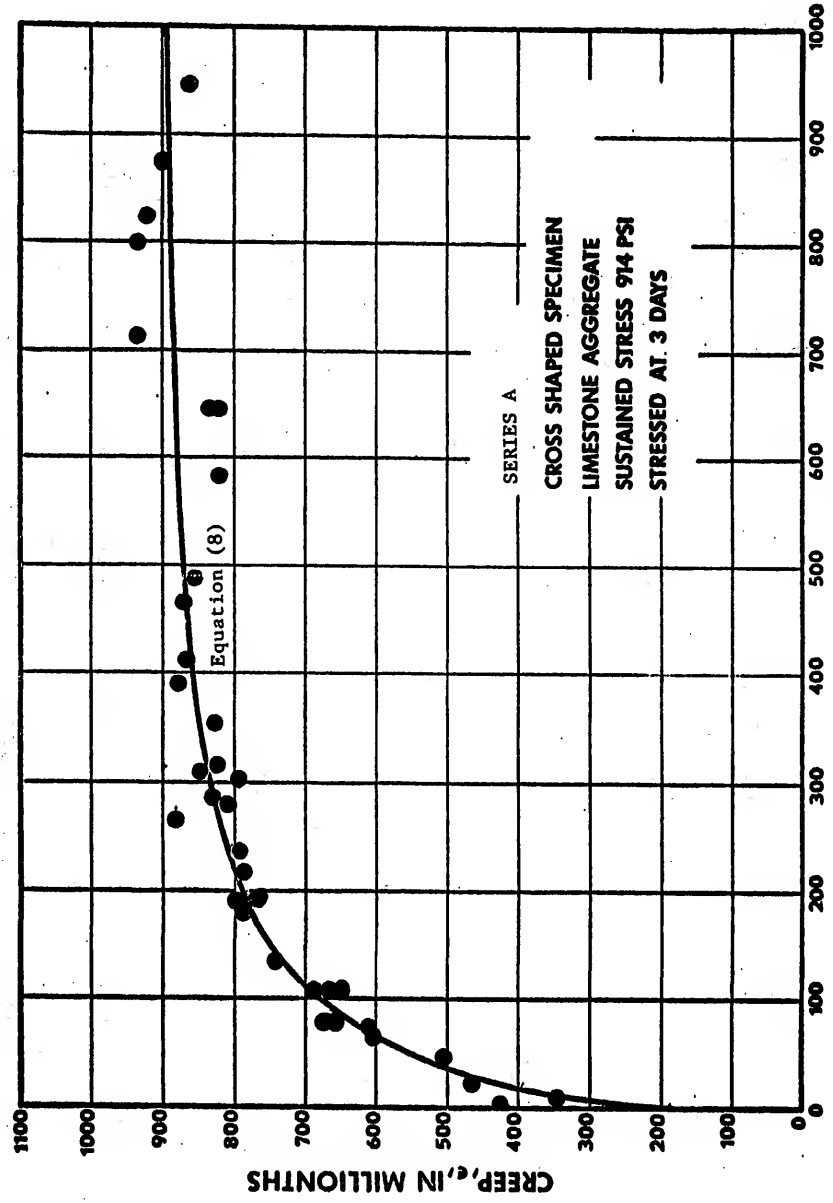

COMPARISON OF RHEOLOGICAL MODEL AND EXPERIMENTAL DATA
FIGURE 18 C

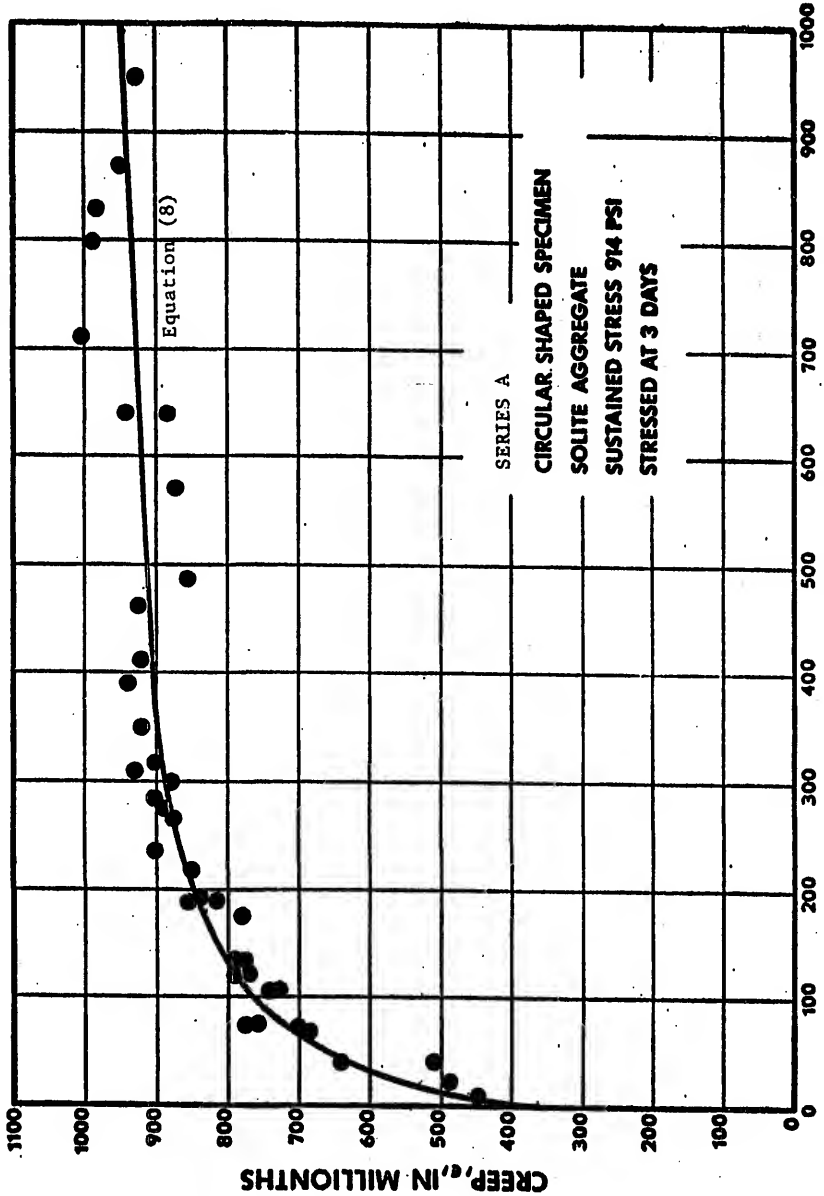

COMPARISON OF RHEOLOGICAL MODEL AND EXPERIMENTAL DATA

FIGURE 18 D

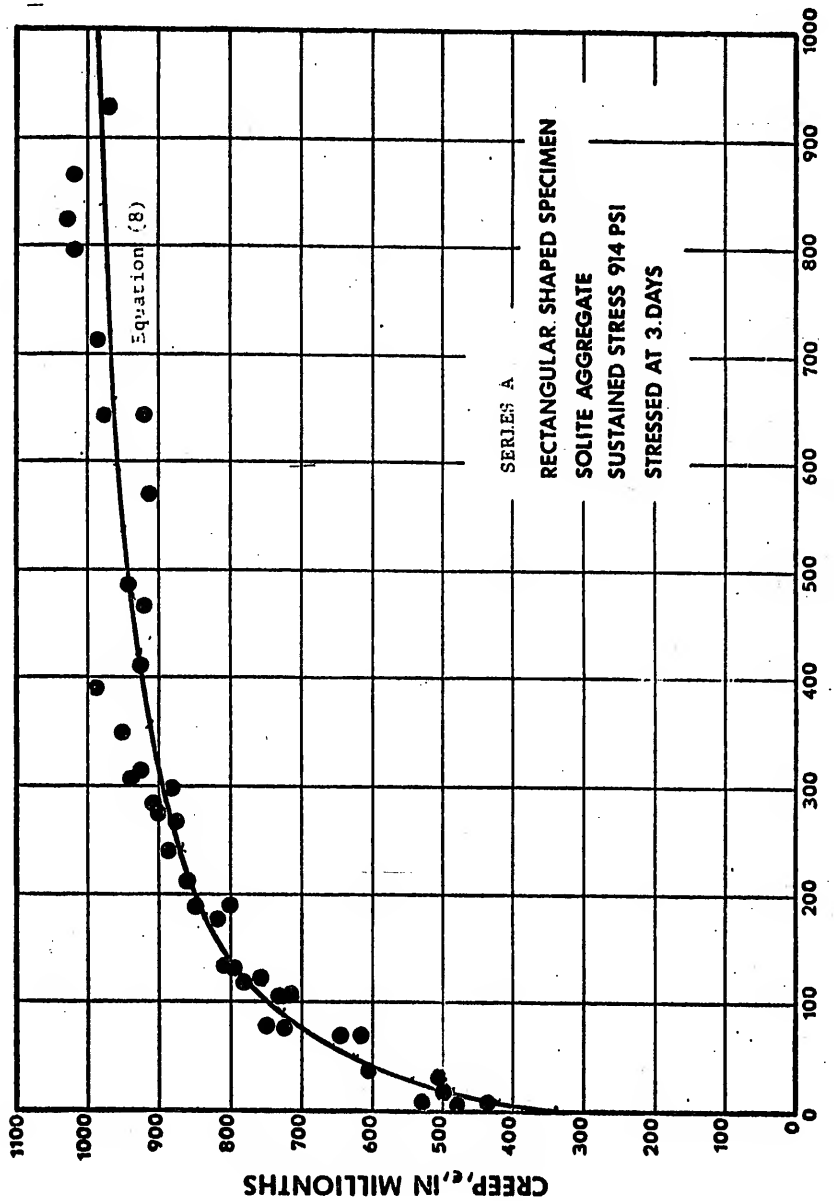

COMPARISON OF RHEOLOGICAL MODEL AND EXPERIMENTAL DATA

FIGURE 18 E

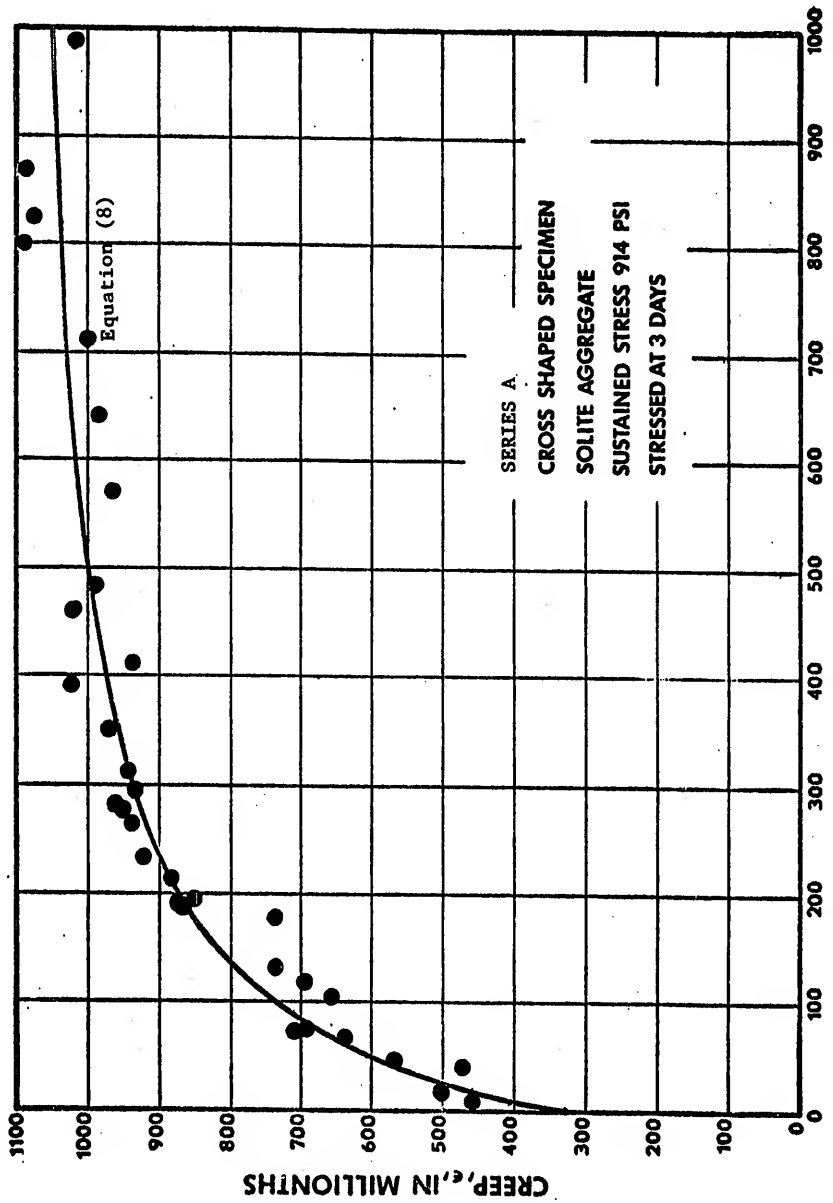

COMPARISON OF RHEOLOGICAL MODEL AND EXPERIMENTAL DATA

FIGURE 18 F

$$\epsilon = \frac{f}{E} + \left[\phi_\infty + (\phi_o - \phi_\infty)\, e^{-(c_t + c_f\,(f_o^2 - f^2))}\right](1 + \rho)\; ft + \frac{f}{E_e}\left[1 - e^{-\phi_e E_e t}\right], \quad (8a)$$

where $\rho = (2.5 + \phi_o \times 10^8)\,(f/f'_c - .30)$.

The ratio f/f'_c represents the ratio of stress level to strength for concrete being evaluated. It is tacitly assumed here that the stress to strength ratio at which proportionality ceases is about 0.30. The value for ρ may not be negative. Therefore, the value for ρ is set equal to zero for all stress levels resulting in values for f/f'_c less than 0.30.

While grouping all inelastic effects in the second term is mathematically convenient there are certain disadvantages with respect to the activity of the third term. When evaluating the delayed elastic recovery upon unloading the concrete the elastic state, or more precisely the quantum state of the molecular structure at the time of unloading determines the amount of recovery. The constant coefficients of the third term are unable to satisfactorily predict this variation. This deficiency may also affect recovery values for concrete under decreasing stress. Further investigation is required to fully understand the manner in which the elastic response coefficients vary.

B. Application of the Model to Concrete Under Decreasing Stress (Test Series B and C)

The model's coefficients were derived from the response of the specimen held under sustained stress for convenience. The application of the model to the specimens of test series B (stress decrease of 65 per cent) and C (stress decrease of 50 per cent) is therefore independent of the test results for these specimens. Figure 19 compares the model with creep test data for specimens of test series B. The model agrees with the data.

Figure 20 compares the model with creep test data for specimens of test series C. The agreement is not as good as for test series B. The apparent cause of the discrepency seems to be related to the delayed elastic element (third term) which recovers a greater amount of strain than it should. This effect was described earlier in connection with delayed elastic recovery of the specimen of series A. Not only was the average value of the structure coefficient A used in connection with elastic recovery, but the coefficient A was also declared independent of time in the derivation of the stress dependent factor for the stability coefficient. These two assumptions, based on an insufficient knowledge of the thermodynamic properties of the material with time, lead to low predicted values of concrete strain. If it were known how the coefficient A decreases with time and mix then a smaller recovery could be predicted and accuracy improved. This effect only influences creep predictions at advanced ages. The model appears to adequately predict creep in the early ages under stress. The early influence of fluidity on creep is controlled to a great extent by the third Kelvin element of the elementary model of Figure 1. This element is not greatly influenced by time beyond 20 days (Table V). Therefore the assumption of constancy of thermodynamic coefficients A for this rheological assembly does not introduce serious error.

The response of the model for test series B agrees better than the response for test series C because the error caused by the discrepency in the third term of equation (8) is proportional to stress. Since series C had a larger average stress the deviation of the model from the data will be greater.

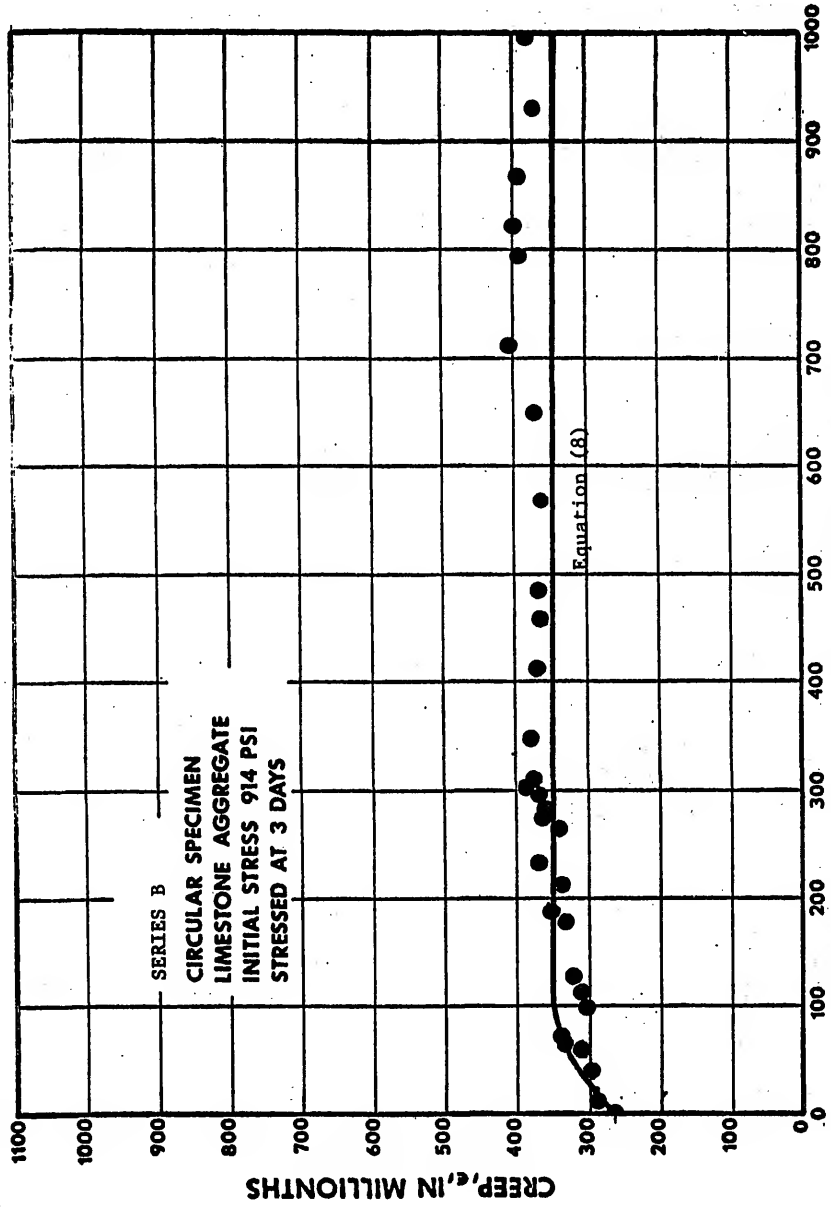

COMPARISON OF RHEOLOGICAL MODEL AND EXPERIMENTAL DATA

FIGURE 19 A

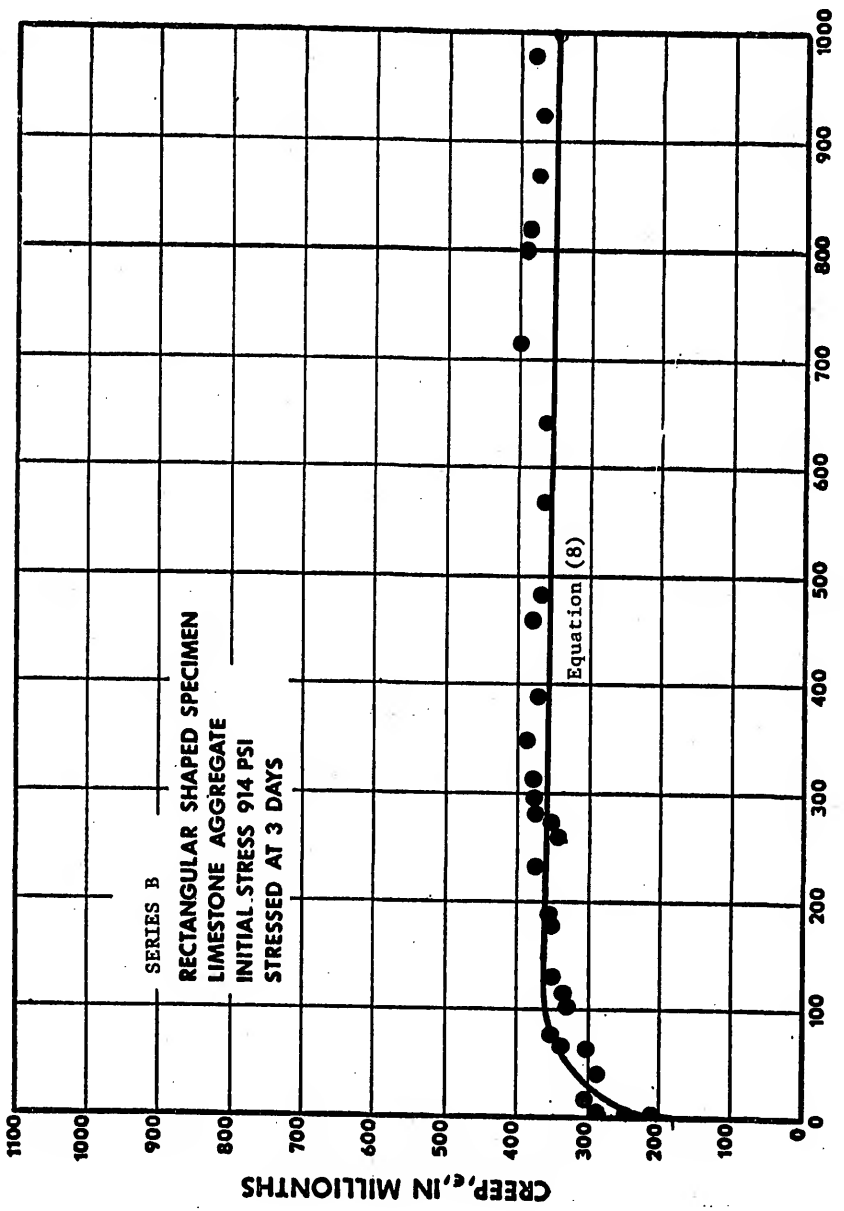

COMPARISON OF RHEOLOGICAL MODEL AND EXPERIMENTAL DATA

FIGURE 19 B

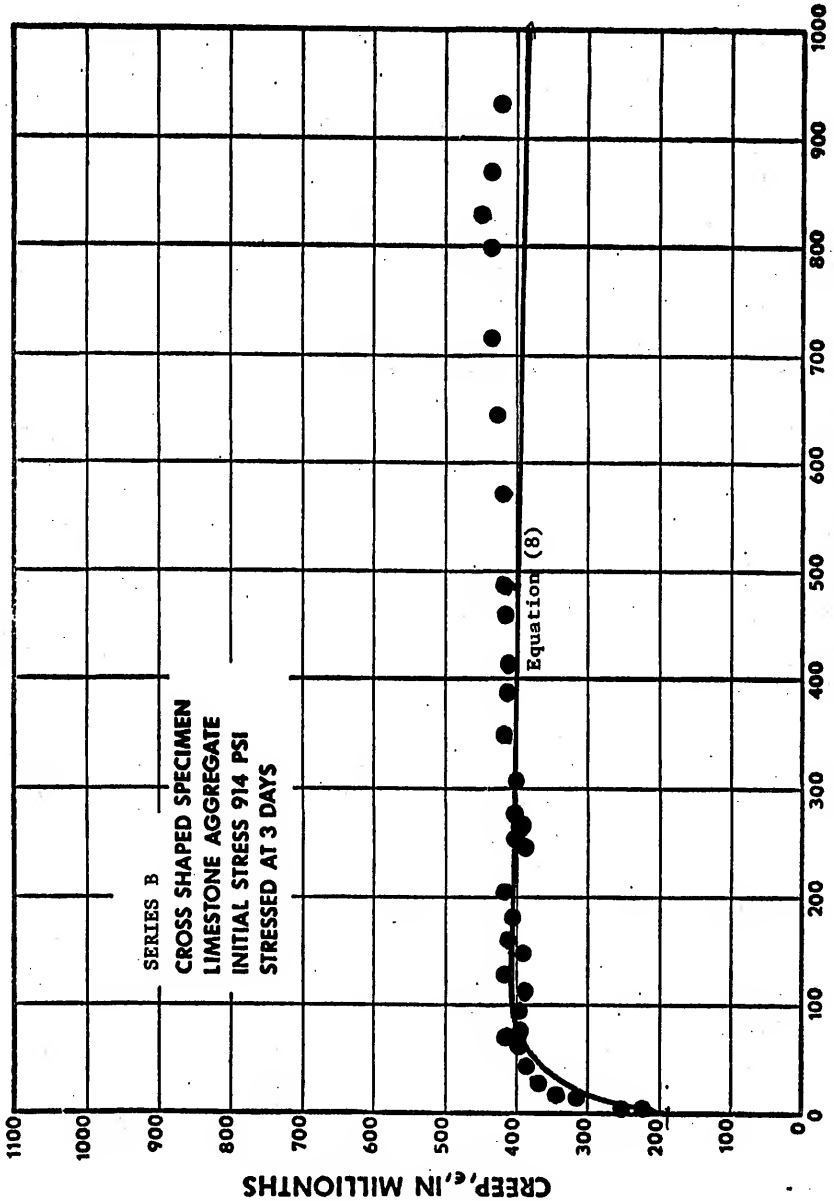

COMPARISON OF RHEOLOGICAL MODEL AND EXPERIMENTAL DATA

FIGURE 19 C

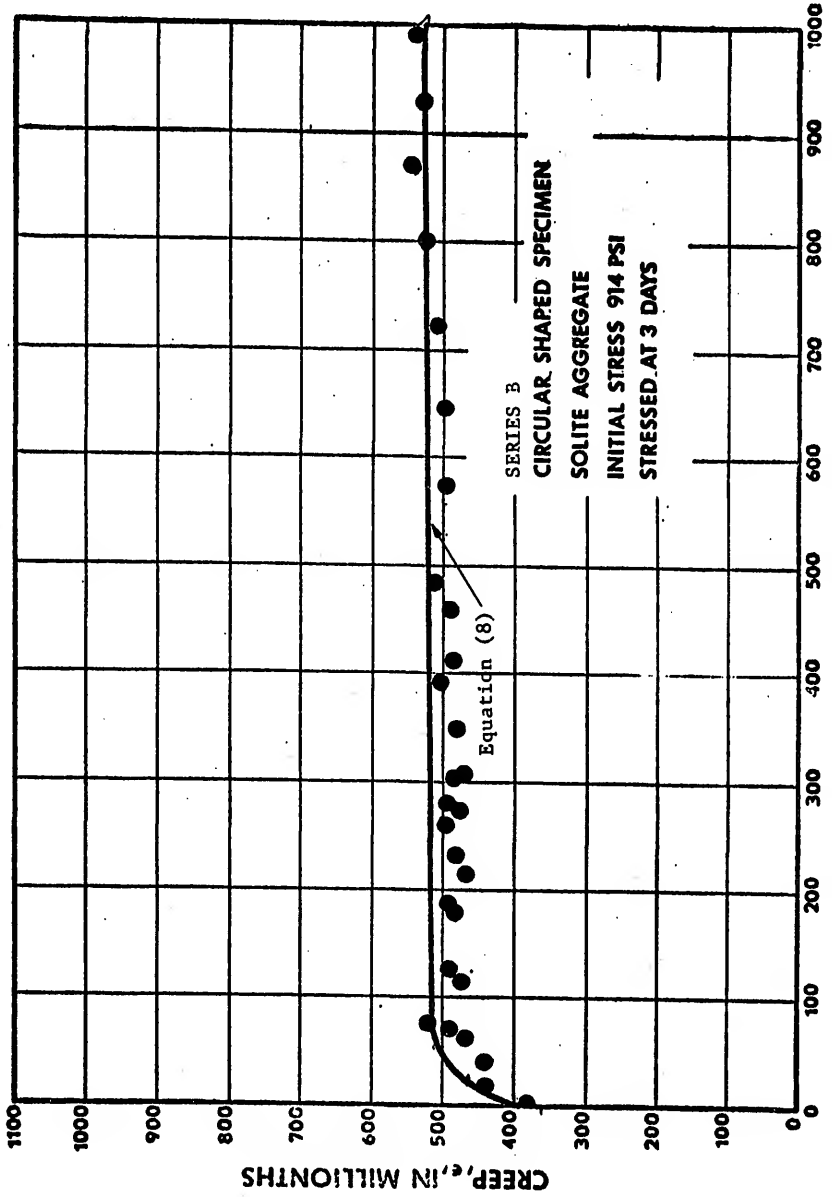

COMPARISON OF RHEOLOGICAL MODEL AND EXPERIMENTAL DATA

FIGURE 19 D

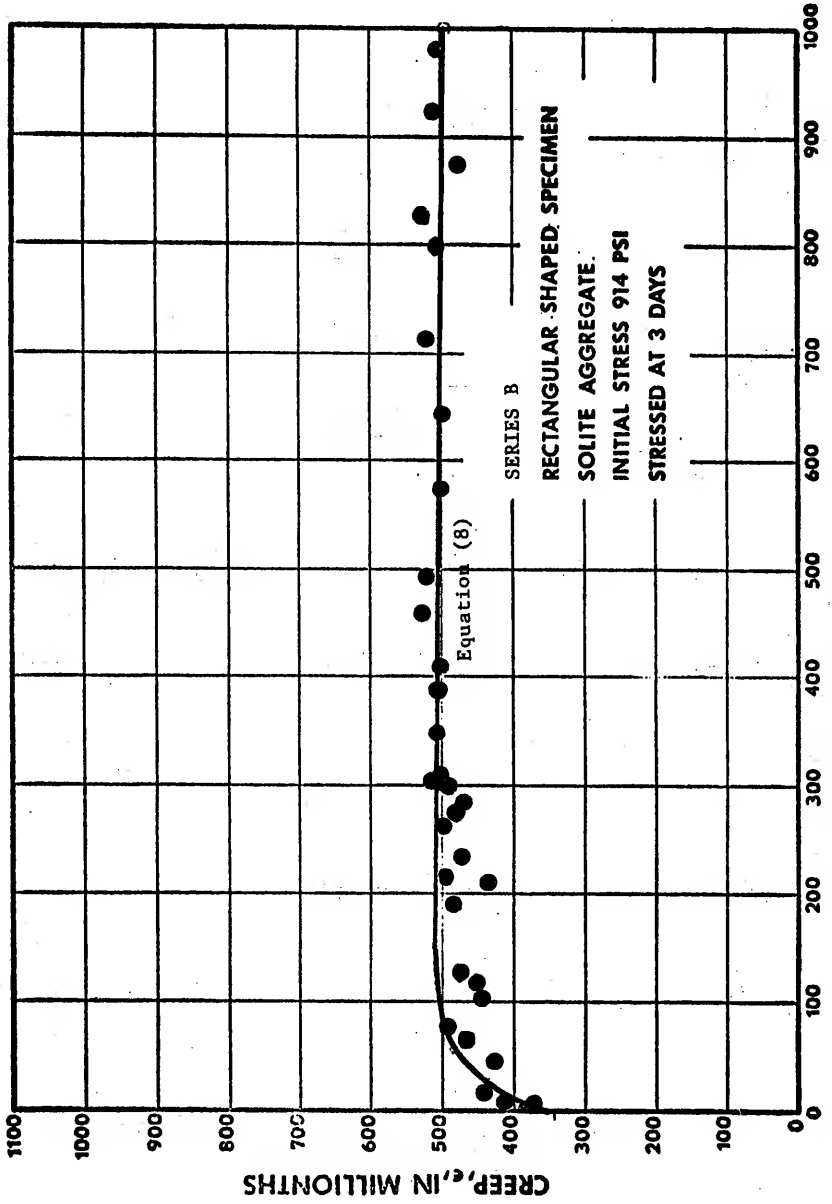

COMPARISON OF RHEOLOGICAL MODEL AND EXPERIMENTAL DATA

FIGURE 19 E

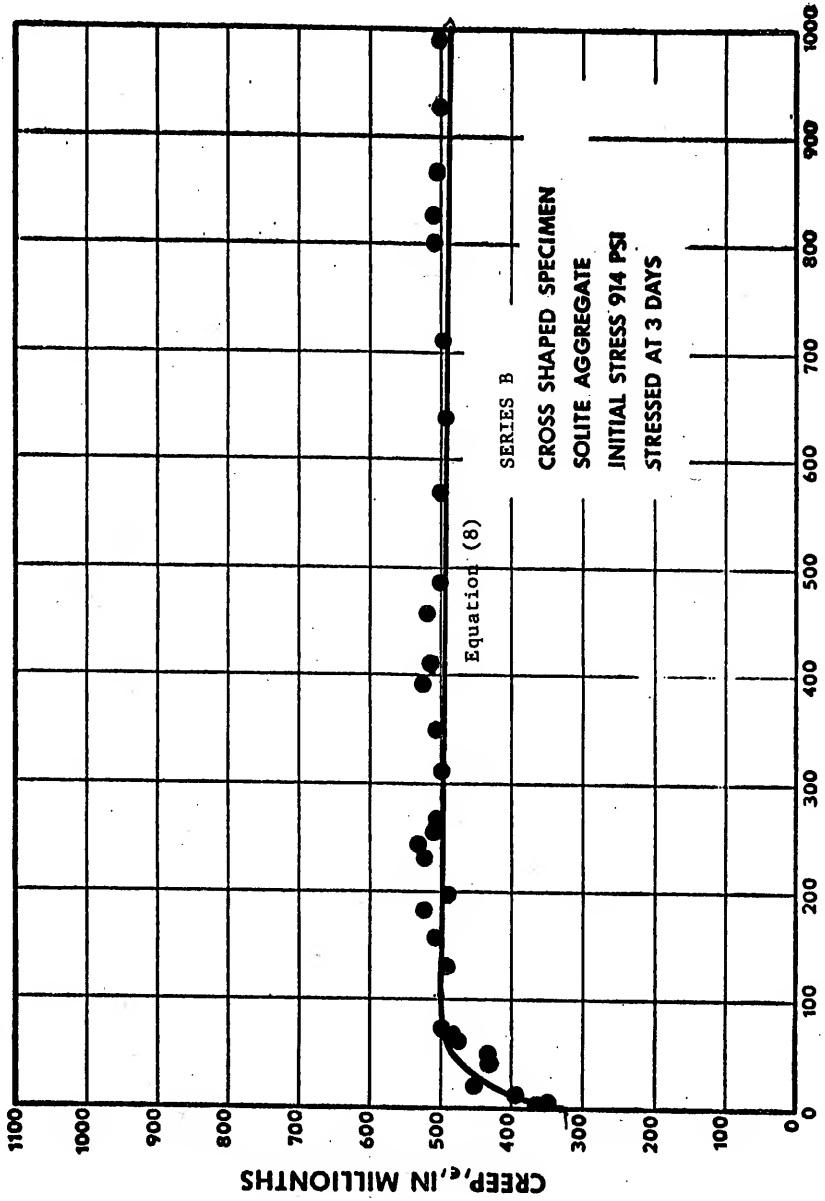

COMPARISON OF RHEOLOGICAL MODEL AND EXPERIMENTAL DATA

FIGURE 19 F

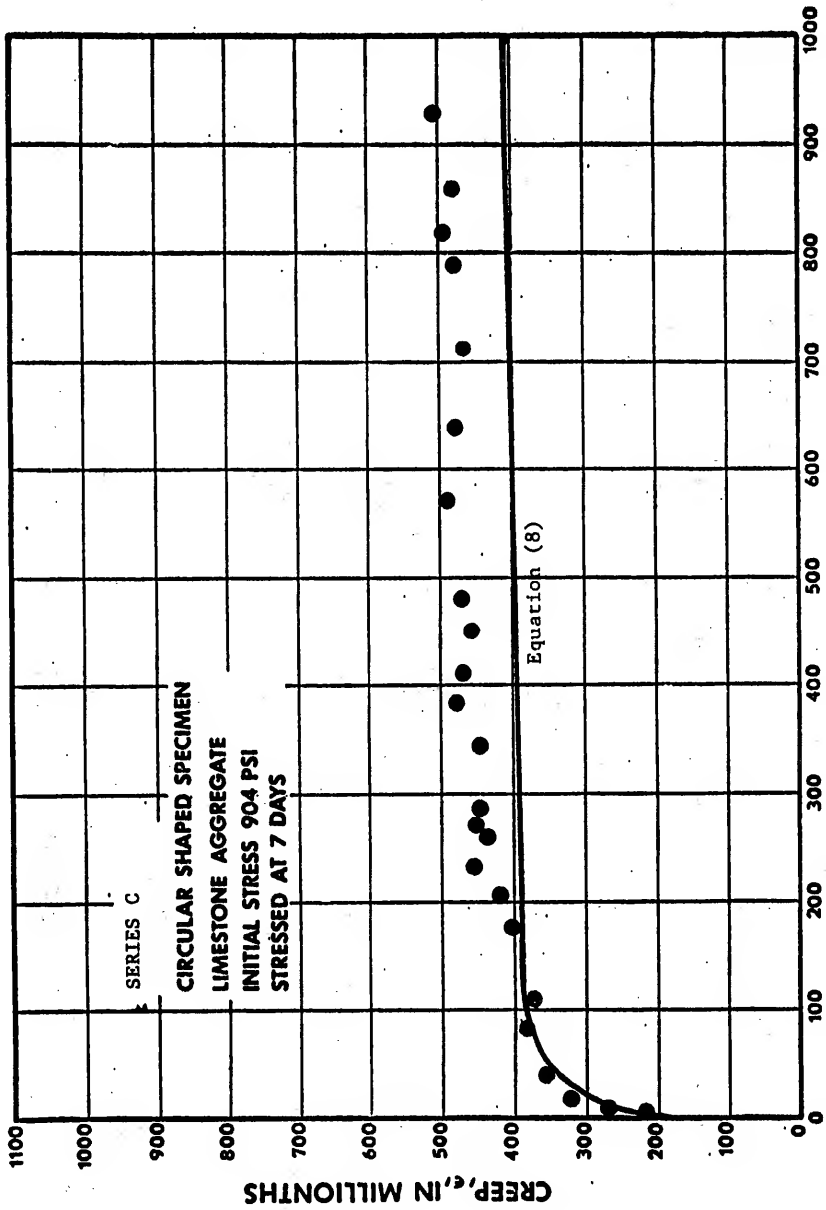

COMPARISON OF RHEOLOGICAL MODEL AND EXPERIMENTAL DATA

FIGURE 20 A

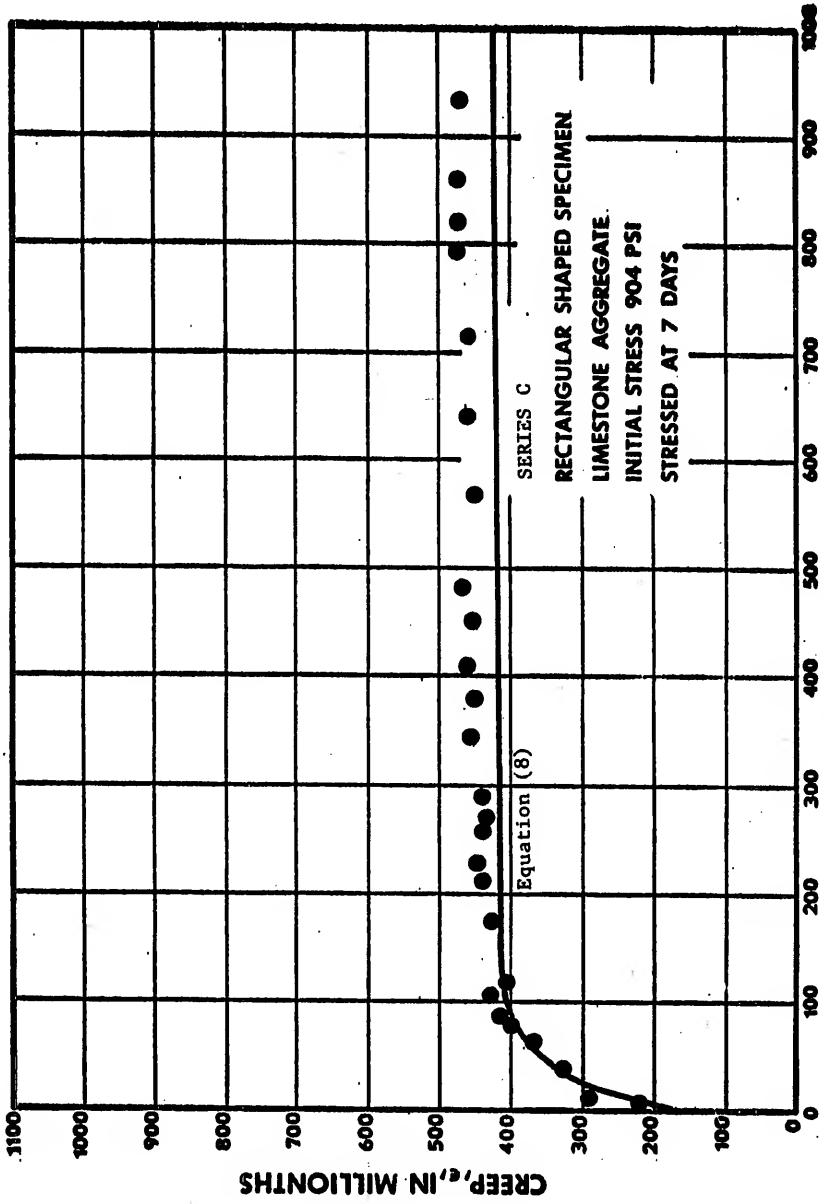

COMPARISON OF RHEOLOGICAL MODEL AND EXPERIMENTAL DATA

FIGURE 20 B

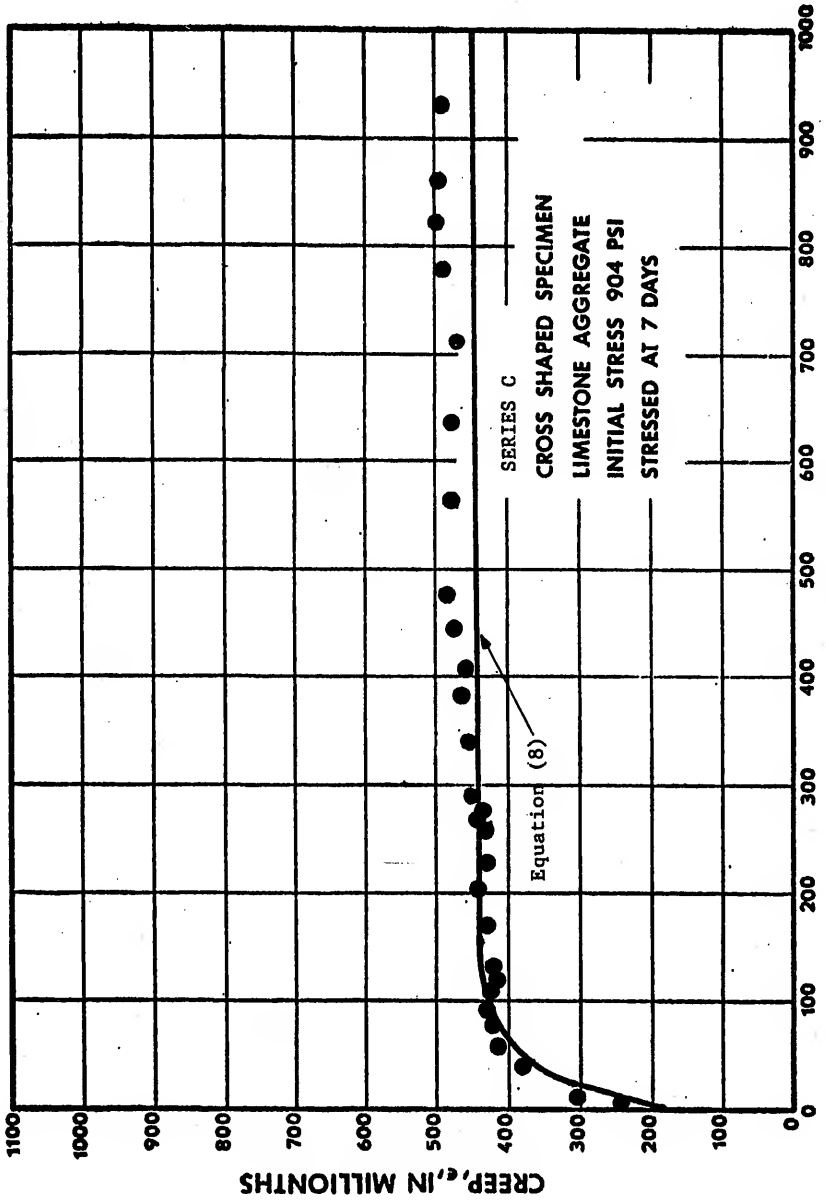

COMPARISON OF RHEOLOGICAL MODEL AND EXPERIMENTAL DATA

FIGURE 20 C

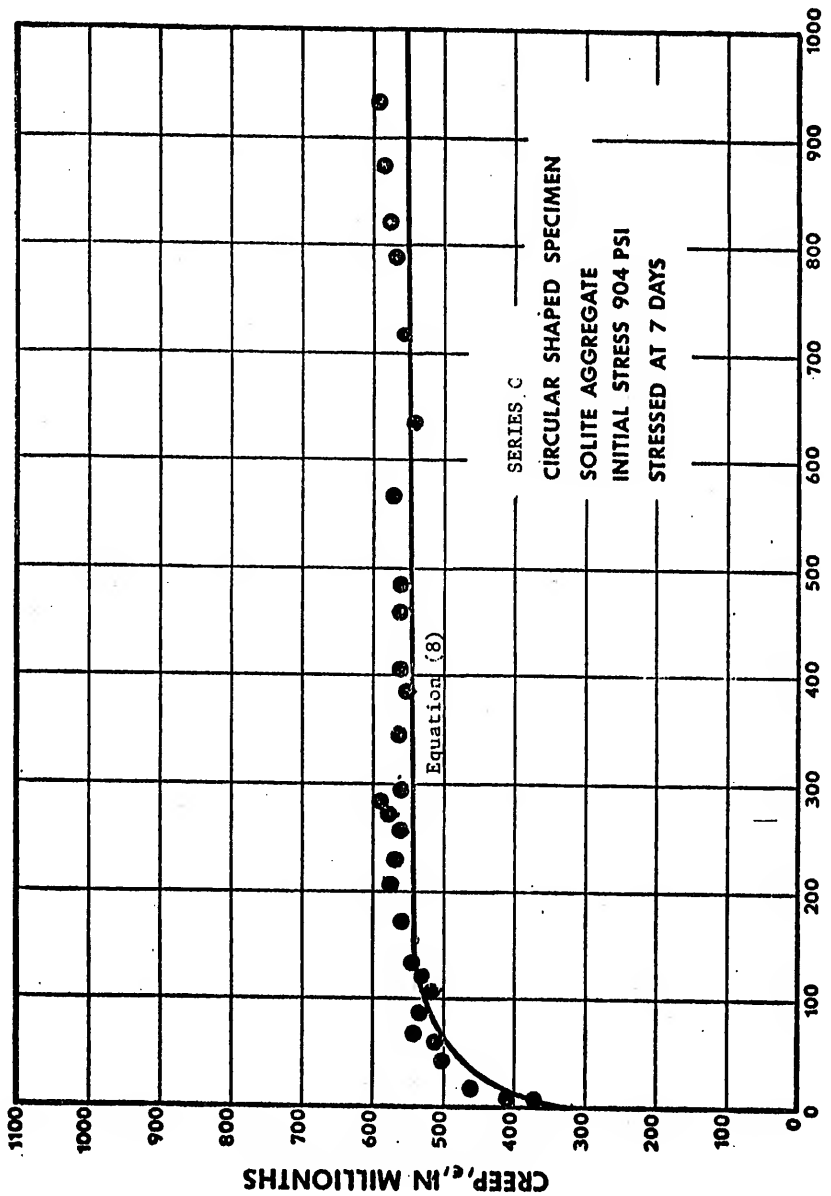

COMPARISON OF RHEOLOGICAL MODEL AND EXPERIMENTAL DATA

FIGURE 20 D

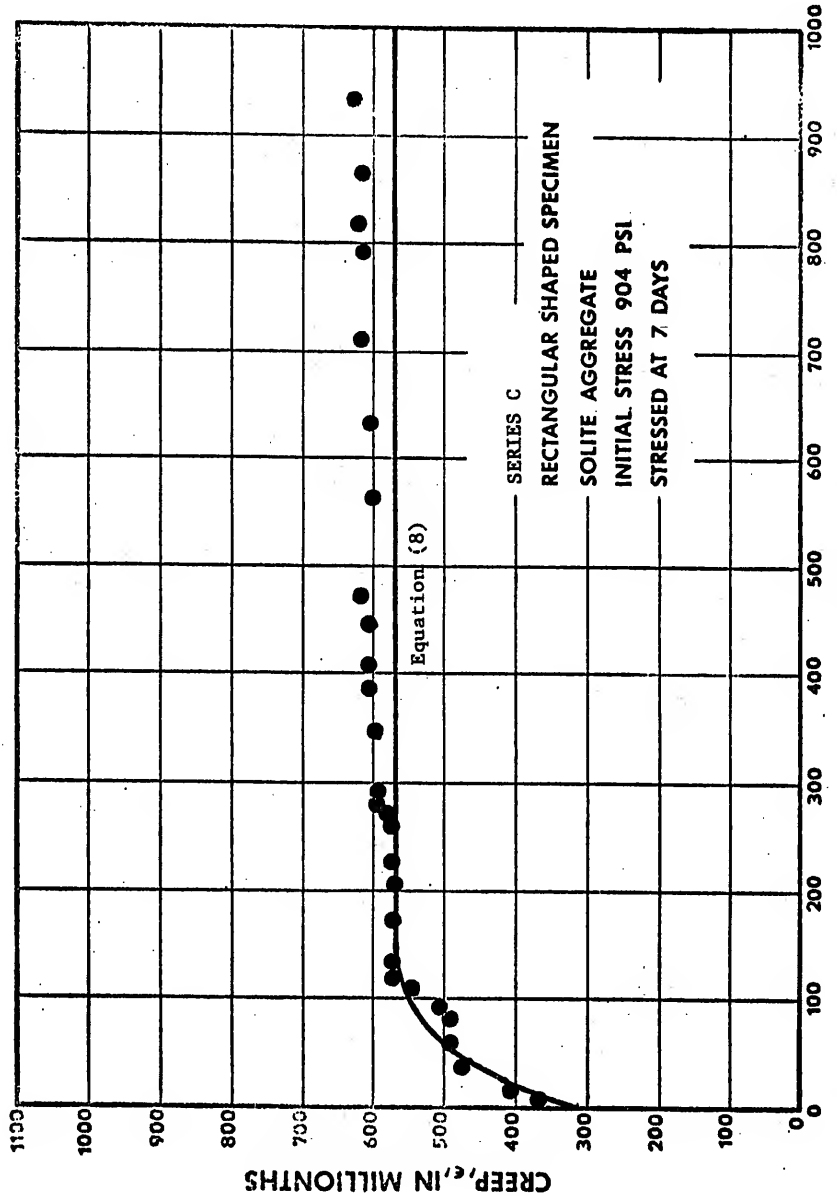

COMPARISON OF RHEOLOGICAL MODEL AND EXPERIMENTAL DATA

FIGURE 20 E

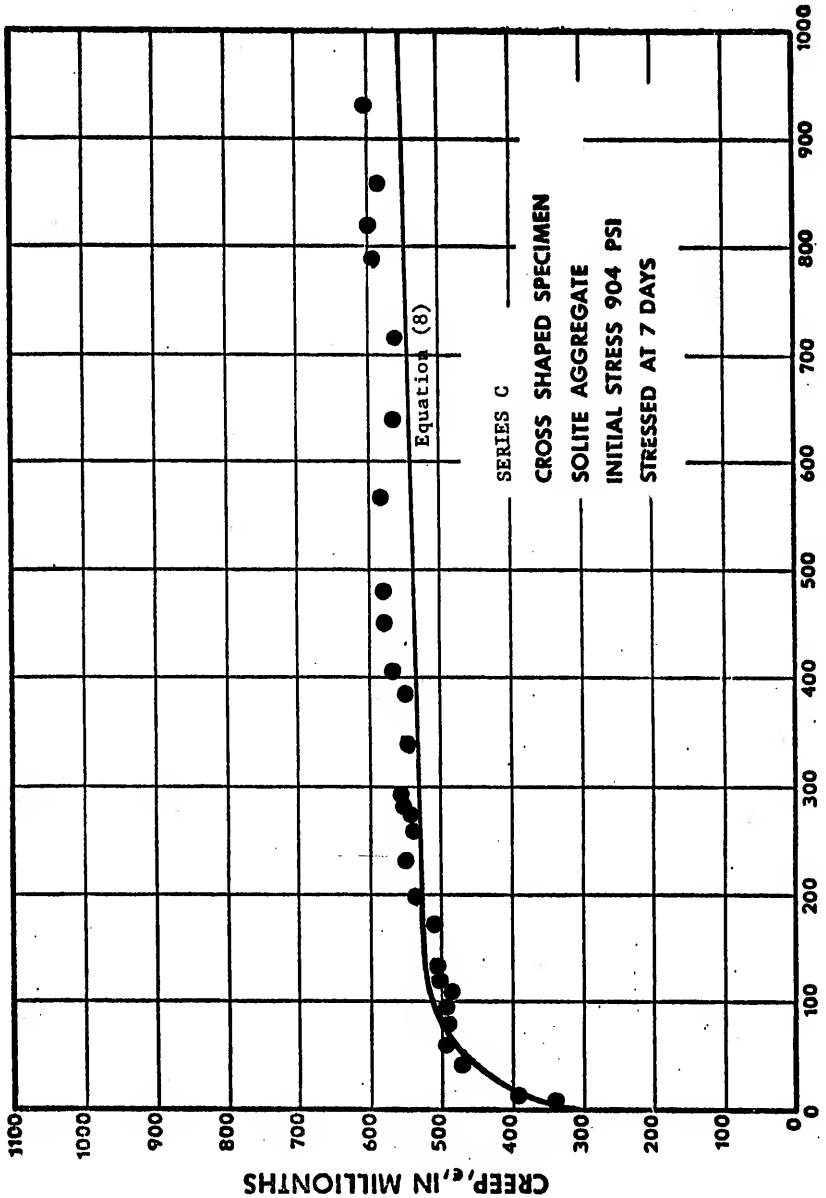

COMPARISON OF RHEOLOGICAL MODEL AND EXPERIMENTAL DATA

FIGURE 20 F

Equations (8) or (8a) are treated like any viscoelastic equation with respect to varying stress. Super-position of responses from each term is made for time intervals over which the applied stress is assumed to be constant. The solutions for test series B and C were obtained by super-position of responses over time intervals for which the stress changed by 2.0% of the original applied stress.

C. Influence of Shape on Creep

A study of the structure constants in Table IV shows the influence of shape on the transient creep components. For the size specimen used in this study shape has only a slight influence on creep behavior in limestone aggregate concrete. This effect is associated almost entirely with the action of the first rheological assembly. However, shape does significantly influence the early creep rate in lightweight aggregate concrete of the type used due to the retarded shrinkage effect. This would lead one to believe that a similar effect would result due to size difference. That is, for sufficiently longer flow paths, even in limestone concrete, where a sufficient amount of free moisture still remains in the concrete after initial hydration is completed, creep may be influenced by fluidity variations similar to the effect caused by shape in the lightweight concrete in this experiment. It seems quite likely that shape effects reported by some authors may really be an interaction between size and shape in the specimen tested.

Even though early viscous creep in the lightweight concrete was influenced by shape there appeared to be no continuation of this behavior into longer periods of time. There was no effective ultimate creep

difference among shapes from which it is concluded that the long term deterioration creep component was inversely influenced by shape and therefore tended to compensate for the initially higher creep in those specimen with high volume-to-surface area ratios.

It may be concluded that shape has a binary effect on creep behavior:

1. An increase in bonds due to greater hydration in connection with longer flow paths results in reduced viscous creep.
2. A reduction in fluidity (resulting in greater bonds) leads to reduced viscous creep. Fluidity is reduced as a result of rapid moisture loss associated with shorter flow paths.

Both effects are influenced by size also, perhaps to a greater extent. These creep effects are further altered by stress to such an extent that shape may appear not to have any influence at all. Evidence of this behavior is indicated in Table VIII wherein specimens under decreasing stress did not exhibit the same shape dependency as specimens under sustained stress over a long term period.

D. Effect of Aggregate on Creep

In addition to the interaction effects of aggregate and shape described in the previous section there was a significant influence noted relative to the stress level after a period of time. The initial elastic modulus which is dependent upon the density of the concrete was naturally smaller for the lightweight concrete thereby producing greater elastic strains. However, in addition to this expected behavior, the lightweight aggregate appeared to influence transient creep in such a way that creep in the lightweight concrete was greater under high stress and less under low stress than creep in the limestone concrete under similar stress conditions.

TABLE VIII

TOTAL OBSERVED TRANSIENT AND STEADY STATE CREEP OF CONCRETE UNDER VARYING STRESS LEVELS

After 1000 days

Type of Concrete	Shape	Creep Test Series A Micro in/in	Creep Test Series B Micro in/in	Creep Test Series C Micro in/in
Limestone	Circle	490	200	310
	Rectangle	610	200	290
Concrete	Cross	705	245	300
	Avg. 3 Shapes	600	215	300
Lightweight	Circle	575	160	275
(Solite)	Rectangle	640	175	310
Concrete	Cross	730	180	280
	Avg. 3 Shapes	650	170	290

Two different factors caused this effect. In a low stress situation the elastic properties dominate the creep behavior of the concrete. It was shown in Chapter VI, Section C that the gel in the lightweight concrete was more elastic than the gel in the limestone concrete. Therefore, elastic recovery was greater in the lightweight concrete resulting in a smaller ultimate creep. Under high stresses the irrecoverable term became dominant.

Due to its greater rate of irrecoverable strain, manifested by the relative magnitudes of the coefficients A (Table IV) for the first rheological assembly, the lightweight concrete experienced greater creep over a long period of time. This creep is undoubtedly a result of the permanent surface distortions of the coarse aggregate particles under stress.

Reference to the comparisons made in Table VIII between average transient creep for the two concrete types provides a clear picture of the stress level effects on creep. Under high stress, test series A, creep in the Solite concrete was greater whereas under low stress, test series B, creep in the Solite concrete was less than in the limestone concrete.

CHAPTER VIII

CONCLUSIONS

A. General

It has been shown that creep behavior may be adequately predicted from macroscopic observations by employing structure parameters in a rheological model. These parameters include the change in fluidity due to natural aging effects under stress and the change in fluidity due to stress variations. A rheological model may be constructed with structure coefficients from statistical mechanics theory which will predict, reasonably well, the creep of concrete from a consideration of the response from a test of several specimens sustained at low constant stress. The parameters which are used in this model represent:

1. The rate of transition of the gel from fluid to solid.
2. The total expected change in the structure of the gel.
3. The purely elastic action of the gel and aggregate system.

The many aspects of the influence of mix on the viscoelastic nature of concrete precludes development of a generalized creep model at this time. It is proposed in this report that an analysis of creep behavior for a particular concrete is possible and a prediction made from test specimens of standard dimensions. The tests should be conducted on concrete from the same mix as the prototype structure and in the same general environment. Using equation (8a) the creep may be predicted at any time under varying stress conditions and for any conventional size or shape of structure. Mass concrete structures do not satisfy conditions for use of this model.

B. Test Results

Maintaining equal paste contents and nearly equal early strength characteristics for two concrete mixes produced creep responses as follows:

1. Shape did not appear to influence the early creep of specimen of the size tested when rapid shrinkage occurred. If for some reason, such as moisture retaining aggregate or greater volume for example, a certain amount of free moisture is maintained in the gel beyond the initial phase of early hydration shape may become influential as it affects the rate of change of fluidity. This creep response, in the early stages of hydration, to shape is due largely to a rapid decrease in fluidity in high early strength concretes. Since it is a rate comparison of fluidity change which is being made therefore, normal strength-gain concretes should show a greater influence of shape on creep than high early-strength concretes.

2. Coarse aggregate has a diverse influence on the elastic properties of concrete. It is already known that density influences the initial elastic modulus (ACI code, 1963). An increase in density results in concrete with greater elastic modulus. However, density also is a measure of the rigidity or stiffness of the aggregate, and aggregates which are stiffer than the gel structure appear to produce a less elastic nature over a long period than aggregates which are less stiff for equal strength concretes. This result stems from the fact that the gel in concrete with stiffer coarse aggregate must have poorer quality than the gel in equal strength concrete made from less stiff coarse aggregate.

Whereas the gel behavior is more elastic in the lightweight concrete, the long term non recoverable creep is greater because of more general

permanent damage to the rough and cellular surface of the softer aggregate by the stiffer gel. In concrete with harder aggregate crushing of the gel is localized and less irrecoverable creep results.

3. Water-cement ratio influences the initial fluidity and the strength gain. Lower water-cement ratios materially reduce the initial creep of concrete by producing a lower initial fluidity and they reduce the over-all creep activity because of an increased level of activation energy.

4. The amount of moisture retained by the coarse aggregate in lightweight concretes has a significant binary affect on the fluidity change after initial hydration. On one hand the supply of moisture during aging produces greater levels of activation energy from increased hydration thereby reducing creep and on the other hand the fluidity is increased as moisture is absorbed by the gel matrix thereby increasing creep. While these two factors tend to offset each other, over the long period either effect may become dominant depending on the test conditions. Therefore the creep response may take different aspects dependent upon the quantity of moisture included in the coarse aggregate at the time of mixing.

C. The Model for Creep Prediction

In order to take into account variations of coarse aggregate, the model was developed with a parameter M. M is considered to repreaent a property of the coarse aggregate of the concrete. Evaluation of M, however, was outside the scope of this inveatigation. In order to satisfy the model M was found to be equal to 0.0 for the limestone concrete used in this study, and it was equal to 1.0 for the lightweight concrete used. It is presumed

that these aggregates represent, to all intent and purpose, the limits of coarse aggregate structure. That is, for soft, porous aggregate, such as Solite, M achieves a maximum value of 1.0 and for hard, dense aggregate, such as limestone, M has a minimum value of 0.0. Thus it is presumed that M varies between the limits of 0.0 and 1.0 for all types of coarse aggregate. However there is no experimental evidence to substantiate this assumption. For this reason it is suggested that these values for M be applied only to structural concretes with similar aggregates to those used in this investigation until verification can be established.

On this basis equation (8) may be employed to predict creep in concrete from a creep test on standard six-inch diameter specimens under low, sustained loading. The parameters in equation (8) may be determined as follows:

ϕ_∞ - Equation (29a)

ϕ_o - Equation (30)

c_t - Equations (22), (25), (31) in consecutive order

c_f - Equation (28) employing equations (32) and (33).

The rheological parameters required to satisfy the above relations are obtained by conventional rheological theory as described in reference 22.

In order to expand the accuracy of equation (8), results from research reported by Freudenthal and Roll[4] were incorporated to account for the non-linear relationship between creep and stress at high stress levels. Accordingly, equation (8a) may be used when stress levels exceed 0.30 f'_c.

D. Procedure for Using the Model

In order to facilitate the use of the model a brief procedural outline is presented.

If it is desired to understand the behavior of a structural concrete in service with regard to its creep character, a test series may be undertaken on about four 6-inch concrete cylinders under low sustained stress of approximately 20 per cent of f'_c.

1. In normal environments subjected to seasonal variations the concrete in the structure will eventually achieve a state where the ultimate fluidity (ϕ_∞) is very small and may be assumed equal to zero. Therefore the test need only be run on the concrete cylinders long enough to establish the slope and intercept of Rosa' parametric creep curve. Perhaps up to 90 days of testing may be required. The averaged data from the four specimens will be plotted in the form of a straight line

$$t = b + a\, t/\epsilon ,$$

where t is the ordinate and t/ϵ is the abscissa. The intercept b and the slope a are obtained directly, and they may be substituted into the creep equation (1)

$$\epsilon = at/(b + t) , \qquad (1)$$

2. Having established the basic parametric relationship between creep strain and time a linear rheological model may be developed as shown in Figure 1 which is represented by equation (2). The method for determining the parameters in equation (2) and the procedure for developing the linear visco-elastic model is presented in reference 22, or any treatise on conventional rheological theory.

3. The solution from step 2 provides knowledge of the parameters ϕ_∞ and E for the final model shown in Figure 9 represented by equations (8) or (8a). E is the elastic modulus. ϕ_∞ is calculated using equation 10. If the preliminary test is not carried sufficiently far to evaluate ϕ_∞, it may be set equal to zero with very little probable error.

4. A rate process solution must then be performed on each of the Kelvin elements from step 2. Equation (12) represents the behavior of each Kelvin element. To represent the rate of creep as a function of stress in the form of equation (13) an iteration procedure is performed. In order to solve for the coefficients A and B in equation (13), $\dot{\epsilon}$ and f_D must be determined for each element in accordance with equations (17) and (16) respectively at corresponding times. Equation (13),

$$\dot{\epsilon} = A \sinh B f_D \tag{13}$$

may now be solved by the iteration procedure outlined in Appendix C. A value for the coefficient B is assumed and substituted into each of the two equations for A given in Appendix C. All values are known for the summations in each equation. The summations are made over time increments and the value of A is calculated from each equation and compared. Each step in the iteration process is performed with a different value for B. When the difference between the calculated values of A begins to deviate from zero, as shown in Appendix C, these values of A and B correspond to solution of the rate equation (13).

The summations taken over time increments are summed to the time at which prediction is required. This process is quite tedious and lends itself quite conveniently to computer solution.

5. The rheological assembly corresponding to elastic behavior is selected as described earlier in the report. The remaining Kelvin elements may then be used to determine ϕ_o from equation (11)

6. To determine the stability coefficient c_t, the viscous strains (ϵ_{vis}) are determined from the simple rheological model of figure 1 by eliminating the elastic components.

$$\epsilon_{vis} = ft/\lambda_\infty \quad + \sum_{viscous} f/E_n \ (1 - e^{-\phi_n E_n t}) \quad .$$

The summation is made over all remaining Kelvin elements after the delayed elastic term has been removed. The coefficient c_t for the test cylinder at any time is determined from equations (22) and (23). This procedure results in a set of values of c_t corresponding to increasing values of time. Therefore a mathematical solution for c_t is required in the form presented by equation (24a)with c_n terms, corresponding to the control cylinder, substituted for the b_n terms.

7. In projecting the test results to predict creep in a prototype member the shape and size influence must be considered. The weighted flow path distance (w) is a measure of each effect. The weighted distance for the 6-inch cylinder is equal to 1.0. For any other member weighted distance may be calculated by dividing the member cross-section into small increments of area, and multiplying these small areas by their respective shortest distance to the member's surface then dividing the product by the total cross-sectional area.

8. The creep behavior of the concrete is influenced greatly by the coarse aggregate. Only two types of aggregate have been tested for their influence on creep, Brooksville limestone and Florida Solite. Since Florida Solite

is a porous aggregate, its capacity to bear moisture is great. Values for the aggregate coefficient M, representing the influence of the aggregate on creep were found to be zero for the limestone aggregate and 1.0 for Solite aggregate with 24 per cent initial moisture by weight. It may be presumed that the value of 1.0 will vary for different moisture contents, however no experimental evidence is available.

9. The aging coefficient of stability may now be projected for the member response from the test results. Employing equations (25) and (24a), c_t may be evaluated for the prototype member.

In similar fashion, ϕ_∞ and ϕ_o may be projected to the prototype member as outlined in section C of this chapter. Also rheological structure coefficients A_n for the long term and short term transient conditions of creep may be projected by using equations (32) and (33) respectively.

10. The creep at any time may now be obtained for any stress history by employing the rheological model of Figure 9 represented by equations (8) or (8a). Since the equation is linear with respect to stress (f), in order to obtain solutions under varying stress conditions piecewise time increments having constant stress must be employed and superposition of the effects must be made. This procedure is outlined in detail in reference 22.

In employing equation (8), the value of the stress dependent stability coefficient (c_f) is obtained simultaneously by equation (28).

If the stress at anytime exceeds $0.30\, f'_c$ the non-linear components of creep must be considered. Then equation (8a) is applicable without variation in the procedure.

APPENDICES

APPENDIX A

CALCULATION OF STRAIN FROM THE ACTIVATION OF A RHEOLOGICAL ASSEMBLY

The strain for one Kelvin element is

$$\epsilon = \frac{f}{E_n} \left(1 - e^{-\phi_n E_n t}\right) \quad . \tag{A-1}$$

The strain rate written in terms of the structure coefficients is

$$\frac{d\epsilon}{dt} = \dot{\epsilon} = A \sinh B f_D \quad . \tag{A-2}$$

The stress f_D may be written in terms of time by substituting equation (A-1) into equation (16)

$$f_D = f - \epsilon E_n = f e^{-\phi_n E_n t} \quad . \tag{A-3}$$

Solving equation (A-3) for time t yields,

$$t = - \frac{1}{\phi_n E_n} \ln \frac{f_D}{f} \quad . \tag{A-4}$$

Also differentiating (A-3) with respect to time yields

$$\frac{df_D}{dt} = - f \phi_n E_n e^{-\phi_n E_n t} \tag{A-5}$$

from which

$$dt = - \frac{1}{f} \frac{1}{\phi_n E_n} e^{\phi_n E_n t} \, d f_D \quad . \tag{A-6}$$

Rewriting equation (A-2) and integrating yields the strain

$$\epsilon = A \int \sinh B f_D \, dt \quad . \tag{A-7}$$

Substituting equation (A-4) and (A-6) into (A-7) produces

$$\epsilon = -A \frac{1}{f} \frac{1}{\phi_n E_n} \int \frac{f}{f_D} \sinh B f_D \, df_D \qquad \text{(A-8)}$$

which when integrated yields

$$\epsilon = -A \frac{1}{\phi_n E_n} \left[\frac{1}{2} \left[\left(\ln f_D + \frac{B f_D}{1 \cdot 1!} + \frac{B^2 f_D^2}{2 \cdot 2!} + \frac{B^3 f_D^3}{3 \cdot 3!} + \ldots \right) - \left(\ln f_D - \frac{B f_D}{1 \cdot 1!} + \frac{B^2 f_D^2}{2 \cdot 2!} - \frac{B^3 f_D^3}{3 \cdot 3!} + \ldots \right) \right] \right] + C \qquad \text{(A-9)}$$

simplifying to

$$\epsilon = -A \frac{1}{\phi_n E_n} \left[\frac{B f_D}{1 \cdot 1!} + \frac{B^3 f_D^3}{3 \cdot 3!} + \frac{B^5 f_D^5}{5 \cdot 5!} + \ldots \right] + C \, . \qquad \text{(A-10)}$$

Initially, at $t = 0$, $f_D = f_o$, $\epsilon = 0$, therefore,

$$C = A \frac{1}{\phi_n E_n} \left[\frac{B f_o}{1 \cdot 1!} + \frac{B^3 f_o^3}{3 \cdot 3!} + \frac{B^5 f_o^5}{5 \cdot 5!} + \ldots \right] \qquad \text{(A-11)}$$

which when substituted into (A-10) yields

$$\epsilon = A \frac{1}{\phi_n E_n} \left[\frac{B (f_o - f_D)}{1 \cdot 1!} + \frac{B^3 (f_o^3 - f_D^3}{3 \cdot 3!} + \frac{B^5 (f_o^5 - f_D^5)}{5 \cdot 5!} + \ldots \right] \qquad \text{(A-12)}$$

or,

$$\epsilon = A \frac{1}{\phi_n E_n} \sum_{j=1,2}^{\infty} \frac{B^i (f_o^i - f_D^i)}{i \cdot i!} \, , \qquad \text{(A-13)}$$

where $i = 2j - 1$.

APPENDIX B

DEVELOPMENT OF THE STRUCTURAL FACTORS FOR COEFFICIENT OF STABILITY

The influence of aging and normal stress, f, is known to change the flow characteristics of concrete. The shear stress on any element is equal to f/2 for a uniaxial stress f. According to Reiner [3] fluidity is related to stress squared ($f^2/4$). The coefficient of stability of the concrete structure may be written as a function of the time, and stress rate of change of fluidity of the material. If all influences on structural stability are included in this coefficient a general relation will result. Fluidity changes differently with time under varying stress conditions. Therefore the structural stability coefficient must be an interaction function of time and stress. Let

$$X = (\phi - \phi_\infty) \Big/ - \frac{\partial^2 \phi}{\partial (f^2/4) \partial t} \qquad \text{(B-1)}$$

be the generalized form of the structural stability coefficient.

According to Reiner [3] aging of the mix alters its physical properties. Since the values of all constants of physical state of the mix are affected, when the numerical value of a constant is given the corresponding physical state must also be given with regard to temperature and pressure. If these are not mentioned, one may assume that the constant is changing with the physical states of the mix. Therefore X may be assumed to vary with time and we may therefore separate the structural stability coefficient into time and time-stress components.

If the structural stability coefficient X is composed of two factors, one a time dependent factor c_t related to aging, and the other a factor c_f related to stress dependent variations with time, then the general form of the structural stability coefficient may take the form

$$\frac{1}{X} = -\frac{\partial c_t}{\partial t}\frac{\partial c_f}{\partial f} + \frac{\partial^2 c_f}{\partial t \partial f} - \frac{\partial c_f}{\partial t}\frac{\partial c_f}{\partial f} \quad , \tag{B-2}$$

where c_t is the aging component of the structural stability coefficient, dependent on time only.

c_f is the stress dependent component of structural stability, dependent on time and stress.

The negative signs are applied because X increases with increasing time whereas X decreases with increasing stress.

The boundary conditions for equation (B-1) are:

$$\text{at } t = 0 , \quad \phi = \phi_o \text{ and } f = f_o \tag{B-3}$$

$$\text{at } t = \infty , \quad \phi = \phi_\infty \text{ approximately} . \tag{B-4}$$

For the boundary conditions (B-3) it is assumed that loading is accomplished before the viscosity changes by a significant amount. In the application of the methods for determining viscosity of the mix, a load must be applied to the concrete. Therefore the initial viscosity is assumed to be the viscosity at the time load is applied.

The solution of equation (B-1) is achieved by rewritting in the form

$$\frac{\partial^2 (\phi - \phi_\infty)}{(\phi - \phi_\infty)} = -\frac{\partial (f^2/4) \partial t}{X} . \tag{B-5}$$

The solution of equation (B-5) is

$$\phi = \phi_\infty + Ae^{-Ct} e^{-Cf} , \tag{B-6}$$

where C_t is a function of time only and C_f is a function of stress and time. Applying boundary conditions (B-3) results in a solution for A

$$A = \phi_o - \phi_\infty \quad . \tag{B-7}$$

This solution tacitly implies that the components C_t and C_f are proportional to time and stress as follows:

$$C_t = c_t\,(t) \tag{B-8}$$

$$C_f = c_f\,(f^2{}_o - f^2) \quad . \tag{B-9}$$

Boundary condition (B-4) is satisfied for any stress change condition. The equation for the change in fluidity under varying time and stress conditions is written

$$\phi = \phi_\infty + (\phi_o - \phi_\infty)\, e^{-(c_t(t) + c_f\,(f^2{}_o - f^2))} \quad . \tag{B-10}$$

Increases in stress over the initial stress is seen to increase fluidity and creep, whereas decreases in stress from the initial applied stress decreases fluidity and creep. Since linear proportionality is implied by the component c_t the parameter t is removed from equation (B-10). Therefore

$$\phi = \phi_\infty + (\phi_o - \phi_\infty)\, e^{-(c_t + c_f\,(f^2{}_o - f^2))} \quad . \tag{B-11}$$

APPENDIX C

METHOD FOR DETERMINATION OF THE COEFFICIENTS IN THE RATE PROCESS EQUATION

$$\dot{\epsilon} = A \sinh Bf$$

The computer program developed by Herrin and used by Majidzadeh[10] determines the value of the coefficient A from the known initial stress and complete strain data for a Kelvin element. The value of A calculated from each of the two solutions

$$A_1 = \frac{\Sigma_t \frac{f}{\lambda_n} e^{-\phi_n E_n t} \sinh Bf_D}{\Sigma_t \sinh^2 Bf_D} \qquad \text{(C-1)}$$

and

$$A_2 = \frac{\Sigma_t \frac{f}{\lambda_n} e^{-\phi_n E_n t} f_D \cosh Bf_D}{\Sigma_t f_D \sinh Bf_D \cosh Bf_D} \qquad \text{(C-2)}$$

are compared for successively approximated values of B. Solution for the values of A and B is declared at the iteration step in which the compared values of A begin to steadily deviate from one another. The development of equations (C-1) and (C-2) were by M. Herrin, Department of Civil Engineering, University of Illinois, Urbana, Illinois.

Figure C-1 illustrates the typical mode of deviation of the A values for each iteration step and the method of solution of the transient creep associated with each rheological assembly for a single specimen.

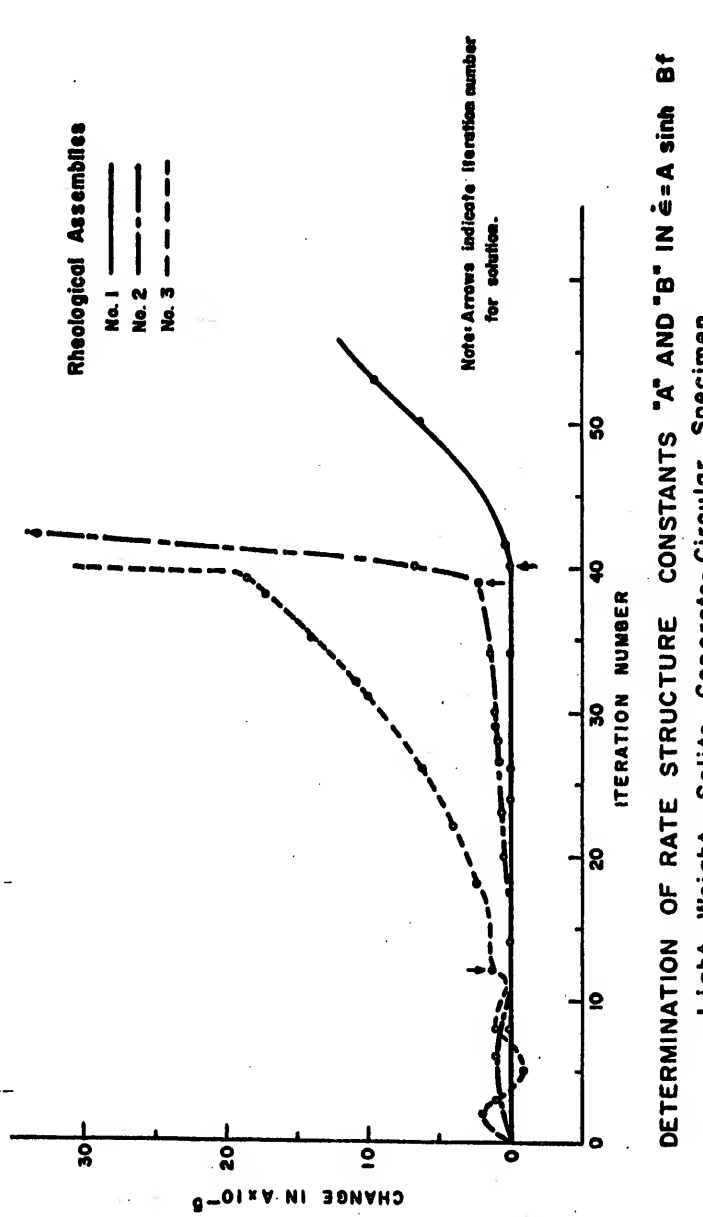

DETERMINATION OF RATE STRUCTURE CONSTANTS "A" AND "B" IN $\dot{\varepsilon} = A \sinh Bf$
Light Weight- Solite Concrete; Circular Specimen

Figure C-1

LIST OF REFERENCES

1. Troxell and Davis, H. E., "Composition and Properties of Concrete," McGraw-Hill Book Company, 1956, New York.

2. Ali, I., and Kesler, C. E., "Rheology of Concrete - A Review of Research," T. and A. M. Report #636, Department of Theoretical and Applied Mechanics, University of Illinois.

3. Reiner, Marcus, "Deformation and Flow," H. K. Lewis and Company Ltd., 1949, London.

4. Freudenthal, A. M., and Roll, F., "Creep and Creep Recovery of Concrete Under High Compressive Stress," Proceedings, American Conc. Inst., V. 54, 1958, pp. 1111-1142.

5. Glucklich, J., and Ishai, O., "Creep Mechanism in Cement Mortar," Proceedings, American Conc. Inst., V. 59, No. 7, 1962, p. 923.

6. Eyring, H., "Viscosity, Plasticity and Diffusion as Examples of Absolute Reaction Rates," Journal of Chem. Physics, V. 4, No. 4, Apr. 1936. Glasstone, Laidler and Eyring, " The Theory of Rate Processes," McGraw-Hill Book Company, 1941, New York.

7. Ross, A. D., "Concrete Creep Data," The Structural Engineer, V. 15, No. 8, 1937.

8. Orowan, E., "Creep in Metals and Polymers," First U. S. National Congress of Applied Mechanics, 1951, p. 453.

9. Abdel-Hady, M. and Herrin, M., "Characteristics of Soil-Asphalt as a Rate Process," Journal of Highway Division, Proceedings, American Society of Civil Engineers, March, 1966.

10. Majidzadeh, K., and Schweyer, H. E., "Non-Newtonian Behavior of Asphalt Cements," Proceedings of the Association of Asphalt Paving Technologists, Vol. 34, pp. 20-44, 1965.

11. Crussard, C., "Transient Creep of Materials," Proceedings of the Joint-International Conference on Creep, American Society for Testing Materials, 1963.

12. Neville, A. M., "The Relation Between Creep of Concrete and the Stress-Strength Ratio," Applied Scientific Research, V. 9, Sect. A, 1960.

13. Powers, T. C., "The Physical Structure and Engineering Properties of Concrete," Research Department Bulletin 90, Portland Cement Association, 1958.

14. Neville, A. M., "Recovery of Creep and Observations of the Mechanism of Creep of Concrete," Applied Scientific Research, V. 9, Sect. A, 1960.

15. Best, C. H., "Creep Characteristics of Lightweight Concretes," M. S. Thesis (Engineering Science), University of California, Berkeley, 1956.

16. Hansen, T. C., and Mattock, A. H., "Influence of Size and Shape of Member on the Shrinkage and Creep of Concrete," Proceedings, American Conc. Inst., V. 63, No. 2, February 1966, pp. 267.

17. Papazian, H. S., "The Response of Linear Viscoelastic Materials in the Frequency Domain with Emphasis on Asphalt Concrete," Proceedings, International Conference on the Structural Design of Asphalt Pavements, University of Michigan, 1963, p. 385.

18. Reichard, T. W., "Creep and Drying Shrinkage of Lightweight and Normal-Weight Concretes," National Bureau of Standards Monograph 74, Dept. of Commerce, March, 1964.

19. Fowler and Guggenheim, "Statistical Thermodynamics," Cambridge University Press, 1956, London.

20. Freudenthal, A. W., "The Inelastic Behavior of Engineering Materials and Structures," J. Wiley and Sons, 1950, New York.

21. Pickett, G., "Shrinkage Stresses in Concrete," Proceedings, American Conc. Inst., Vol. 42, No. 3, Jan-Feb, 1946, pp. 165-204, 361-400.

22. Cassaro, M. A. and Holsonback, J.L., "A Rheological Analysis of Creep in Concrete," Report to Florida State Road Department and Bureau of Public Roads, Washington, D. C. on the progress of research in connection with HPR Project 99630-7201, Job 7534. Report in preparation.

BIOGRAPHICAL SKETCH

Michael A. Cassaro was born on March 15, 1931, in Brooklyn, New York. He graduated from Fort Hamilton High School in 1949. In September, 1951, he entered Rensselaer Polytechnic Institute in Troy, New York, and was graduated in June, 1954, with a B. S. degree in Civil Engineering. From August, 1954, through November, 1957, he served with the United States Navy as a division officer in a photo intelligence unit in the far east. In January, 1958, he was employed as a structural engineer by the Prescon Corporation of Corpus Christi, Texas. From March until July of 1960, he served as acting manager of the Pacific Coast Division of the Prescon Corporation in Los Angeles, California. In August, 1960, he was transferred to San Francisco, California to establish a permanent engineering and construction office in that area. In September, 1960, he entered the University of California at Berkeley as a graduate student in Structural Engineering while concurrently continuing his assignment with the Prescon Corporation. He was graduated in August, 1961, from the University of California with the degree of M.S. In September, 1961, he accepted the appointment to join the faculty of the Department of Civil Engineering of the University of Florida. In September, 1962, he was accepted into graduate school of the University of Florida and commenced working toward a doctorate degree in Civil Engineering.

Mr. Cassaro is married to the former Kay O'Gara and they have six children. He is an Associate Member of the American Society of Civil Engineers, and a member of the American Concrete Institute. He is a registered professional engineer in the state of Florida, and has been awarded the honors of membership in Tau Beta Pi, Sigma Xi, and Chi Epsilon.

This dissertation was prepared under the direction of the chairman of the candidate's supervisory committee and has been approved by all members of that committee. It was submitted to the Dean of the College of Engineering and to the Graduate Council, and was approved as partial fulfillment of the requirements for the degree of Doctor of Philosophy.

April 22, 1967

Dean, College of Engineering

Dean, Graduate School

Supervisory Committee:

Chairman